

Geochronologic Connections between the Chinle Formation and Dockum Group

By:

BLAKE BENJAMIN BEZUCHA

Bachelor of Science, 2018
The University of Texas at Austin
Austin, Texas

Submitted to the Graduate Faculty of the
College of Science and Engineering
Texas Christian University

Master's of Science
December 2022

Copyright by
Blake Benjamin Bezucha
2022

GEOCHRONOLOGIC CONNECTIONS BETWEEN THE CHINLE FORMATION
AND DOCKUM GROUP

Major Professor

For the College of Science and Engineering

Acknowledgements

First, I would like to thank my advisor, Dr. John Holbrook, for his guidance, encouragement, and patience through the process and development of this thesis and general study of some novel rocks in Texas and New Mexico, as well as giving me a sedimentological and scientific basis to complete this study. I would also like to thank Dr. Holbrook, Dr. Neil Tabor from SMU, and Dr. Xiangyang Xie of TCU, for their help in working out problems that arose during the completion of this thesis, as well as providing guidance to help me stay sane throughout this whole process. A special consideration is given to Dr. Neil Griffis of the USGS for his help in providing analytical simplicity to the complex data that was produced throughout the study. A special thanks should be given to all other TCU Faculty that helped me in general with a wide variety of things. Another thanks is made to the LaserChron lab at the University of Arizona, for making the data produced in this thesis available during the remote times of 2020/2021.

Secondly, I would like to thank my friends Anthony, Clayton, Josh, and Shaun for their help in this whole process, providing great times, and providing the opportunity to form life-long friendships just by studying some rocks. Yall's help and friendship will always be appreciated. A special thanks is needed for my friend Sam Grier, who always helped out, even if the conditions were sometimes not ideal.

Lastly, I would like to thank my family. Without them I would not have ever had the opportunity to get this degree. They are the real MVPs of this thesis, and the real rocks of my life.

Table of Contents

Acknowledgements.....	ii
Table of Contents.....	iii
List of Figures.....	iv
List of Tables.....	v
Introduction.....	1
Geologic Background.....	4
Dockum Group.....	4
The Chinle-Dockum Connection.....	6
The Santa Rosa Enigma.....	8
Potential Protolith Provenance Terranes.....	11
Methods.....	13
Results.....	19
Provenance.....	21
Statistical Results.....	33
Lithofacies and Architecture of the Santa Rosa Formation.....	38
Lithofacies.....	38
Architectural Analysis Results.....	41
Depositional Model for the Santa Rosa Formation.....	60
Provenance for the Santa Rosa Group and Greater Dockum Group.....	61
Provenance Changes within the Santa Rosa Formation.....	66
Regional Provenance Comparison.....	76
Regional Samples – Westward Correlations Dockum Group Samples.....	76
Lithological Effects on Data Abundance and Potential Implications.....	78
Paleotectonic and Paleoclimate Implications of the Dockum Group and Santa Rosa Formation.....	81
Regional Tectonics.....	81
Santa Rosa Formation.....	82
Conclusions.....	92
References.....	95
Vita.....	102
Abstract.....	103

List of Figures

1. Paleogeography – Page 17
2. Sample Locations – Page 19
3. Kernel Density Estimates – Palo Duro Canyon – Page 26
4. Kernel Density Estimates – Highway 256 – Page 27
5. Kernel Density Estimate – Santa Rosa – Page 28
6. Kernel Density Estimate – S8 – Page 29
7. K-S Tests – Page 38
8. Cumulative Density Function – Highway 256 – Page 39
9. Cumulative Density Functions – Palo Duro – Page 40
10. Cumulative Density Function – Santa Rosa – Page 41
11. Lithological Sections – Palo Duro, Highway 256 – Page 43
12. Lithological Section – Santa Rosa – Page 44
13. Paleocurrent Data – Page 45
14. Architecture Results – Middle Sandstone Unit – Page 52
15. Architecture Results – Middle Sandstone Unit – Detailed –Page 53
16. Architecture Results – Lower Sandstone Unit – Page 53
17. Architecture Results – Lower Sandstone Unit – Detailed – Page 54
18. Detailed Architecture – Middle Sandstone Unit – Page 55
19. Architecture Results – Lower Sandstone Unit – Page 57
20. Architecture Results – Mudstone Unit – Page 58
21. Architecture Results – Upper Sandstone Unit – Page 61
22. Architecture Results – Upper Sandstone Unit – Detailed – Page 62
23. Large Scale Surfaces – Middle Sandstone Unit – Page 64
24. Paleodrainage Interpretation – Lower Sandstone – Santa Rosa Formation – Page 92
25. Paleodrainage Interpretation – Middle/Upper Sandstone – Santa Rosa Formation – Page 93
26. Paleodrainage Interpretation – Tecovas Formation – Page 94
27. Paleodrainage Interpretation - Trujillo Formation – Page 95
28. Paleodrainage Interpretation – Cooper Canyon Formation – Page 96

List of Tables

1. Sample Location – Page 23
2. Analysis of Samples and Grains – Page 25
3. Architectural Analysis Results – Page 47
4. Architectural Elements – Page 48
5. Lithofacies – Page 50

Introduction

The Late Triassic Chinle Formation and the correlative Dockum Group spans most of the southwestern United States, exposed in outcrop from Texas (Dockum) to Nevada (Chinle) (Van der Voo et al., 1976; Blakey and Gubitosa, 1984; Dubiel et al., 1991; Parrish, 1993; Riggs et al., 2003; Lehman and Chatterjee, 2005; Prochnow et al., 2006b; Tanner and Lucas, 2006; Cleveland et al., 2007; Dickinson and Gehrels, 2008; Irmis et al., 2011; Lucas et al., 2012; Howell and Blakey, 2013; Lamb, 2019; Kent et al., 2019). Although the Chinle Formation west of the Rocky Mountains is extensively studied and dated and shown to be lithostratigraphically and broadly time equivalent to the more eastern Dockum Group (Riggs et al., 1996; Steiner and Lucas, 2000; Riggs et al., 2003; Zeigler et al., 2008; Dickinson and Gehrels, 2008; Cleveland et al., 2008; Martz and Parker, 2010; Dickinson et al., 2010a; Dickinson et al., 2010b; Ramezani et al., 2011; Irmis et al., 2011; Lucas et al., 2012; Jiang et al., 2018; Olsen et al., 2018; Kent et al., 2019; Parrish et al., 2019; Giesler, 2019), a more refined geochronologic correlation is needed to confirm western Chinle strata is equivalent to Dockum strata east of the Rockies in basins such as the Palo Duro and Tucumcari Basins.

Initial assessments for provenance of the Dockum Group and paleogeographical ties to the Chinle (Dickinson and Gehrels, 2008) also require more testing and refinement.

The Chinle-Dockum fluvial system is critical to understanding the climate of the Triassic, and leaves behind climatic evidence in the form of diverse paleosols, upper flow regime bedding structures, perennial and ephemeral stream deposits, and other sedimentary structures such as petrified wood (Dubiel et al., 1991; Ash and Creber, 1992; Prochnow et al.,

2006a; Tanner and Lucas, 2006; Cleveland et al., 2007; Plink-Björklund, 2015; Lamb, 2019). Paleogeography of the Chinle system is examined extensively (Blakey and Gubitosa, 1984; Steiner and Lucas, 2000; Prochnow et al., 2006a; Prochnow et al., 2006b; Dickinson and Gehrels, 2008; Dickinson et al., 2010b; Howell and Blakey, 2013), but the tectonic and climatic factors that control the potential proximal end of the system in the Dockum Group have not been well investigated. Paleogeographic trends across the Chinle-Dockum system are thus also uncertain.

This study provides geochronological and sedimentological evidence that tests temporal correlation and depositional continuity between the Chinle Formation and Dockum Group.

Particularly, this study of the Dockum Group focuses on connecting existing literature from the distal Chinle Formation to new information from the Dockum Group to assess potential for a unified Triassic drainage basin which spanned from modern-day Texas to Nevada, at least. Correlation of Dockum and Chinle strata remains a persistent problem in studies of Triassic rocks of Pangea because erosion due to post-depositional tectonic uplift made most studies regional to either side of the modern-day Rocky Mountains. Thus, any direct large-scale study of correlation to date has proved futile. Potential issues tied to a unified drainage include, coexistence of the two units in timing, dynamics of the Triassic megamonsoon across a potential unified drainage, and paleogeographic trends in fluvial style. Previous paleomagnetism studies argue that the Chinle Formation is equivalent in stratigraphic age to the Dockum Group, and both include a change from reverse to normal polarity coinciding with the Carnian to Norian boundary (Lucas et al., 2012). Recent research argues that the Chinle Formation is younger than previously believed, with evidence that the

Chinle is completely of Norian age (Irmis et al., 2011). This geochronologic revelation draws question to whether geochronologic, tectonic, and climatic factors that affected Dockum Group deposition are in common to the Chinle, particularly as to whether the waning climatic effects of a global monsoonal atmospheric circulation system, the so-called “Megamonsoon” which are recorded in strata around the Triassic-Jurassic boundary in Chinle strata (Parrish et al., 2019) correlate physically or temporally with the precieved records preserved within Dockum strata.

If the Dockum and Chinle constitute a unified drainage, they should coexist in time and show evidence for a similar source area. Comparison and correlation of geologic U-Pb detrital zircon dates of the Dockum Group to previous U-Pb studies of the Chinle Formation, as well as detailed architectural analysis of the Dockum Group and distally equivalent Chinle Formation will help constrain the duration, and extent of this continental fluvial system. Zircon analysis will be used to determine if the Dockum Group and Chinle Formation coincide in age and source area as a test of the unified drainage theory.

Geologic Background

Dockum Group

The Late Triassic Dockum Group in west Texas comprises four formations. A regional, well-developed geosol marks the base of the Dockum Group. The geosol is followed by the sand-dominant Tecovas and Trujillo Formations, each of which records several episodes of fluvial cut-and-fill events. The Dockum Group in west Texas is capped by the fluvio-lacustrine Cooper Canyon Formation. The Cenozoic Ogallala Formation incises the Cooper Canyon in all study locations in west Texas. The basal unit of the Dockum Group is thought to be the Santa Rosa Sandstone, interpreted as an amalgamated fluvial channel complex with multiple phases of incision and aggradation (Lehman and Chatterjee, 2005). The Santa Rosa Formation is not present in west Texas study locations, but is thought to equate to the boundary between the geosol and Tecovas Formations (McGowen et al., 1979; Lamb, 2019).

Carboniferous uplift caused by the Ouachita orogeny, a byproduct of collision between southern Laurentia and Gondwana, was coupled with subsidence of Paleozoic basins such as the Palo Duro Basin into which Dockum sediments accumulated (Dickinson and Gehrels, 2008). Basin subsidence was due to lithospheric flexure during the Late Carboniferous to Early Permian adjacent to collision related basement-cored uplifts such as the Matador Arch and Amarillo-Wichita Uplift (Walper, 1977; Dickinson, 1981; Martz, 2008). These basins subsequently filled with sediment up until the late Permian Period, when accommodation generated by the Ouachita orogeny had filled (McGowen et al., 1983). The Dockum Group was deposited during the Late Triassic, when Pangea had reached maximum terrestrial extent and the basin was reactivated by Triassic rifting with the

initiation of the Gulf of Mexico (McGowen et al., 1983). The surface and subsurface extent of the Dockum Group encompasses a majority of west Texas and eastern New Mexico. Overall thickness of the Dockum Group in west Texas is dependent on location within the Palo Duro Basin. Units tend to thin over the Matador Arch to the south and extend beyond in the subsurface into the Midland Basin. Thicknesses range from 600 meters in the center of Palo Duro Basin to tens of meters towards the arch (McGowen et al., 1983; Lamb, 2019). At this time, Pangea encompassed both sides of the equator and the Dockum fluvial system formed in paleolatitudes of 5° to 15° N (Bazard and Butler, 1991; Dubiel et al., 1991). Dockum equivalents are preserved in rift basins of northeast Mexico on the south side of the Ouachita Mountains (Rubio Cisneros and Holbrook, 2021).

The end of the Permian and start of the Mesozoic marked an increase in humidity and an increase in precipitation (Dubiel, 1994; Winguth and Winguth, 2013). This climatic change is argued to reflect incipient breakup of Pangea beginning in the Late Triassic, that prompted a climatic gradient to form due to rifting that opened ocean basins, causing atmospheric pressure imbalances and increased precipitation (Van der Voo et al., 1976; McGowen et al., 1983; Dickinson et al., 2010b; Winguth and Winguth, 2013; Lamb, 2019). The result of the breakup of Pangea was initiation of the Gulf of Mexico, caused by thermal doming due to elevated mantle temperatures (McGowen et al., 1983). This thermal uplift reactivated subsidence in the Palo Duro Basin and Midland Basin during the Late Triassic, thus accommodating Dockum Group deposition (McGowen et al., 1983).

Evidence for thermal uplift and subsequent reactivation of relict basins such as the Palo Duro Basin is seen in paleocurrent data. Eolian paleocurrent trends point to northerly trade winds sourced initially by perennial trade winds, before the formation of the Dockum

Group in the Late Triassic (McGowen et al., 1983). Sediment sourcing switched to the south to southeast during the Late Triassic (Dickinson et al., 2010b) and was a result of the incipient formation of the Gulf of Mexico and thermal uplift of the Ouachita fold belt, which corresponded with subsidence in the Palo Duro and Midland Basins (Riggs et al., 1996; Lehman and Chatterjee, 2005; Dickinson et al., 2010b). This reactivation formed a fluvial paleogeographic gradient from uplifted sediment sources in the Ouachita foreland toward Dockum depocenters such as the Palo Duro Basin in the Late Triassic (McGowen et al., 1983).

Pangea in the Late Triassic underwent drastic climatic changes. The alignment of Pangea along the paleoequator in the Late Triassic promoted increased climatic seasonality, as well as monsoonal conditions (Parrish, 1993). Vertic paleosols, cyclical lacustrine strata, and lungfish burrows are some examples that point to seasonal climate during the Late Triassic in the Chinle formation west of the Rocky Mountains (Dubiel et al., 1991; Ash and Creber, 1992; Parrish, 1993; Dubiel, 1994; Tanner and Lucas, 2006). More recently, Lamb (2019) found upper flow regime channel deposits in the Dockum Group of Texas, proposed to be a byproduct of rare and intense monsoonal storms that reached inner Pangea.

The Chinle-Dockum Connection

Previous studies of the Late Triassic Chinle Formation point to a continental-scale fluvial system spanning the present day southwest United States from Texas to Nevada. The headwaters of this paleodrainage are hypothesized to be located near the reactivated Ouachita Foreland (Dickinson et al., 2010a), and the terminus of the system is argued to be the Auld Lang Syne marine back-arc basin, which was located in present day Nevada (Riggs et al., 1996). Paleocurrent data in both the Chinle Formation as well as the Dockum Group show

similar northwest trends in fluvial paleoflow (Cazeau, 1962; Seni, 1978; Boone, 1979; Pavlak, 1979). Dickinson and Gehrels (2008) argued that this data is evidence of a stable northwest continental gradient that lasted throughout the Late Triassic and that these two fluvial systems are connected as proximal (Dockum) and distal (Chinle) equivalents.

Analogous lithostratigraphy of the Chinle Formation and Dockum Group also point to a potentially connected fluvial system. Regional, basal unconformities in both units cut into underlying Permian strata. The fluvial units of the Shinarump Member at the base of the Chinle Formation are often described as being deposited in paleovalleys bounded at the base by a regional unconformity, similar to the Santa Rosa Formation (Dubiel et al., 1999). In west Texas, the Tecovas Formation is described as being deposited in a mixed floodplain system with local terminal lakes that experienced seasonal lake levels, recorded in lapping relationships in lacustrine delta deposits (Lamb, 2019). Similar to the Tecovas, the Monitor Butte Member is described as a fluvial system having lacustrine deltaic deposits (Dubiel et al., 1991). Above the Tecovas Formation in west Texas is the Trujillo Formation, described as a sand-dominated multi-story channel complex (Lehman and Chatterjee, 2005; Lamb, 2019). Similar sand-dominant deposits in the Chinle Formation include the stratigraphically equivalent Sonsela Member and Moss Black Member (Tanner and Lucas, 2006; Dubiel and Hasiotis, 2011). The youngest depositional units in both reaches of the proposed paleodrainage are mud-dominated lacustrine deposits that contain non-amalgamated channel bodies. The Cooper Canyon Formation of the Dockum Group and the Painted Desert Member of the Chinle Formation are examples of these types of deposits, and both occupy similar stratigraphic positions in the upper part of the Triassic section (Lehman and Chatterjee, 2005; Tanner and Lucas, 2006).

Provenance studies of the Chinle Formation indicate evidence of a potential sourcing of sediment from the southeast. Riggs et al. (1996) was the first to find a signature of the Amarillo-Wichita uplift (515 Ma to 540 Ma) in a limited set of zircon grains found in a Santa Rosa Formation sample. Riggs et al. (1996) stated that the signature was evidence for a fluvial system that spanned southwest Laurentia, as Chinle Formation deltaic deposits in Nevada showed a similar provenance signature. Dickinson and Gehrels (2008) were the first study to rigorously test the unified paleodrainage hypothesis, obtaining 17 samples in the Chinle Formation and Dockum Group. Dockum Group samples included samples from the Trujillo and Cooper Canyon Formations in west Texas, as well as Santa Rosa Formation samples in New Mexico and Texas. Three separate drainages are identified during the fluvial evolution of the Chinle Formation and Dockum Group, each with a distinct provenance signal differentiating different source terranes and timing within the fluvial system (Dickinson and Gehrels, 2008).

The Santa Rosa Enigma

The Santa Rosa Formation is commonly placed as a sedimentary unit within the Dockum Group (Lucas and Hunt, 1987; Finch and Geological, 1988; Lucas et al., 2001). There is some debate as to where the Santa Rosa Formation should be placed stratigraphically with relation to Triassic units in Southwest Laurentia, and a goal of this study is to identify whether the Santa Rosa Formation should be included in the Dockum Group or excluded as a separate unit.

The Santa Rosa Formation was first identified as a Late Triassic fluvial sedimentary unit by Darton (1922), and named the Santa Rosa Sandstone (Darton, 1922). Gorman and Robeck (1946) divided the Santa Rosa Sandstone into four units based on lithological

properties, the lower sandstone unit, the middle sandstone unit, the shale unit, and the upper sandstone unit (Gorman and Robeck, 1946). These four distinct units were kept, with minor name changes in future studies (Lupe, 1977; McGowen et al., 1983; Finch et al., 1988). The unit was renamed the Santa Rosa Formation, and paleontological findings also pointed to an older age for the lower sandstone unit in comparison to the upper three units (Lucas, 1985). Lucas and Hunt (1987) were the first to describe the lower sandstone unit as a separate lithological formation, the Middle Triassic Anton Chico Formation, based on the lithological features. The Anton Chico Formation (lower sandstone unit) contains higher amounts of lithics and lithic conglomerates and has a distinct purplish-red color in contrast with the upper three members of the Santa Rosa Formation (Lucas and Hunt, 1987). Lucas and Hunt (1987) also renamed the middle sandstone, mudstone, and upper sandstone units the Tecolotito, Los Esteros, and Tres Lagunas Members, respectively, of the Santa Rosa Formation. Finch et al. (1988) reverted back to Gorman and Robeck (1946) when describing each of the units, and lowered the Anton Chico Formation to member status. This study, for simplicity, will use the stratigraphy of Gorman and Robeck (1946).

Though complex stratigraphically and with disputed correlations, the lithology of the Santa Rosa Formation is well understood. The lower sandstone is predominantly a red-brown-purple cross-laminated litharenitic sandstone (Lucas and Hunt, 1987; Finch et al., 1988; Fritz, 1991). This unit is unique with regard to the other units in that it contains a significant amount of lithic fragments. The lower sandstone unit overlies Permian red beds, and the base of the unit is marked by extraformational conglomerates containing Permian clasts (Lucas et al., 2001). The middle sandstone member commonly incises the lower sandstone member, and is mineralogically distinct from the lower sandstone, with a lack of

lithics and a high proportion of quartz. The middle sandstone member is a greyish orange trough cross-bedded quartzarenitic sandstone containing minor extrabasinal conglomerates (Lucas and Hunt, 1987; Finch et al., 1988). The middle sandstone grades conformably upward into the finer grained mudstone unit. The yellow-to-red colored mudstone member is often intertongued with middle sand bodies, and commonly contains thin, very fine-grained sandstone beds. The youngest of the units, the upper sandstone member, is an orange-yellowish brown quartzarenitic sandstone, displaying planar and trough cross-bedding. A limestone-cobble conglomerate marks the base and signifies an erosive contact between the upper sandstone and mudstone members (Lucas and Hunt, 1987; Finch et al., 1988; Fritz, 1991; Lucas et al., 2001).

Finch et al. (1988) provided a detailed depositional history of the Santa Rosa Formation at its type section in Santa Rosa, New Mexico. Overall, the Santa Rosa Formation, including the lower sandstone member, records multiple sedimentary cycles. The lower sandstone is described as deposition from ephemeral streams flowing in a northern direction, incorporating clasts of the underlying Permian sediment into the formation (Finch et al., 1988). The lower sandstone unit is alternatively described as originating from an alluvial fan environment (McGowen et al., 1979). The lower sandstone is interpreted as lower energy braided river deposits established after the initial conglomerate-generating incision. The middle sandstone is interpreted as conglomerate lags and upper flow regime deposits that quickly waned to lower flow regime deposits with transverse bars in a stream system that flowed south (Finch et al., 1988). There is also speculation that these sands are correlative to the Tecovas Formation of west Texas (Fritz, 1991). Once sediment supply waned, lacustrine and floodplain deposits of the mudstone member were deposited. Alternatively, these strata

are interpreted to include a prodeltaic lacustrine sequence (McGowen et al., 1979). The final depositional cycle of the Santa Rosa Formation resulted in deposition of the upper sandstone member, consisting of lower flow regime deposits similar to those of the middle sandstone member (Finch et al., 1988). Other interpretations of this member include a mix of fluvial to terrestrial deltaic environments (Fritz, 1991), as well as a progradational fan delta complex (McGowen et al., 1979).

Potential Protolith Provenance Terranes

A primary prediction for the hypothesis that a paleodrainage was sourcing sediment through the Palo Duro Basin, and to Chinle Formation basins in the Four Corners Area is whether both share a common provenance. Provenance suites in the Chinle Formation show different source distributions for each of the three paleorivers described vertically in Dickinson and Gehrels (2008). The upper Chinle Cottonwood paleoriver has a dominant southeast source, with predominant ages of pre-Paleozoic Appalachian terranes (300-540 Ma), Neoproterozoic Peri-Gondwanan terranes (540-700 Ma), and Grenville orogenic terranes (900-1350 Ma). The contributive Shinarump trunk paleoriver is considered to contain a predominant southern source from adjacent Mogollan Highlands that represent uplifted Yavapai-Mazatzal ages (1600-1800 Ma) and anorogenic granite (1440-1420). Another south to southwestern source inferred for the Shinarump drainage is the adjacent nascent Cordilleran Arc, which supplied Permian-Triassic grains to the lower paleoriver deposystem via tributary drainages and plinian ash-fall deposits (Dickinson and Gehrels, 2008; Dickinson, 2018; Riggs et al., 2020). The Eagle paleoriver is the youngest of the three, and is inferred to have traversed the Ancestral Rocky Mountains of Colorado with headwaters sourcing distinct ages (515-525 Ma) of the Amarillo-Wichita Uplift, a direct

result of Ancestral Rocky Mountain Paleozoic tectonism.

Potential contributive provenance sources of the Dockum Group are proposed to be similar to southeast sources of the Chinle Formation, and thus Appalachian, Gondwanan, and Grenvillian aged sources could be significant sources funneling into the Palo Duro Basin during the Late Triassic (Dickinson and Gehrels, 2008). Other potential sources include northeasterly sourced Amarillo-Wichita Uplift sediments, local erosion of uplifted Midcontinent Granite-Rhyolite basement, and potential Permian-Triassic arc input from the East Mexico Arc and/or Cordilleran Arc of western Pangea. These sources previously mentioned will be considered, as well as any other potential sources supported by the data.

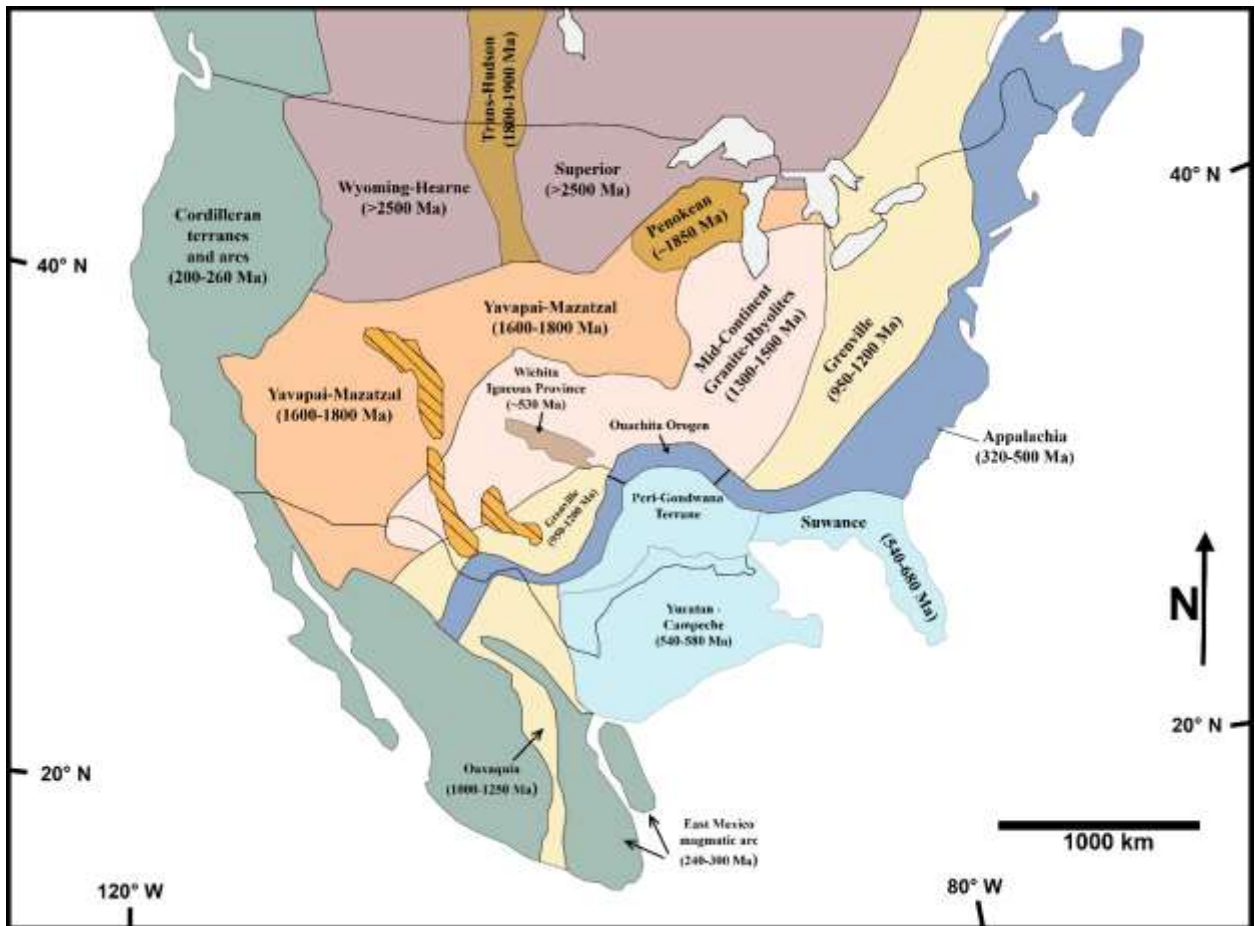


Figure 1. Major source terranes of North America. Modified after Gehrels et al. (2011). Protolith

terrane and representation used for interpretation are modified from previous studies (Gehrels et al., 2011; Fildani et al., 2016). The provenance suites include: Archean terranes (>2500 Ma), Paleoproterozoic terranes (1600-2500 Ma), Midcontinent Granite-Rhyolite province (1300-1500 Ma), Grenville orogenic terranes (900-1350 Ma), Neoproterozoic/Gondwanan terranes (540-800), Pre-Paleozoic/Appalachian terranes (300-540 Ma), as well as Permian-Triassic ages (300-200 Ma).

Methods

This study comprises of lab, field, and statistical elements. Field expeditions to areas in west Texas were made for sample collection. Field locales in New Mexico were used for sample collection, as well as for taking a stratigraphic section through the Santa Rosa Formation in the type area within Santa Rosa State Park, Santa Rosa, New Mexico.

Samples collected for U-Pb analysis span the Late Triassic Dockum Group in west Texas and areas of east-central New Mexico. Samples of the Middle Triassic Santa Rosa Formation were collected in areas just south of Los Esteros Dam in Santa Rosa, New Mexico from a section measured for this study. Samples were also collected from the overlying Dockum deposits in west Texas (Figure 2). These samples were collected from stratigraphic sections of previous workers, such as Lamb (2019) and Skaleski (pers. comm.). Samples were generally decimeter-scaled and targeted channel sandstones, as heavy minerals such as zircons preferentially group with lighter minerals such as quartz in stratified siliclastic rocks (Gehrels, 2011). Mud-rich samples were also collected from outcrops, targeting floodplain mudstones, well-defined paleosols, laminated lacustrine deposits, as well as potential ash-fall layers. Mud-rich samples were preferentially selected based on lack of bioturbation. Samples were collected near contacts between individual formations of the Dockum Group, as well as informal lithological units that lie within the Santa Rosa Formation. In total, 33 raw samples were obtained via two field expeditions.

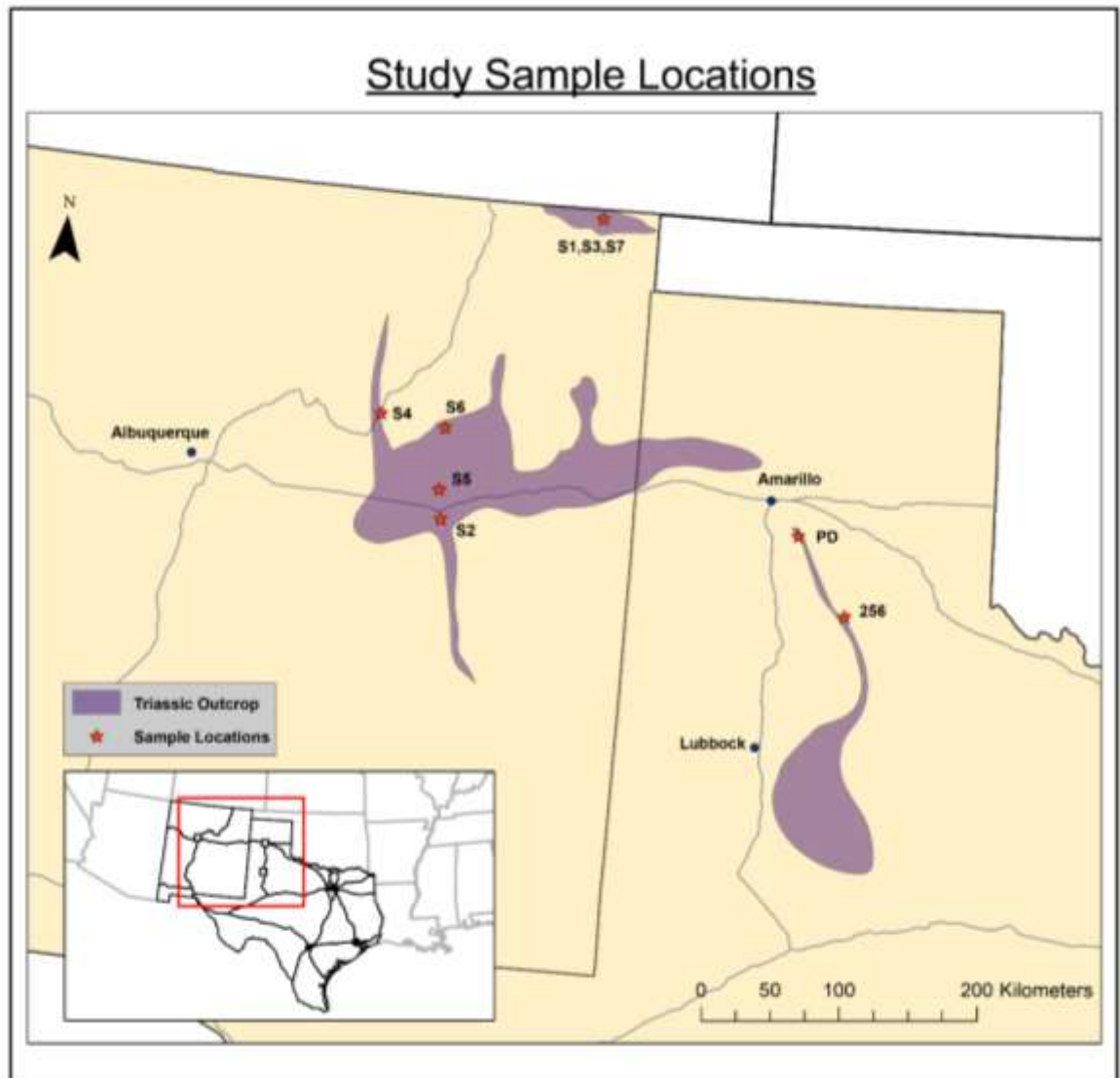


Figure 2. Outcrop locations of samples collected for this study. See Table 1 for Unit descriptions.

Mud-rich samples were sent in tact to the UA LaserChron lab for further zircon extraction and analysis, while select sandstones were extracted at TCU. Sandstone samples from the field were broken down mechanically to gravel-sized pieces using a jaw crusher at TCU and then pulverized using a disk mill for each sample. Sandstones at TCU underwent

heavy mineral separation using a Frantz-LB-1 magnetic separator, and heavy liquids to separate heavy minerals like zircon grains from other detritus. Zircons were then microscopically analyzed and grouped in an alcohol solution and transported to a weigh sheet, and finally packaged for transport to the LaserChron lab in Arizona.

Mud-rich samples that were sent to the UA LaserChron lab after pulverization underwent similar separation techniques, as well as undergoing sonication using an ultrasonic sonicator. Zircons were then polished in an epoxy and mounted for analysis. Radiometric dates were acquired using the University of Arizona's LaserChron lab. Specifically, detrital zircons were analyzed using Laser Ablation- Inductively Coupled Plasma-Mass Spectrometry (LA-ICPMS). A population target of $n=300$ zircons per sample was used for this study. Due to travel restrictions, selection of grains was done by using a remote picking program, Chromium Offline Targeting. SEM BSE greyscale images were used in this program via a Hitachi 3400N to determine if grains were composed of homogenous zircon, as well as to tell if grains were absent of cracks and overgrowths. These are signs of potential Pb (lead) loss within the grain that could lead to error in true age. Grains selected for chemical analysis were absent of these traits. Grains were analyzed via LA-ICP-MS using the Thermo-Element 2 (E2) with a spot diameter of 20 microns (Gehrels et al., 2006). The laser used was the Photon Machines Analyte G2 Eximer Laser.

Statistical Methods

Statistical tests are used to examine regional and temporal similarities and differences between samples. Cumulative Density Functions (CDFs) were produced for the three sections using the same excel macro used to produce K-S tests. CDF's are similar to probability density plots, except that they provide information on the probability that a zircon

will be younger than a specific age when plotted on the y-axis. CDFs display the same data as kernel distance estimates, but allow for easier identification of patterns.

A Kolmogorov-Smirnov (K-S) statistical test was done to show correlations or variations between two individual samples based on their population distributions (Guynn and Gehrels, 2010). K-S tests are based on cumulative distribution functions, and the product of two different samples are analyzed. K-S tests produce p values, which are the probability that the difference between samples is a result of statistical error versus true error. P values that have values greater than 0.05 are considered to not be dissimilar. This were calculated using a excel macro from (Guynn and Gehrels, 2010).

Likeness tests were also used for this study, based on the statistical difference between two individual samples. Likeness tests use probability density plots (PDPs) of two different samples, and creates a difference summation based on the number of grains and density of ages. These tests were conducted based on a excel workbook created by Satkoski et al. (2013).

Data Reduction

U-Pb radiometric ages were examined using the Excel-based Isoplot program (Ludwig, 2008). Data was reduced at the 2-sigma error value for the data set. Grains with raw ages under 1 billion (1 Ga) were reduced using Concordia plot comparison of U^{235}/Pb^{207} to U^{238}/Pb^{206} . Grains younger than 1 Ga that fell on concordia within 2-sigma were included in this study. Grains with raw ages older than 1 Ga were filtered using a discordance filter of 20%, as well as a reverse discordance filter of 5%. This filtered data is used for data analysis.

Field Methods Description

Outcrop descriptions were compiled of the Santa Rosa Formation and underlying Permian sediments in Santa Rosa, New Mexico. Descriptions of the measured section were used to identify sedimentary characteristics, such as lithology, grain characteristics, as well as bedding characteristics. The outcrop is in the type area, and samples S2 and S5 were analyzed at the base and top contact of the Santa Rosa Formation, respectively. Outcrop photos were taken using Canon EOS Rebel T3i handheld camera. These photos were used for architectural analysis. Measured sections were digitized using the program Adobe Illustrator.

Architectural Analysis was done on the Santa Rosa section, using a set of principles by Holbrook (2001). Surface relationships were based on guidelines that each surface is considered to be unique and laterally continuous, unique surfaces can truncate but cannot cross, and the fact that a surface is younger if it is bound by another surface. First order surfaces are considered bound lamina sets, lower order surfaces are bound by higher order surfaces, a surface order is one higher than the one it truncates, surfaces can only truncate surfaces of equal or higher order, and a set of equal ordered surfaces will be bounded by higher order surfaces.

Section	Sample	Unit	Latitude	Longitude
Palo Duro Canyon	PDG2	Geosol	34.977924	-101.680648
Palo Duro Canyon	PDG1	Geosol	34.978120	-101.680793
Palo Duro Canyon	PDTE1	Tecovas Foramtion	34.978631	-101.682554
Palo Duro Canyon	PDTE3	Tecovas Formation	34.980079	-101.684127
Palo Duro Canyon	PDTJ2	Trujillo Formation	34.982245	-101.684969
Palo Duro Canyon	PDCC4	Cooper Canyon Formation	34.983857	-101.685347
Highway 256	256paleosol	Geosol	34.470347	-101.095461
Highway 256	256TC3	Tecovas Formation	34.469771	-101.096585
Highway 256	256TC2	Tecovas Formation	34.469795	-101.096687
Highway 256	256TR4	Trujillo Formation	34.470317	-101.099421
Highway 256	256TR3	Trujillo Formation	34.470238	-101.099832
Highway 256	256TR2	Trujillo Formation	34.470063	-101.100349
Highway 256	256CCS4	Cooper Canyon Formation	34.470021	-101.101067
Highway 256	256CCS3	Cooper Canyon Formation	34.470092	-101.102806
Highway 256	256CCS2	Cooper Canyon Formation	34.470236	-101.103368
Highway 256	256CCS1	Cooper Canyon Formation	34.468985	-101.106794
Santa Rosa State Park, NM	S2	Santa Rosa Formation	34.91935	-104.65834
Dry Cimmaron Valley, NM	S3		36.97334	-103.40967
I-25, Las Vegas NM	S4		35.51214	-105.25631
Santa Rosa State Park, NM	S5		35.02870	-104.68455
Trujillo Hill, NM	S6		35.51480	-104.68778
Dry Cimmaron Valley, NM	S7		36.97350	-103.40967

Table 1. GPS coordinates of study samples.

Results

Lithology versus Zircon Yield

One objective of this study is to determine what types of lithologies produce the greatest yield of analyzable zircon grains. Samples were collected from a range of lithologies with different textures from contrasting depositional environments. Lithologies, with environments, included channel-fill conglomerates, floodplain mudstones, channel-fill sandstones, and ash-rich floodplain deposits. These lithotypes were compared for grain abundance and distribution of zircon ages. Table 2 shows each sample analyzed and the total number of grains analyzed, along with the amount of Late Triassic Grains, and are sorted by location and percentage of Late Triassic grains. A conservative estimate was used for this number, accounting for grains with 2σ error ranges within Late Triassic time intervals. Samples S2 and S5 were omitted, as these represent Santa Rosa Formation deposits that are likely Middle Triassic in age based on this study.

Sample	Lithology and Interpreted Depositional Environments	*Number of Late Triassic grains analyzed (<237 Ma)	Total number of grains analyzed	% of Late Triassic grains within sample
Palo Duro Outcrop				
PDG2	Floodplain paleosol mudstone	4	82	4.878049
PDG1	Floodplain paleosol mudstone	12	278	4.316547
PDCC4	Lacustrine Mudstone	8	248	3.225806
PDTE1	Channel-fill fine-grained sandstone	2	268	0.746269
PDTE3	Lacustrine mudstone	0	287	0
PDTJ2	Lacustrine mudstone	0	296	0
256 Outcrop				
256TC3	Channel -fill fine-grained sandstone	4	93	4.301075
256CCS3	Ash-rich Floodplain mudstone	11	274	4.014599
256CCS2	Lacustrine mudstone	10	260	3.846154
256CCS1	Channel-fill siltstone	9	286	3.146853
256TR4	Channel-fill conglomerate	4	201	1.99005
256CCS4	Lacustrine mudstone	3	287	1.045296
256TR2	Lacustrine mudstone	2	283	0.706714
256TR3	Lacustrine mudstone	1	212	0.471698
256paleosol	Floodplain paleosol mudstone	0	294	0
Regional Samples				
S6	Floodplain paleosol mudstone	5	191	2.617801
S7	Channel-fill fine-grained sandstone	5	246	2.03252
S3	Channel-fill fine-grained sandstone	1	179	0.558659
S4	Channel-fill fine-grained sandstone	0	296	0

Table 2. Analysis of Late Triassic Grains. Samples are also distinguished by grain size based on shading. Brown-Clay-sized samples, Yellow-Sand-sized samples. Orange-Silt-sized samples. Blue-Gravel-sized samples.

Provenance

The following are results from provenance analysis. Relative percentages of grains with respect to source terranes, as well as prominent and secondary peak ages present in kernel density estimates are described below. Kernel Density Estimates for the Palo Duro section, the Highway 256 section, as well as the additional regional samples are shown in Figure 3, Figure 4, and Figure 5.

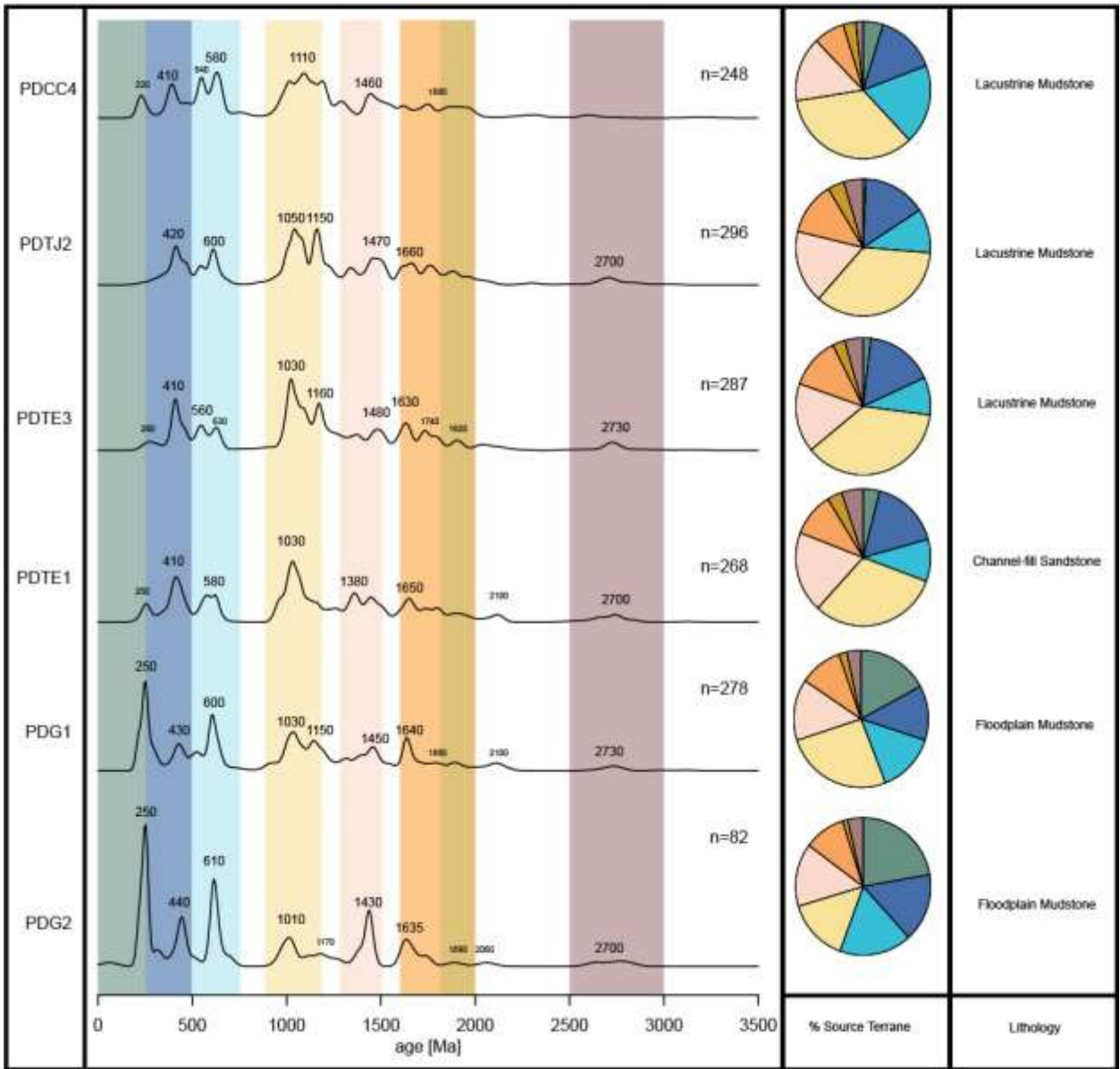


Figure 3. Kernel Density Estimates of Palo Duro Outcrop Samples in Stratigraphic Order

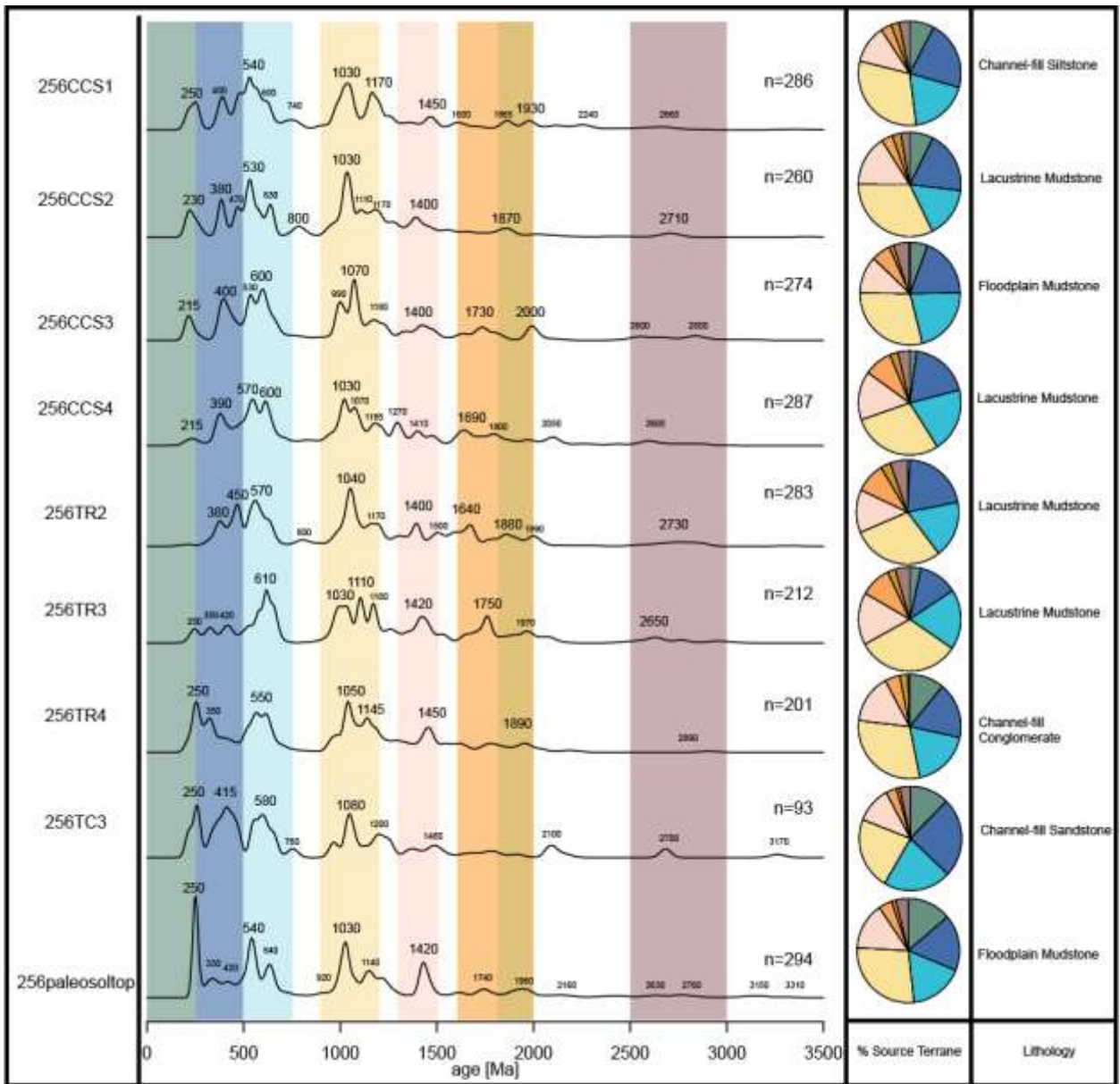


Figure 4. Kernel Density Estimates of Highway 256 Samples in Stratigraphic Order

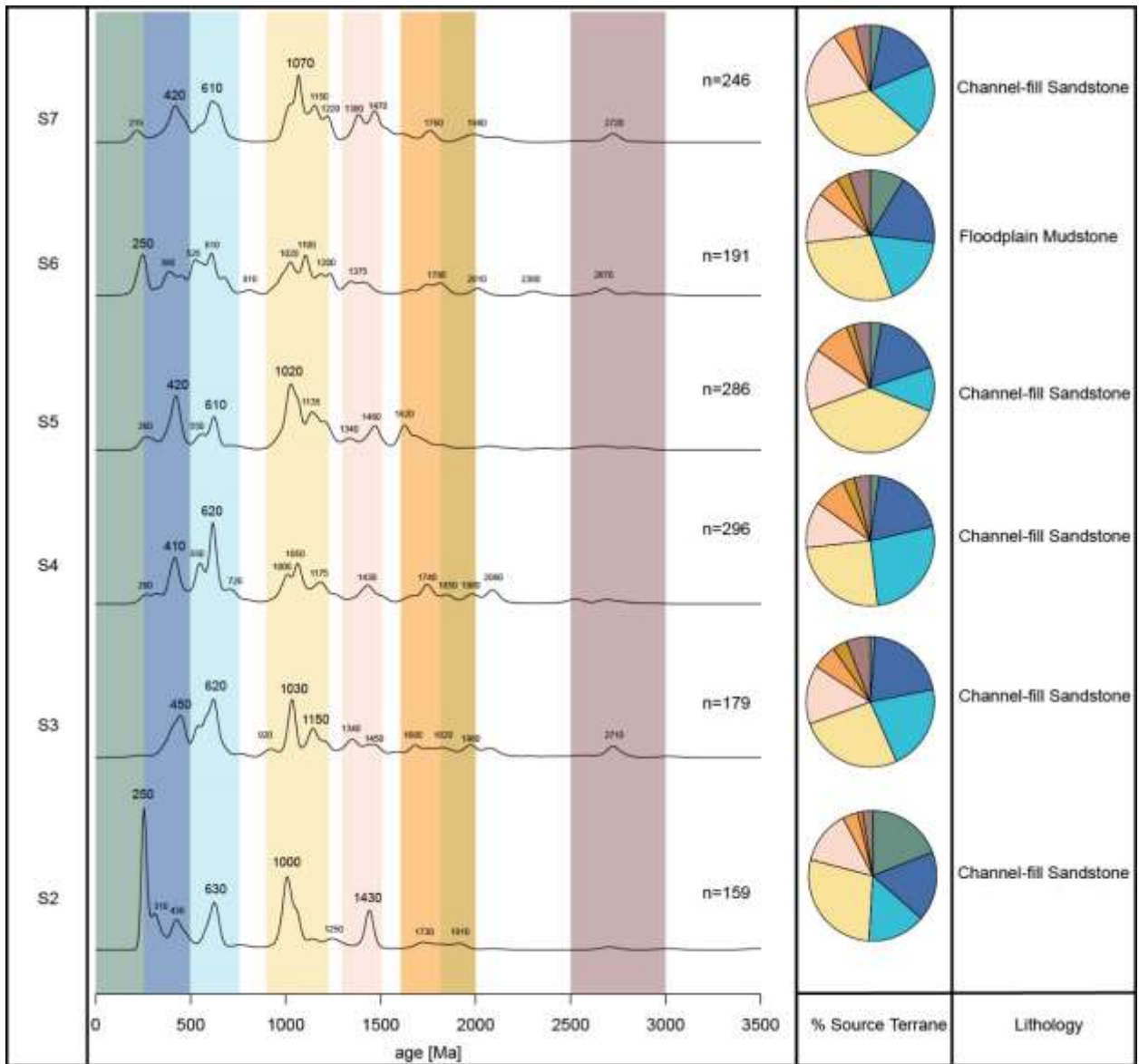


Figure 5. Kernel Density Estimates of Santa Rosa Formation (S2, S5) and Regional Samples (S3, S4, S6, S7) in Stratigraphic Order

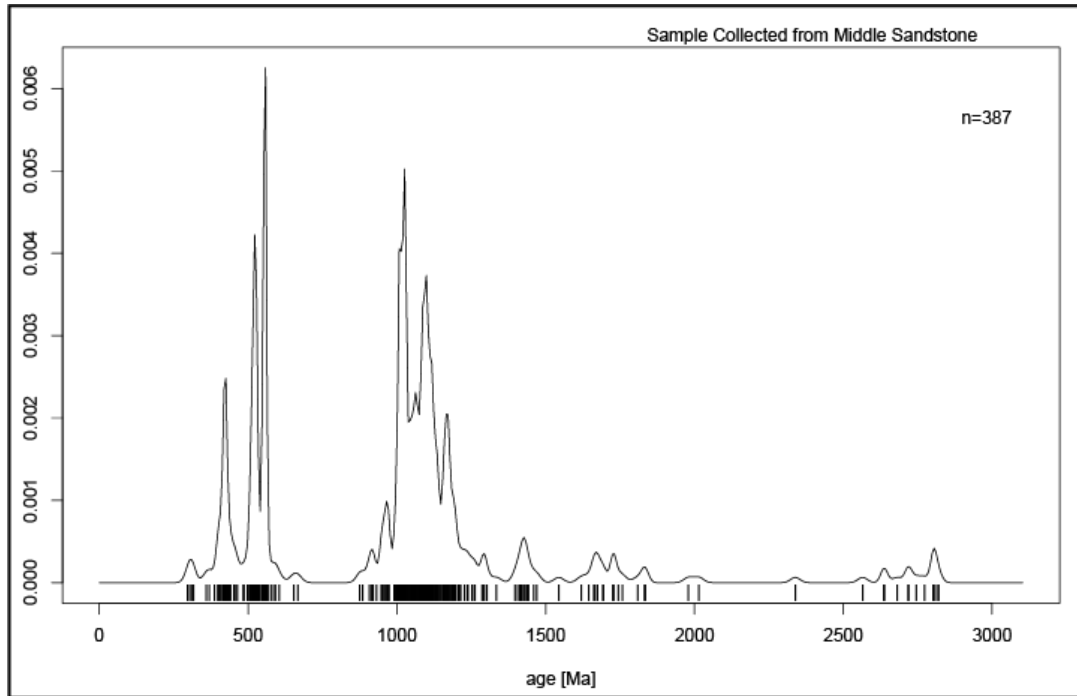


Figure 6. Analysis of Middle Sandstone of the Santa Rosa Formation (Sample S8) in Santa Rosa, NM.

Zircon Samples

Santa Rosa Formation, Santa Rosa, New Mexico: Samples S2 and S5

The Santa Rosa Formation was analyzed for similarities in provenance and age with the remaining strata of the Dockum Group. Two samples, S2 and S5, of the Santa Rosa Formation, near its type section in New Mexico, were collected from the same lithologic column for zircon analysis in the type section near Santa Rosa, New Mexico. Sample S2 is a fine-grained parallel-laminated purplish sandstone that lies at the base of the lower sandstone unit of the Santa Rosa Formation. Sample S5 is a medium-grained, trough cross-bedded tan sandstone that was collected at the top of the lithologic section, in the upper sandstone member of the Santa Rosa Formation.

The most abundant source of grains in sample S2 are from Grenville aged terranes (28%), with significant amounts of grains also coming from Permian-Triassic terranes (19%), Appalachian terranes (17%), and Gondwanan terranes (15%). Primary KDE peak ages of the sample include peaks at 250 Ma, 630 Ma, 1000 Ma, and 1430 Ma. Other secondary peak ages include 310 Ma, 430 Ma, 1250 Ma, 1730 Ma, as well as 1910 Ma.

The highest amount of grains in sample S5 derives as well from Grenville aged terranes (38%). A remarkable amount of grains derive from Appalachian aged terranes (17%), Midcontinent aged terranes (15%), as well as Gondwanan aged terranes (11%). Prominent peak ages from the KDE plot of sample S5 include peaks at 420 Ma, 610 Ma, and 1020 Ma, with secondary peaks of 260 Ma, 550 Ma, 1135 Ma, 1340 Ma, 1460 Ma, 1620 Ma.

Dockum Formation Geosol

All three Geosol samples are part of the regional geosol across west Texas that lies at the base of the Dockum Group. PDG2, the base of the Palo Duro section, is maroon in color, with a mottled, pedogenic, heavily bioturbated structure. PDG1 is a brown paleosol with a platy soil structure, containing evidence of rooting. 256Paleosol is poorly-drained, purplish with a blocky pedogenic structure. These three samples represent a range of stratigraphic expressions in the well-developed and mature regional geosol.

These paleosols include a range of zircon ages from a dominance of Grenvillian to Late Triassic ages. All geosol samples show a prominent abundance of Permian-Triassic ages, with samples PDG2 and PDG1 having 22% and 17% abundance of Permian-Triassic aged grains. Sample 256paleosol has a Permian-Triassic abundance of 14%. A distinct abundance of Grenvillian aged grains was found in sample PDG1, composing 26% of the

sample. A distinct abundance of Grevillian aged grains was found in sample 256paleosol as well, composing 28% of the sample. Grains ages > 1250 Ma predominately make up the paleosol samples, with 70% of grains being 1250 Ma or younger in samples PDG2 and PDG1, as well as 76% in 256paleosol. Lesser, but potentially significant, amounts of grains aged 1200-1800 Ma are present in all paleosol samples. Prominent peak ages in the kernel density estimate of sample PDG2 include 250 Ma, 610 Ma, 1430 Ma. Secondary peak ages for sample PDG2 include ages 440 Ma, 1010 Ma, 1635 Ma. Prominent peak ages in the kernel density estimates of sample PDG1 include 250 Ma and 600 Ma. Secondary peak ages of sample PDG1 include 430 Ma, 1030 Ma, 1150 Ma, 1450 Ma, 1640 Ma. Prominent peak ages in the kernel density estimate of sample 256paleosol include 250 Ma, 540 Ma, 1030 Ma, 1420 Ma. Secondary peak ages of sample 256paleosol include 330 Ma, 420 Ma, 640 Ma, 1140 Ma.

Tecovas Formation, Dockum Group, west Texas

Three samples of the Tecovas Formation contained adequate grains (>80 grains) for provenance analysis. PDTE1 is a fine-grained sandstone that forms the basal channels of the Tecovas Formation in Palo Duro Canyon and cuts into the geosol. PDTE3 is a bioturbated floodplain mudstone that lies on top of the basal trunk channels of the Tecovas Formation. 256TC3 is a fine-grained sandstone, part of an upper flow regime sheet channel like those commonly found in the Tecovas Formation at the 256 outcrop (Lamb, 2019; Walker, 2020).

Sample PDTE1 contains a significant amount (31%) of grains in between 900-1250 Ma, an indication of grains derived from Grenville orogenic terranes. Other notable abundances include a 19% abundance of grains from Midcontinent Granite-Rhyolite terranes, as well as a 17% abundance from Appalachian terranes. Prominent peak ages from sample

PDTE1 include 410 Ma and 1030 Ma. Smaller secondary peak ages of 250 Ma, 580 Ma, 1380 Ma, and 1650 Ma are also present.

Sample PDTE3 has a kernel density estimate (KDE) signature similar to sample PDTE1. The highest abundance of grains (37%) lie within 900-1250 Ma, indicating an influence from Grenvillian aged terranes. Similar to sample PDTE3, the other age suites with the highest abundance are Appalachian terranes at 16%, as well as Midcontinent terranes at 16%. Prominent peak ages for PDTE3 are 410 Ma, 1030 Ma, and 1160 Ma, while secondary peak ages are 260 Ma, 560 Ma, 610 Ma, 1480 Ma, 1630 Ma, and 1740 Ma.

Sample 256TC3 shows a high abundance of Grenvillian aged grains (22%) when compared to other Tecovas Formation samples. In contrast, there is an approximately even distribution of abundance between Appalachian, Gondwanan, and Grenvillian terranes with amounts of 25%, 21%, and 22% respectively. Prominent age peaks of 250 Ma, 415 Ma, 580 Ma, and 1080 Ma are seen in sample 256TC3. This sample has minor secondary age peaks at 760 Ma, 1200 Ma, 1480 Ma, and 2100 Ma.

Trujillo Formation, Dockum Group, west Texas

Four samples of Trujillo Formation sediments yielded sufficient zircons for provenance analysis (>80 grains). PDTJ2 is a fine-grained laminated lacustrine mudstone interpreted to be abandoned channel fill or open lake in origin. 256TR4 is a conglomerate lag with pebble-sized rip up clasts, interpreted to be the base of the sand-dominated Trujillo Formation, and generated by incision into the underlying Tecovas Formation. 256TR3 is a fine-grained laminated mudstone interpreted as an abandoned channel fill. 256TR2 is a fine-grained muddy channel fill 3 meters below the contact with the overlying Trujillo Formation and Cooper Canyon Formation.

Sample PDTJ2 shows a predominant abundance of Grenvillian grains, with 35% of grains being sourced from Grenville aged terranes. Other significant sources of grains in this sample include Appalachian aged terranes (15%), Midcontinent aged terranes (17%), as well as Yavapai-Mazatzal aged terranes (13%). Prominent peak ages for sample PDTJ2 include 1050 Ma, and 1150 Ma, with secondary age peaks including ages 420 Ma, 600 Ma, 1470 Ma, 1660 Ma, 1750 Ma, 1900 Ma, and 2700 Ma.

Sample 256TR4 shows a predominant abundance of Grenvillian grains, composing 30% of the sample. Secondary abundances of grains in this sample include grains sourced from Appalachian aged terranes (17%), as well as from Gondwanan aged terranes (18%). Prominent peak ages for sample 256TR4 include 270 Ma, 550 Ma, and 1050 Ma. Secondary peak ages include peaks at 350 Ma, 1145 Ma, 1450 Ma, and 1890 Ma.

Sample 256TR3 shows a primary abundance of grains that are sourced from Grenville aged terranes, composing 32% of the grains in the sample. Other significant abundances include Gondwanan aged terranes (19%), Midcontinent aged terranes (16%), as well as Appalachian aged terranes (12%). Prominent peaks include peaks at 610 Ma, 1030 Ma, 1110 Ma, and 1180 Ma. Secondary age peaks are present at 250 Ma, 350 Ma, 420 Ma, 1420 Ma, 1750 Ma, 1970 Ma, and 1650 Ma.

Sample 256TR2 shows a primary abundance of grains sourced from Grenville aged terranes (29%). Other significant abundances of grains in the sample are sourced from Appalachian aged terranes (21%) as well as Gondwanan aged terranes (18%). Primary peak ages of the sample show at 380 Ma, 450 Ma, 570 Ma, as well as 1040 Ma. Secondary peak ages arise at 800 Ma, 1170 Ma, 1400 Ma, 1500 Ma, 1640 Ma, 1880 Ma, and 1990 Ma.

Cooper Canyon Formation, Dockum Group, west Texas

Five samples of the Cooper Canyon Formation were used for provenance analysis (Figure 3 and Figure 4). PDCC4 is a fine-grained, laminated purplish mudstone from 2 meters below the contact between the Cooper Canyon Formation and Ogallala Formation in the Palo Duro measured section (Figure 11). 256CC4 is a fine-grained purplish laminated lacustrine mudstone that lies at the base of the Cooper Canyon Formation at the 256 outcrop. 256CCS3 is a fine-grained faint greenish-grey ash bed that lies on top of laminated lacustrine sediment in the upper part of the Cooper Canyon Formation. 256CCS2 is a fine-grained laminated mudstone that is interpreted to be lacustrine in origin. 256CCS1 is a fine-grained rippled siltstone between laminated mudstone, interpreted to be a splay from a distributary channel in a lacustrine delta present in the lower part of the Cooper Canyon Formation. 256CCS1 lies 3 meters below the contact between the Cooper Canyon Formation and overlying Ogallala Formation.

The highest abundance of grains in sample PDCC4 is from Grenville aged terranes, composing 34% of the sample. Other significant sources for detrital zircon grains derive from Gondwanan aged terranes (19%), Midcontinent aged terranes (15%), as well as Appalachian aged terranes (14%). Prominent peak ages for this sample include 540 Ma, 580 Ma, and 1110 Ma. Secondary peak ages of this sample include 220 Ma, 410 Ma, 1460 Ma, and 1880 Ma.

Sample 256CCS4 derives from Grenville aged terranes (29%), with other abundant sources from Appalachian (19%), Gondwanan (20%), and Midcontinent (15%) aged terranes. Prominent age peaks for sample 256CCS4 include peaks at 390 Ma, 570 Ma, 600 Ma, 1030 Ma, and 1070 Ma. Secondary minor age peaks include 215 Ma, 1185 Ma, 1270 Ma, 1410 Ma, 1690 Ma, 1800 Ma, 2050 Ma, as well as 2800 Ma.

Sample 256CCS3 derives from Grenville aged terranes (29%), with other significant

abundances of Gondwanan aged terranes (21%), as well as Appalachian aged terranes (19%). Significant peak ages for this sample include 400 Ma, 530 Ma, 600 Ma, 990 Ma, and 1070 Ma. Secondary age peaks of this sample include 215 Ma, 1180 Ma, 1400 Ma, 1730 Ma, and 2000 Ma.

Sample 256CCS2 contains a significant amount of Grenville aged grains (32%), with other significant amounts of grains from Appalachian (19%), Gondwanan (16%), and Midcontinent (16%) aged terranes. Prominent peak ages for this sample include 230 Ma, 380 Ma, 530 Ma, and 1030 Ma. Secondary peak ages for this sample include peaks at 470 Ma, 630 Ma, 800 Ma, 1110 Ma, 1170 Ma, and 1400 Ma.

Sample 256CCS1 shows the greatest abundance of grains from Grenville aged terranes (31%). Other distinct sources of grains include Appalachian aged terranes (22%) and Gondwanan aged terranes (19%). Prominent peak ages for this sample include 250 Ma, 400 Ma, 540 Ma, 600 Ma, 1030 Ma, and 1170 Ma. Smaller secondary peaks of ages 740 Ma, 1450 Ma, 1600 Ma, 1865 Ma, and 1930 Ma are also present.

Regional New Mexico Samples: S3, S4, S6, S7

Various samples from Dockum Group sediments in eastern New Mexico were collected for zircon radiometric analysis to see if any regional correlation exists with these lithostratigraphically equivalent strata and the two sections in west Texas (Figure 2). Sample S3 is a faintly laminated purplish-brown fine-grained sandstone from the base of the Travesser Formation in the Dry Cimmaron Valley of northeastern New Mexico, and sample S7 is a purplish faintly laminated fine-grained sandstone taken from the top of the Travesser at the same locality. The Travesser Formation is thought to be the youngest Dockum Formation strata present in southwest Laurentia (Lucas et al., 1987). Sample S4 is a trough

cross-laminated fine-grained tan sandstone of the Trujillo Formation taken from Romeroville Gap on I-25, in Las Vegas, New Mexico. Sample S6 is a fine-grained laminated tan lacustrine mudstone of the Redonda Formation at Trujillo Hill, New Mexico.

Samples S3 and S7 record the Travesser Formation in far northeastern New Mexico, and reflect broadly similar zircon sources. Sample S3 shows a dominant abundance of grains spread from Appalachian aged terranes and Gondwanan aged terranes (both 21%) to Grenville aged terranes (26%). Prominent age peaks on the KDE of sample S3 are 450 Ma, 620 Ma, and 1030 Ma. Secondary peaks of this sample include 920 Ma, 1150 Ma, 1340 Ma, 1450 Ma, 1680 Ma, 1820 Ma, 1980 Ma, and 2710 Ma. Sample S7 contains grains primarily from Grenville aged terranes (35%), with other abundant sources of Midcontinent (19%), Gondwanan (18%), and Appalachian aged terranes (16%). Prominent age peaks for sample S7 include 420 Ma, 610 Ma, and 1070 Ma. Minor age peaks are present at 215 Ma, 1150 Ma, 1220 Ma, 1380 Ma, 1470 Ma, 1760 Ma, 1980 Ma, and 2720 Ma.

Sample S4 Shows a dominant abundance of grains from Gondwanan aged terranes (27%), as well as a significant amount of grains derived from Grenville aged terranes (25%). Appalachian aged terranes also have a high abundance of grains in this sample (19%). Prominent peak ages for sample S4 include peaks at 410 Ma, 620 Ma, and 1050 Ma. Other secondary peaks include 260 Ma, 550 Ma, 720 Ma, 1000 Ma, 1175 Ma, 1430 Ma, 1740 Ma, 1850 Ma, 1980 Ma, and 2080 Ma.

The most abundant age range for grains in sample S6 are Grenvillian (29 %). Other significant sources include Appalachian (18%) and Gondwanan aged terranes (17%). Prominent age peaks of sample S6 include 250 Ma, 525 Ma, 610 Ma, 1020 Ma, and 1100 Ma. Secondary peak ages are present at ages 380 Ma, 810 Ma, 1375 Ma, 1780 Ma, 2010 Ma,

2300 Ma, and 2670 Ma.

Sample S7 contains grains primarily from Grenville aged terranes (35%), with other abundant sources of Midcontinent (19%), Gondwanan (18%), and Appalachian aged terranes (16%). Prominent age peaks for sample S7 include 420 Ma, 610 Ma, and 1070 Ma. Minor age peaks are present at 215 Ma, 1150 Ma, 1220 Ma, 1380 Ma, 1470 Ma, 1760 Ma, 1980 Ma, and 2720 Ma.

Statistical Results

Statistical analyses compare local and regional variability or likeness within samples using population distributions (Figure 7, Figure 8, Figure 9, and Figure 10). These results allow for better interpretation of provenance and potential drainage patterns between samples analyzed. The results of these statistical tests are shown in the following figures, and interpretations in following sections.

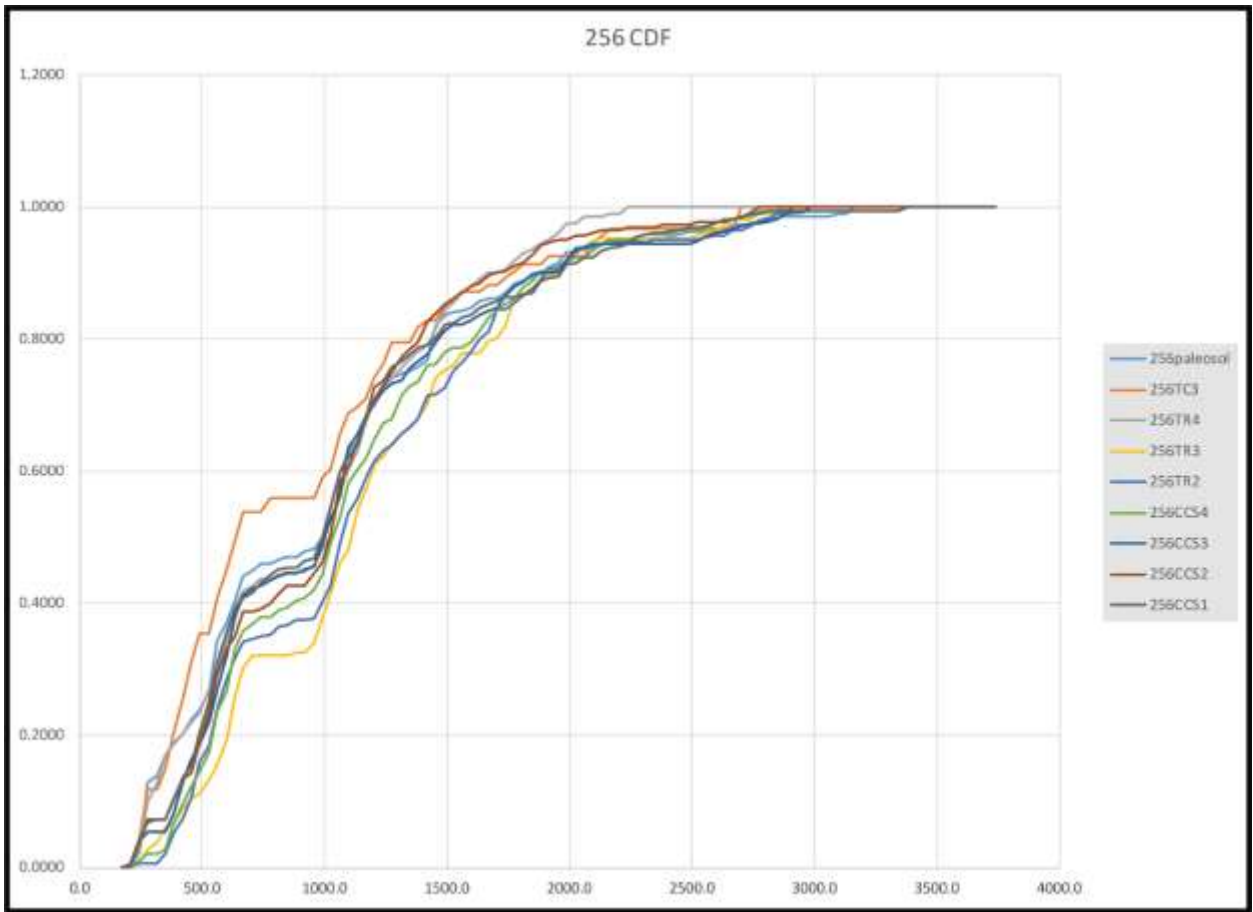


Figure 8. Cumulative Density Function of Highway 256 samples. Y-axis values represent the probability that a zircon will be younger than the corresponding x-axis value (in Ma).

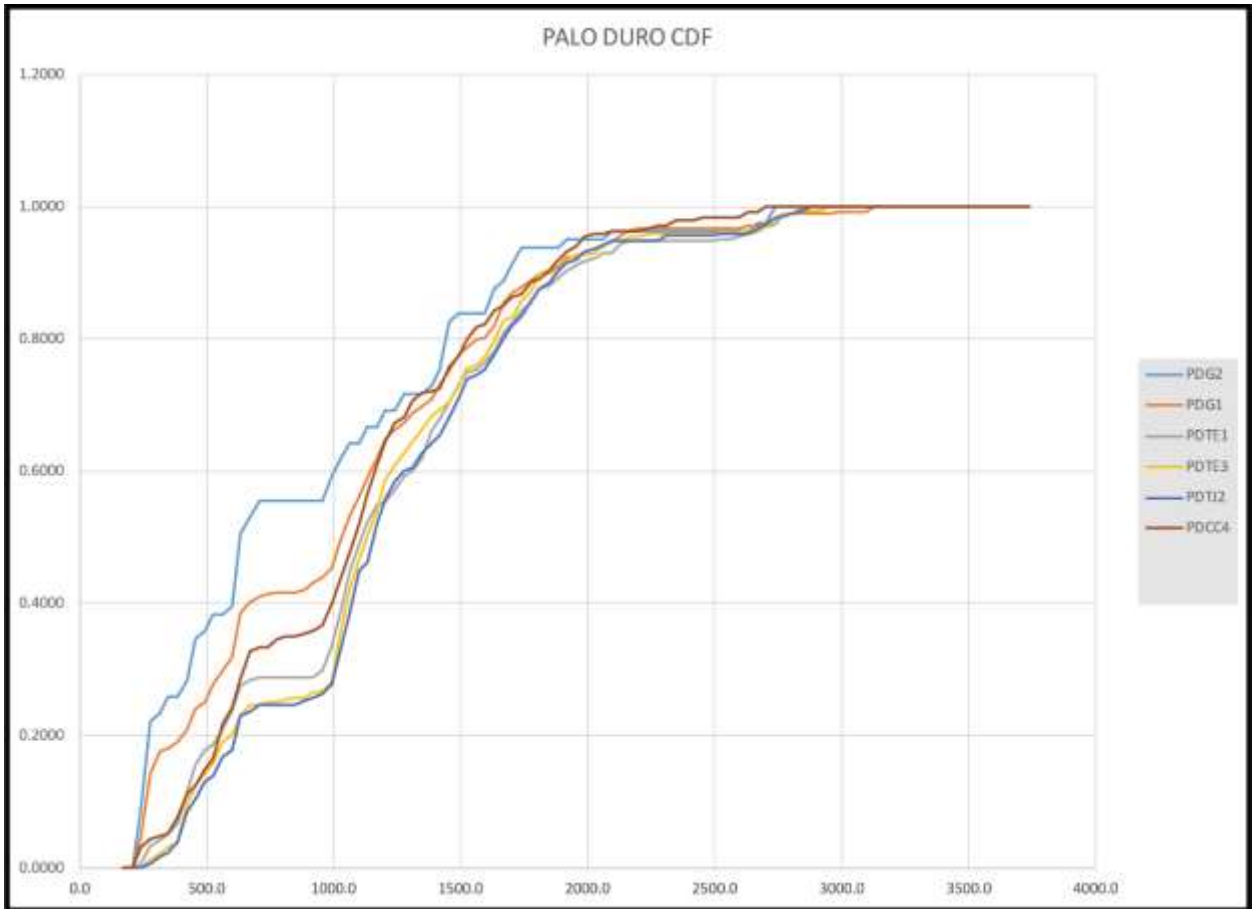


Figure 9. Cumulative Density Function of Palo Duro samples. Y-axis values represent the probability that a zircon will be younger than the corresponding x-axis value (in Ma).

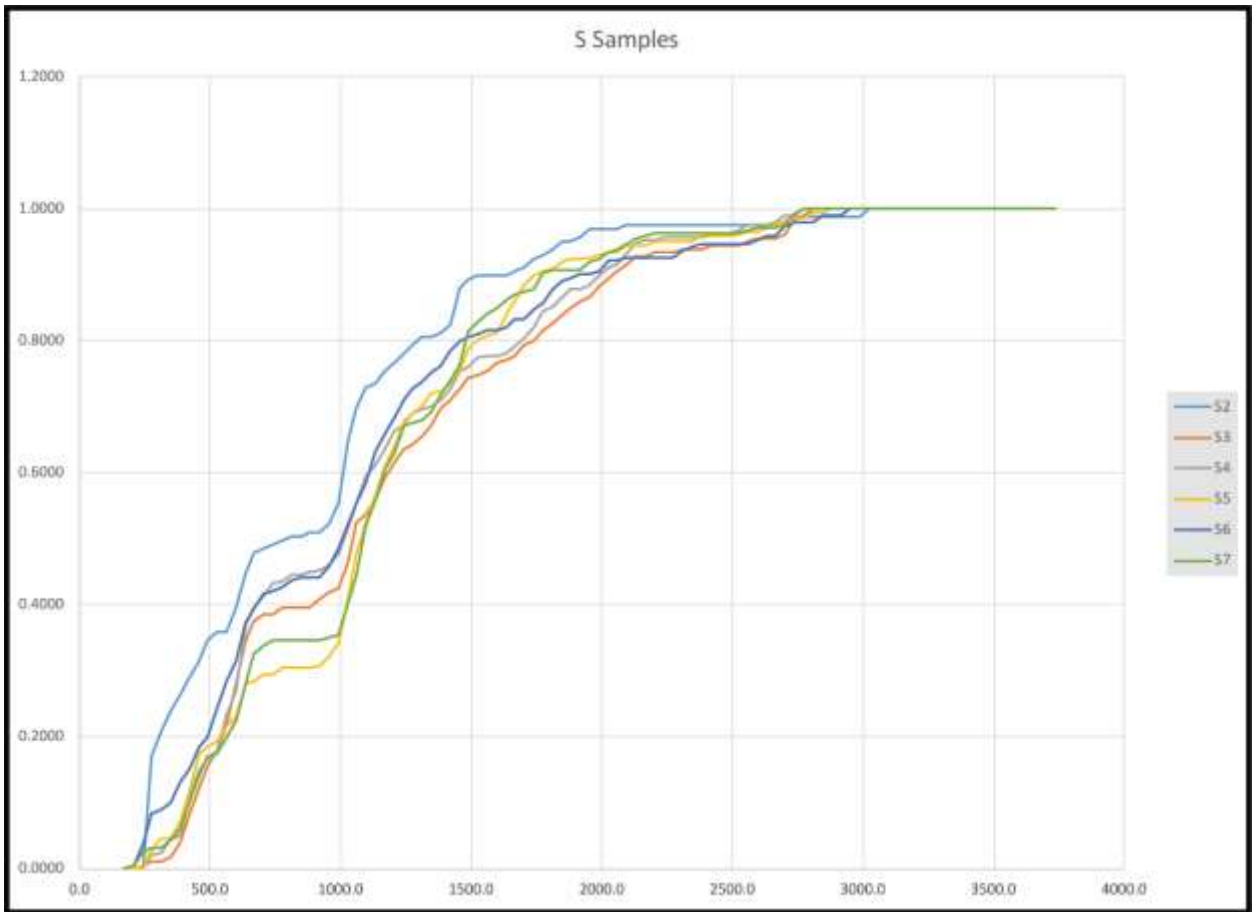


Figure 10. Cumulative Density Function of Santa Rosa Formation and regional samples. Y-axis values represent the probability that a zircon will be younger than the corresponding x-axis value (in Ma).

Lithofacies and Architecture of the Santa Rosa Formation

Lithofacies

Lithofacies and lithofacies associations are defined for the Santa Rosa Formation from two measured sections compiled for a complete stratigraphic section of the Santa Rosa Sandstone in the type area of Santa Rosa, NM (Figure 12). Nine lithofacies were identified and interpreted in this composite stratigraphic section, based on lithofacies principles of Miall (1996). Lithofacies were distinguished predominately based on composition and sedimentary structure (Table 2).

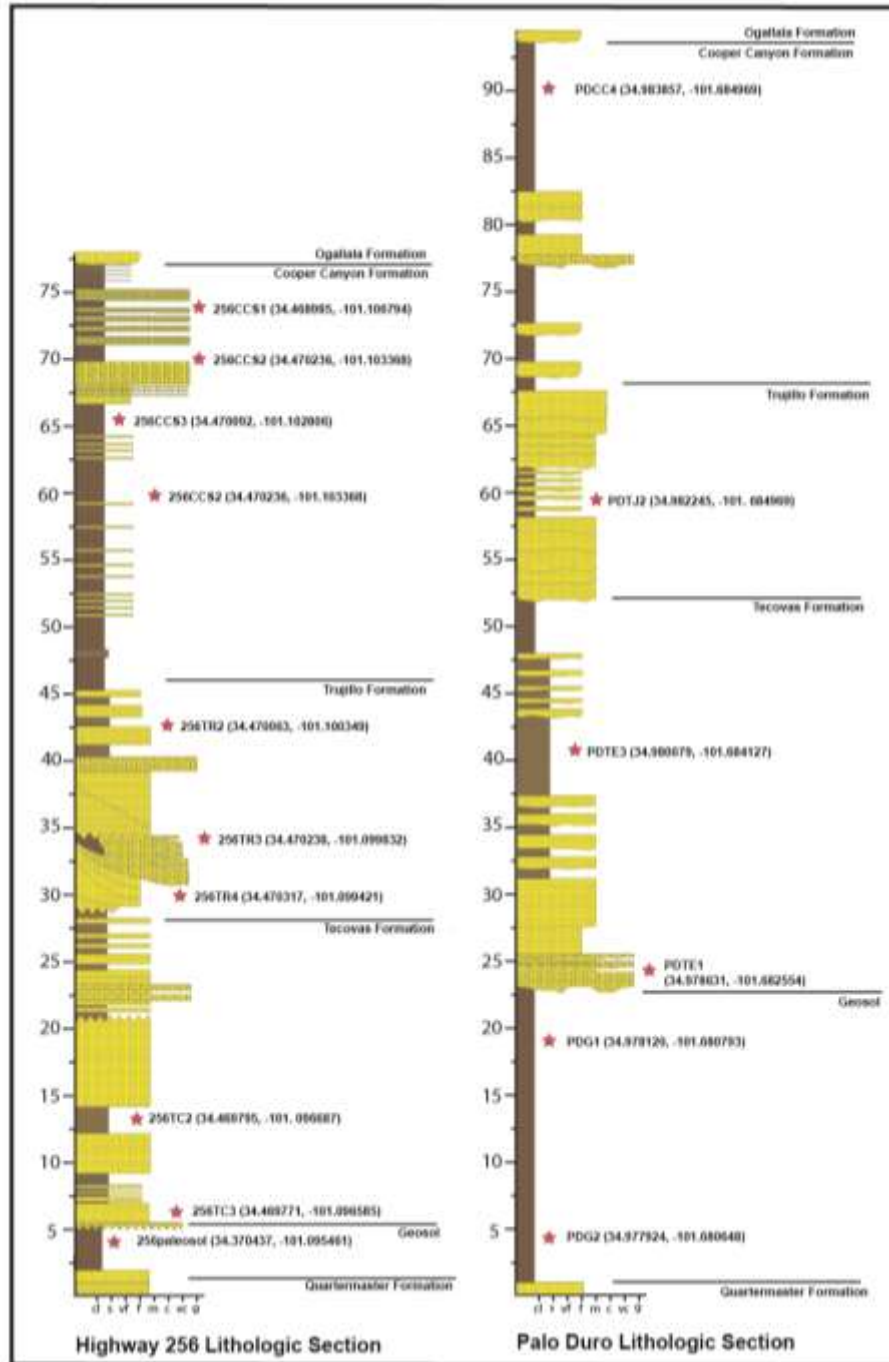


Figure 11. Lithologic section of Palo Duro and Highway 256, redrafted from Lamb (2019) and Skaleski (pers. comm). Latitude and longitude coordinates are located to the right of each sample star in the figure.

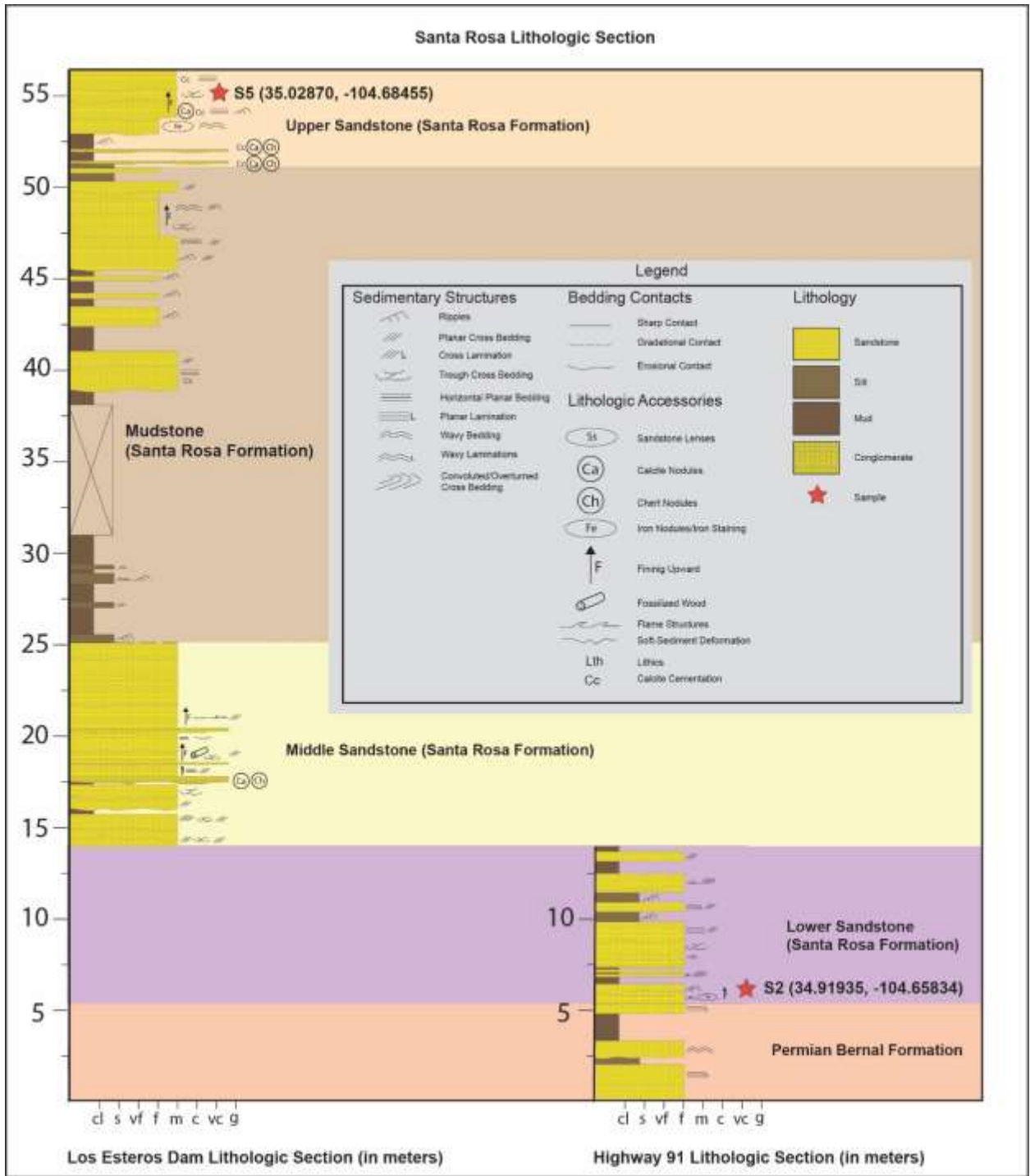


Figure 12. Composite lithologic section of the Santa Rosa Formation at Highway 91 and Los Esteros Dam. Latitude and longitude coordinates are located to the right of each sample star in the figure.

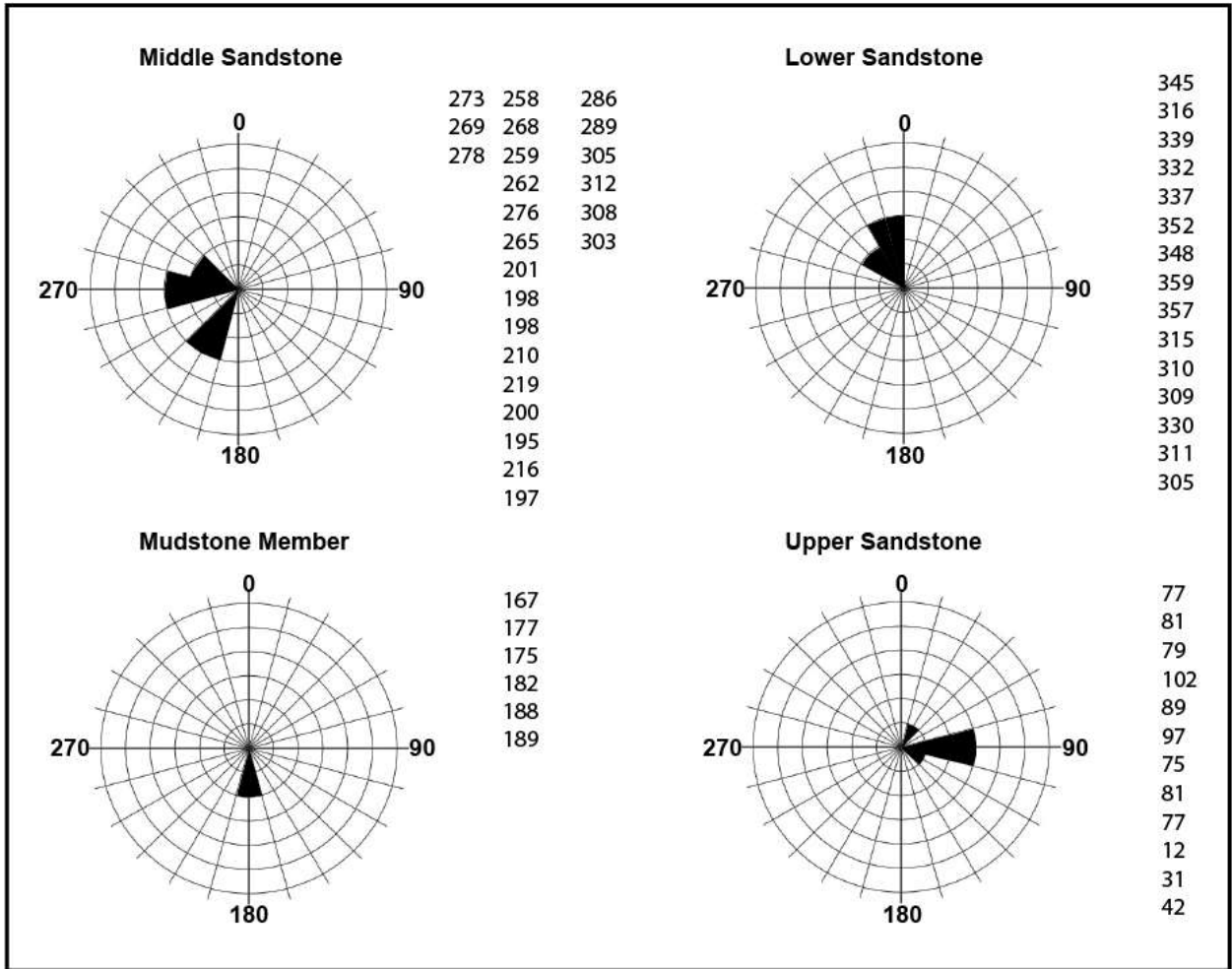


Figure 13. Paleocurrent readings of each informal unit of the Santa Rosa Formation in Santa Rosa, NM. Paleocurrents were taken from 1st order sedimentary structures identified in the field. Numbers to the right of each figure represent an individual measurement of the paleocurrent trend.

Architectural Analysis Results

Code	Lithofacies	Structure	Texture/Composition	Thickness	Other Features	Geometry	Interpretation
G _h	Pebble-Sized conglomerat	Thin-bedded, cross stratified to Massive.	Pebble sized clast-supported extrabasinal (chert/calcite) conglomerates. Clasts are subrounded to subangular. Dark brown color.	0.1 m – 0.5 m	Some imbrication present. Calcite cemented in top sandstone unit.	Erosive, tabular	Bedload deposition in highly concentrated and erosive sediment flows. Incipient channel formation. Typically found in the braided stream facies associations common in the middle and lower sandstone units of the Santa Rosa Formation, more specifically in elements such as CFB, CFF, and DA (Table 3).
S _r	Laminated sandstone	Thin-bedded. Parallel lamination, wavy laminations.	Fine-grained, well-sorted, laminated sandstone. Parallel to wavy laminations. QFR 80/20/0. Beds fine upwards. Dark red to faint purple.	0.1 to 1 m	Calcite cemented in top sandstone unit.	Planar to sheet-like	Upper plane deposition in upper flow conditions. This lithofacies is typically found in upper flow regime deposits, such as elements UPM and SS. It is also a minor component of braided channel fill elements such as CFF and CFB.
S _p	Small-scale laminated sandstone	Thin to thick-bedded, trough and planar cross-bedding. Cross lamination.	Medium-grained purple sandstone. Interbedded with thin mudstone beds. QFR 50/50/0. Moderately sorted. Subangular to subrounded grains. .	0.3 m – 2 m	Contains white fine-grained sandstone lenses at the base. Fines upward into finer grained material. Beds are locally discontinuous. Convoluted bedding present.	Lenticular, Interbedded with inclined sandstone bodies.	Migrating, sinuous and straight crested dunes or bars in lower flow regime conditions. Lithofacies S _{ma} is found in subcritical, migrating, and sinuous fluvial dune forms common to fluvial elements such as channel fills and sheet elements described in Table 3.
S _p	Large-scale, planar cross-bedded Sandstone	Thick-bedded, planar cross-bedding	Light grey to brown medium-grained sandstone. Well-sorted and well-rounded to subangular Quartzarenite.	1- 3.5 m	Well-indurated. Convoluted bedding. Feeding trace burrows present.	Lens, concave-up,	Migrating, straight crested dunes or bars in lower flow conditions. Longitudinal or transverse bars. These elements are commonly seen in accretion elements such as DA and LA.
S _t	Large-scale trough-cross-bedded Sandstone	Thick-bedded, trough cross-bedding. Beds are .5 m to 2 m.	Yellowish –brown medium-grained sandstone. Quartzarenite. Well-sorted, subangular grains.	2 m – 4 m	Tangential contacts at bounding surface. Bedding thins upward.	Lens, concave-up	Migrating, sinuous crested dunes or bars in lower flow conditions. Longitudinal or transverse bars. These elements are commonly seen in accretion elements such as DA and LA which are typical of the braided stream deposits of the Santa Rosa Formation.
S _t	Rippled sandstone	Thin-bedded, wavy ripples.	Grey rippled very fine-grained sandstone. QFR 60/30/10.	.3 m – 1 m	Asymmetrical ripples. Beds locally discontinuous. Thin limestone nodules locally present.	Lenticular to tabular and sheetlike. locally discontinuous.	Downstream migration of asymmetrical ripples in low flow, slow sedimentation conditions. This lithofacies is often associated with fluvial environments such as the overbank channelized deposits of the Santa Rosa Formation (element CFF), as well as sheetflow deposits (element SS).
S _r	Silt, rippled	Thin-bedded, wavy, current ripples.	Dark purple, wavy rippled silt. Interbedded with S _{ma} . Well-sorted. Grains subangular to subrounded.	0.2 m – 0.6 m	Interbedded with inclined sandstone. Locally discontinuous	Lenticular, planar	Deposition during decelerating low flow regime conditions on top of bar deposits. Drape-like deposits. Typical of subcritical flow deposits seen in the overbank environments of the Santa Rosa Formation, but also seen in accretionary elements of associated with braided fluvial environments commonly seen in the Santa Rosa Formation.
S _m	Massive Mudstone	Thin to thick-bedded, massive, no stratification	Massive mudstone, minor faint lamination. Brown and grey in color.	0.5- 5 m	No internal structure. Locally Micaceous. Bioturbated, with Rooting present	Tabular	Overbank deposition of suspended fines on the floodplain with weak paleosol development. This lithofacies is seen in overbank environments of the Santa Rosa Formation with slow sedimentation rates. This lithofacies is mostly associated with Element OF.

Table 3. Lithofacies

Element	Lithofacies Association	Description (geometry, bounding surfaces)	Interpretation
Braided Channel Fill- CFb	Fluvial Channel: G _h S _p S _r	Predominately cross-bedded, medium-grained sandstone. Often amalgamated ribbon to lenticular geometries. Bounded by 5 th order surfaces at the base. Often topped by macroscale barforms, or incision of other channel elements. 3 rd order surfaces composite to form boundaries. A common stacking trend of element CFb is conglomerates at the base of the channel (lithofacies Gx), grading up into small-scale cross-bedded sandstone (Sma) and into laminated and rippled sandstones at the top of channel forms (lithofacies Sff and Sfr).	Anabranch hannels within a low-sinuosity, braided river system that show high amalgamation rates. Channel bases contain small scale 3D sinuous dune fields.
Floodplain Channel fill- CFF	Floodplain Channel Fill: G _h S _p S _r S _r	Predominantly cross-bedded, sandstone. Common ribbon to tabular geometries. Channel fills are bounded by 4 th order surfaces and often capped by overbank elements. Lateral trending 2 nd order surfaces with little abundance of 3 rd order surfaces. The dominant lithofacies is Sfr, as rippled sandstone is seen throughout the mudstone member of the Santa Rosa Formation.	Confined subcritical fluvial channels deposited on an alluvial plain.
Downstream Accretion -DA	Fluvial Bar: G _h S _p S _t S _r	Cross-bedded sandstone. Lenticular to planar sigmoidal amalgamated geometries with concave-up bases and convex-up tops. Barforms that are bounded by 4 th order surfaces with common internal 3 rd order macroform geometries. Often incised by channel fill elements. Common large-scale sigmoidal 2 nd order surfaces. Downstream accreting barforms are commonly incised by channel-fill elements of CFb. Common to DA elements are large-scale 2 nd order surfaces that represent bar surfaces. This element typically has lenticular to planar amalgamated geometries with concave-up to planar bases and convex-up top bounding surfaces, representative of barforms.	Downstream accretion of longitudinal mid-channel bars in a braided stream with barforms trending in the direction of paleoflow.
Lateral Accretion -LA	Fluvial Bar G _h S _p S _t S _r	Cross-bedded sandstone. Lenticular to planar sigmoidal amalgamated geometries with concave-up bases and convex-up tops. Barforms that are bounded by 4 th order surfaces with common internal 3 rd order macroform geometries. Often incised by channel fill elements. This element is similar to downstream accreting (DA) elements, but differs in the typical perpendicular orientation of cross sets with regard to paleoflow. Similarly to DA elements, LA macroforms tend to fine upwards as a result of decreasing water depth, and large scale trough or planar sets tend to grade into ripple-dominated sands.	Lateral accretion of side-attached bars in a braided stream. Barforms trending oblique to direction of paleoflow
Scour Fill -SF	Fluvial Thalweg: G _h S _p	Medium-grained sandstone. Common conglomerate lags. Erosive nature creates concave-up bases that are associated with Channel fills and bounded at the base by 5 th order surfaces. Commonly overlain by channel fill elements.	Erosive cuts into channel bed representing a channel thalweg or confluence.
Upper Plane Macroforms- UPM	Fluvial Channel-to-Sheet: S _r	Medium to fine-grained sandstone. Sheet-like geometries. Predominant horizontal to slightly undulatory laminations. Bounded by 4 th order surfaces. Lack of high angle surfaces, with some 4 th order reactivation surfaces present.	Supercritical flash-flood events in shallow depth, laterally extensive channels migrating on floodplain.
Sand sheets- SS	Fluvial Sheet: S _{fl} S _{fr}	Medium to fine grained sandstone. Rippled to laminated. Beds are continuous to discontinuous. Bounded by 4 th order surfaces with multiple internal 3 rd order reactivation surfaces. Sand bodies are laterally extensive and sheet-like in geometry (>50 m)	Subcritical to supercritical flood events with deposition representing overbank flood events onto floodplains or laterally extensive shallow channels.
Overbank Fines -OF	Overbank Mudflat: F _b	Tabular to sheet-like bodies of clay-sized particles that show little to no stratification. Laterally extensive. Often intertongued with CFF. Bounded by planar to sharp bases. Often incised by Channel elements. Thickness ranges from 1 m to 20 m. Presence of paleosols is evidence of subaerial soil formation on elevated terrain, or on uninterrupted floodplain terrain with little evidence of flooding.	Floodplain deposits depositing clay-sized particles during waning flood stage events that have evidence of bioturbation. Paleosol development on elevated terrain.

Table 4. Architectural elements were identified in order to aide in determination of fluvial style and depositional environment.







	S_t
	S_r
	S_r
	S_p, S_{fl}
	S_t, S_p
	G_h

Table 5. Lithofacies of the Santa Rosa Formation.

Lower and Middle Sandstone member – Perennial Mixed Meandering and Braided Fluvial System

Both the lower and middle sandstone units of the Santa Rosa Formation (named by Gorman and Robeck, 1946) are interpreted as deposits of perennial mixed braided and meandering fluvial systems. They show predominant amalgamated bar-generated elements, as well as repeated fining-upward sequences consistent with braided and/or meandering rivers, but generally lack of overbank-generated elements. These are consistent with both meandering and braided fluvial systems (Miall, 1996). The main architectural elements seen in this environment are small amalgamated laterally accreting and downstream bars, larger lateral accretion elements forming point bars, scour fill elements, as well as overbank fines. Figure 18 shows the typical fining-upward sequence of a bar element capped by either upper-plane bed or subcritical ripple deposition. 5th order surfaces mark the bases of channels, and are highly amalgamated within the middle sandstone member. Large LA elements with consistent accretion direction are typical of point bars and the smaller amalgamated LA elements with multiple accretion directions are more typical of deposition from midchannel bars (Bridge, 2003; Holbrook and Allen, 2021).

The lower sandstone member is not as pronounced in thickness as the middle member in Santa Rosa, but still shows a similar architecture. This mixed perennial braided and meandering fluvial is similarly reflected in element preservation, though in a differing flow direction. The mobility of these braided channels caused erosion of overbank fines that may have accumulated on floodplains. Any overbank deposition preserved is modified into soil throughout both members.

These upper and lower sandstone members also contrast with overlying Dockum

sediments in west Texas, The Dockum rivers were much more upper-flow regime and ephemeral (see following sections). Abundance of bar elements with second order accretion sets with lower flow regime structures and lack of desiccation features is typical of midchannel and lateral lower-flow regime bars from perennial channelized flow (Wakefield et al., 2015). Bar size is relatively constant, especially in the upper reaches of the middle sandstone unit.

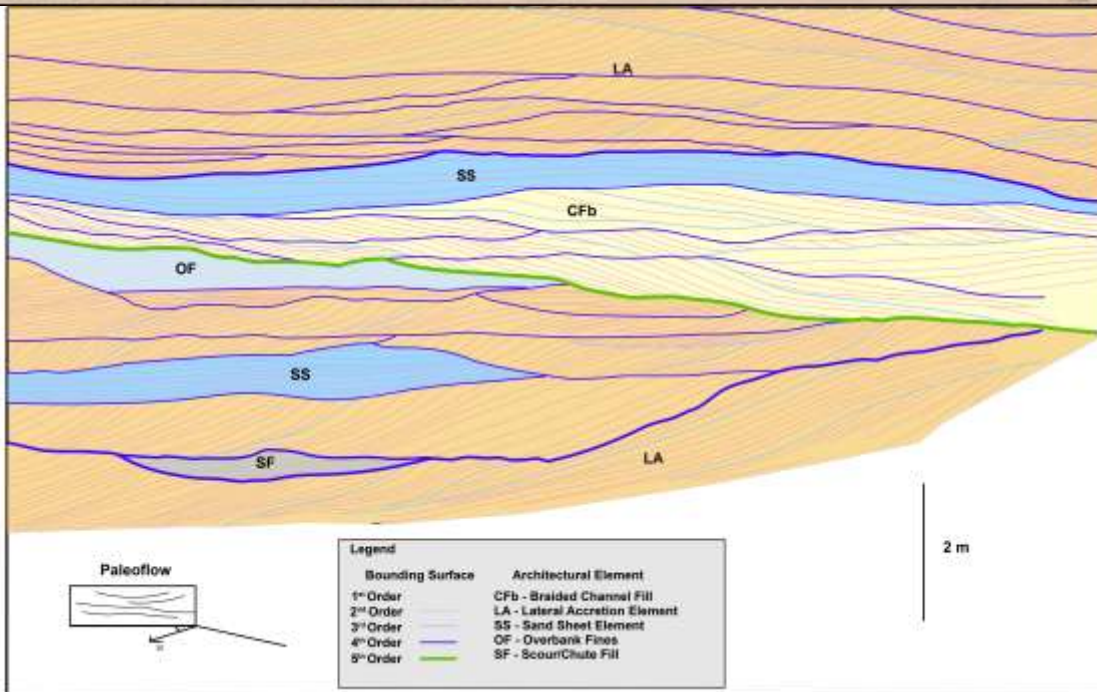


Figure 14. Architectural Analysis of the Middle Sandstone Unit at the channel fill (5th order) scale. Elements are distinguished by color. Cfb, Braided Channel Fill = light yellow. LA, Lateral Accretion = dark yellow. OF, Overbank Fines = blue. SF, Scour/Chute Fill = grey. SS, Sand Sheets, dark blue.



Figure 15. Architecture of the Middle Sandstone. Paleoflow to the left of the figure.

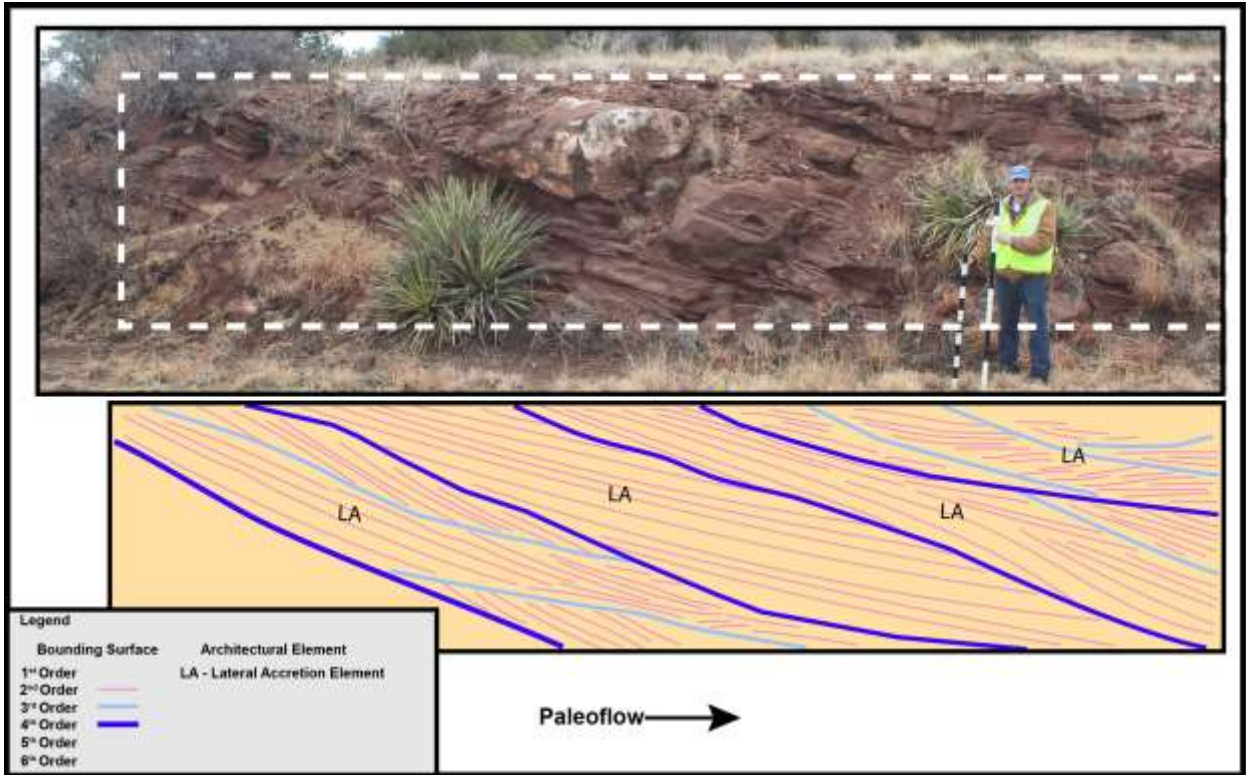


Figure 16. Architectural Analysis of the Lower Sandstone Unit at the channel fill scale. Elements are distinguished by color. LA = Lateral Accretion

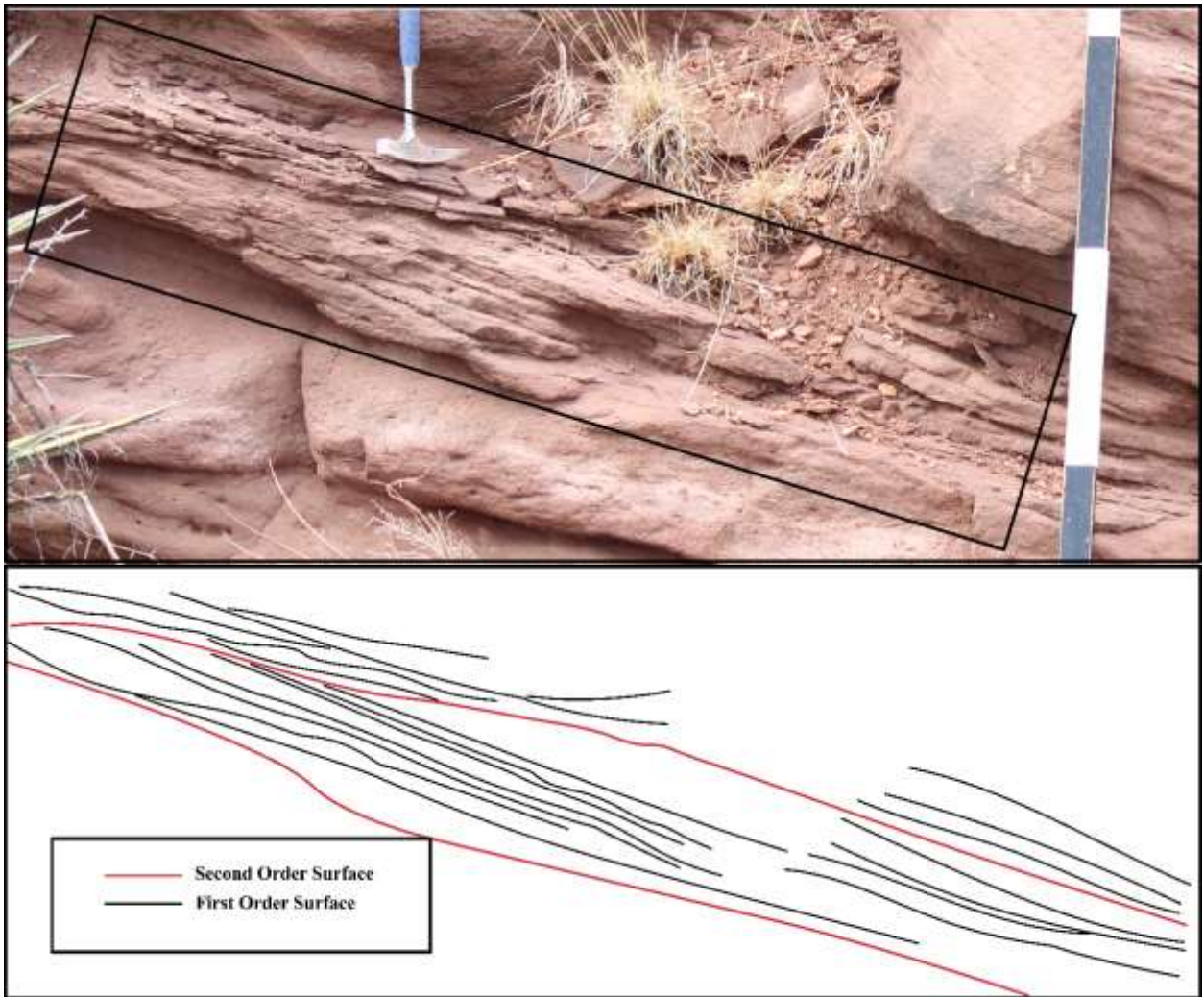


Figure 17. Architecture of the Lower Sandstone from the same section and LA elements as Figure 16. Paleoflow to the right.

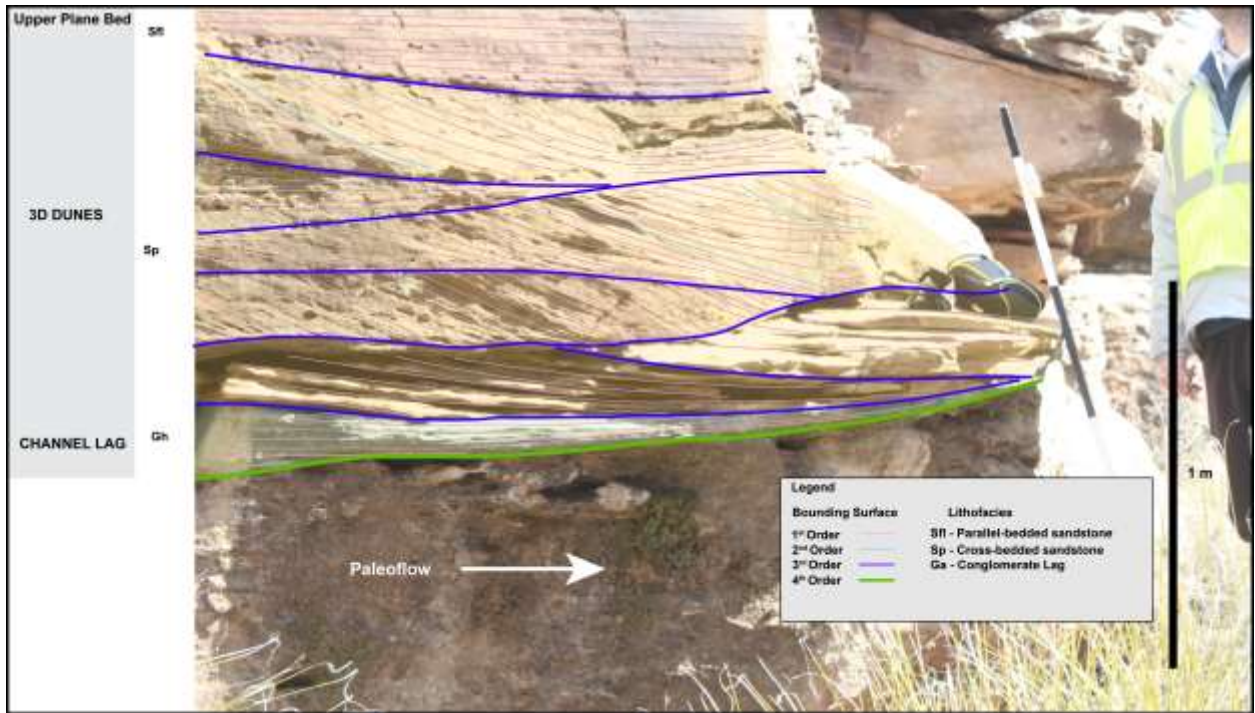


Figure 18. Typical upward-fining sequence of the Middle Sandstone Unit of the Santa Rosa Formation

Mudstone unit – Santa Rosa Fm - Floodbasin.

The mudstone unit, overlying the middle sandstone unit, and underlying the upper sandstone unit, is interpreted as a distal floodplain environment. The major architectural elements that define this environment are OF, overbank fines, as well as CFF, floodplain channels. OF elements are thick, laterally extensive fine-grained deposits bounded by 4th order surfaces that represent overbank mudflat deposition during waning flood stages. The amount of bioturbation and lack of laminated lacustrine sediments in this mudstone unit signifies that the floodplain was subaerially exposed and vegetated for extended periods of time, but not deflated regularly by wind erosion. Thin, subcritical channels deposited at the base of the unit are probably a result of minor flood events or minor distal splay events, with dominant ripple lithofacies and southerly flowing paleocurrents. Sand intervals increase in abundance and thickness towards the upper reaches of the unit, and are mostly single channel

fills of CFf that are encased with OF elements. The decrease of fining-upward small-scale single channel fills from the base to the middle of the unit probably represents the gradual loss of channel intrusion into the floodplain, with the channel source being situated the farthest away in the finest intervals. Thicker CFf elements (Figure 20) are interpreted as being closer to channel margins, as bedload grain size and the amount of lithofacies Gh tends to increase deposition closer to channel margins (Miall, 1996; Bridge, 2003). Overall, the abundance of thick, fine-grained deposits and subcritical, thin, single story fine-grained channels points to deposition on relatively low-energy distal floodplain, away from trunk channels, with minor single-story splay elements isolated within the mudstone unit (Miall, 1996).

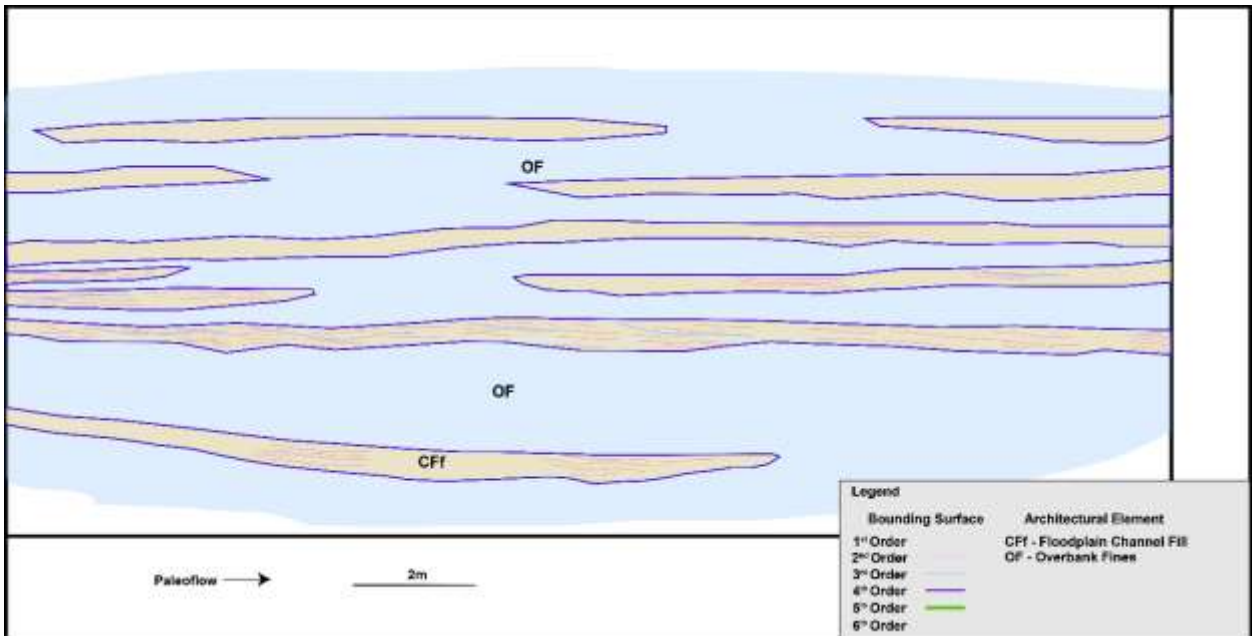


Figure 19. Architectural analysis of the Mudstone Unit near the contact with the middle sandstone unit. Elements are distinguished by color. CFf, Floodplain Channel Fill = light yellow. OF, Overbank Fines = blue.

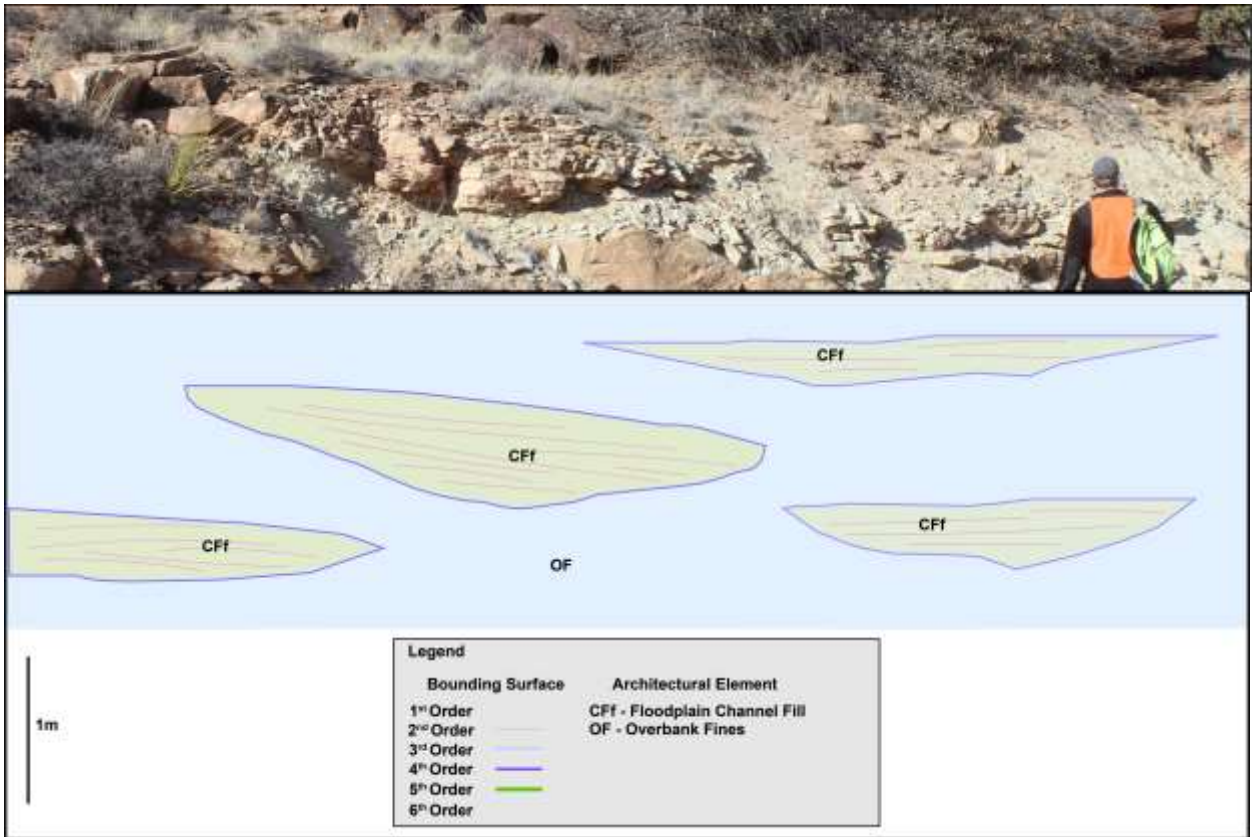


Figure 20. Architectural analysis of the mudstone unit, showing single channel fills. Elements are distinguished by color. Cff, Floodplain Channel Fill = light yellow. OF, Overbank Fines = blue.

FA2 – Ephemeral Sheet Channel Fluvial System – upper sandstone unit – Santa Rosa Fm

The youngest unit of the Santa Rosa Formation, the upper sandstone unit, shows a dominant ephemeral sheet-like channel fluvial system. This model is characterized by high velocity, episodic discharge on an alluvial plain during seasonal flood events, with runoff not sufficiently steady enough to generate the deeper and more narrow channels and well as well-developed bars typical of the lower and middle sandstone unit (Miall, 1996). The dominant architectural elements seen are wide and thin upper-plane-bed macroforms (UPM), Scour Fills (SF), and ripple-dominated sand sheets (SS). Deposition of the sands were in broad, unconfined channels active during flood events. These flood events occur in different orientations, and are marked by the abundant 3rd order-bound channel fill surfaces seen in

the upper sandstone unit. These surfaces were a result of seasonal ephemeral flow. This is in contrast to the lower-flow regime large-scale dunes and bars formed by consistent flow observed in the middle sandstone unit. The abundance of upper-plane-bed deposition is evidence for dominance of upper-flow regime stages in peak flow, with waning flow represented by subcritical dune. Wide and shallow scour fills formed during flood initiation that gave way to upper-plane bedforms, and in some cases DA elements, recording transverse unit bars (Figures 21 and 22). Element SS is similar to element UPM, but contains lower-flow-regime subcritical bedforms. This is interpreted to record different flood events of variable energy, preserving both subcritical dunes and the upper plane sheets that commonly erased lower flow regime bedforms during flood events. Overall, the upper sandstone member represents an ephemeral, unconfined sheetflood fluvial system marked by broad, sheet-like sandstone deposits with predominant upper-plane-bed deposition. Channel initiation is evident where scour fills are present. When flow energy waned, subcritical dune formation initiated but was commonly eroded by higher velocity flows.

There are many similar sheet-flood environments discussed in literature, particularly in Triassic deposits across Pangea (Meadows and Beach, 1993; Bordy et al., 2004; Horn et al., 2017). The ephemeral deposits identified in Santa Rosa are similar to the flash flood deposits of the Dockum Group in west Texas (Lamb, 2019; Walker, 2020), with the exception of the abundance of preserved antidune and higher Froude sedimentary structures, which are more common in the Dockum Group of west Texas, but not seen in Santa Rosa deposits abundantly.

The shift from the middle to the upper sandstone member records a fundamental shift in climate conditions for the Triassic that persists into Late Triassic Dockum deposition. The

upper sandstone member is overlain by Dockum/Chinle Formation deposits that similarly record ephemeral conditions. The lower and middle sandstone record deposition from more perennial rivers and less discharge variation (Plink-Björklund, 2015). The climate shift from more humid to arid conditions between the middle and upper Santa Rosa deposition has implications on the climate record of the east of the Rockies in the Triassic Period.

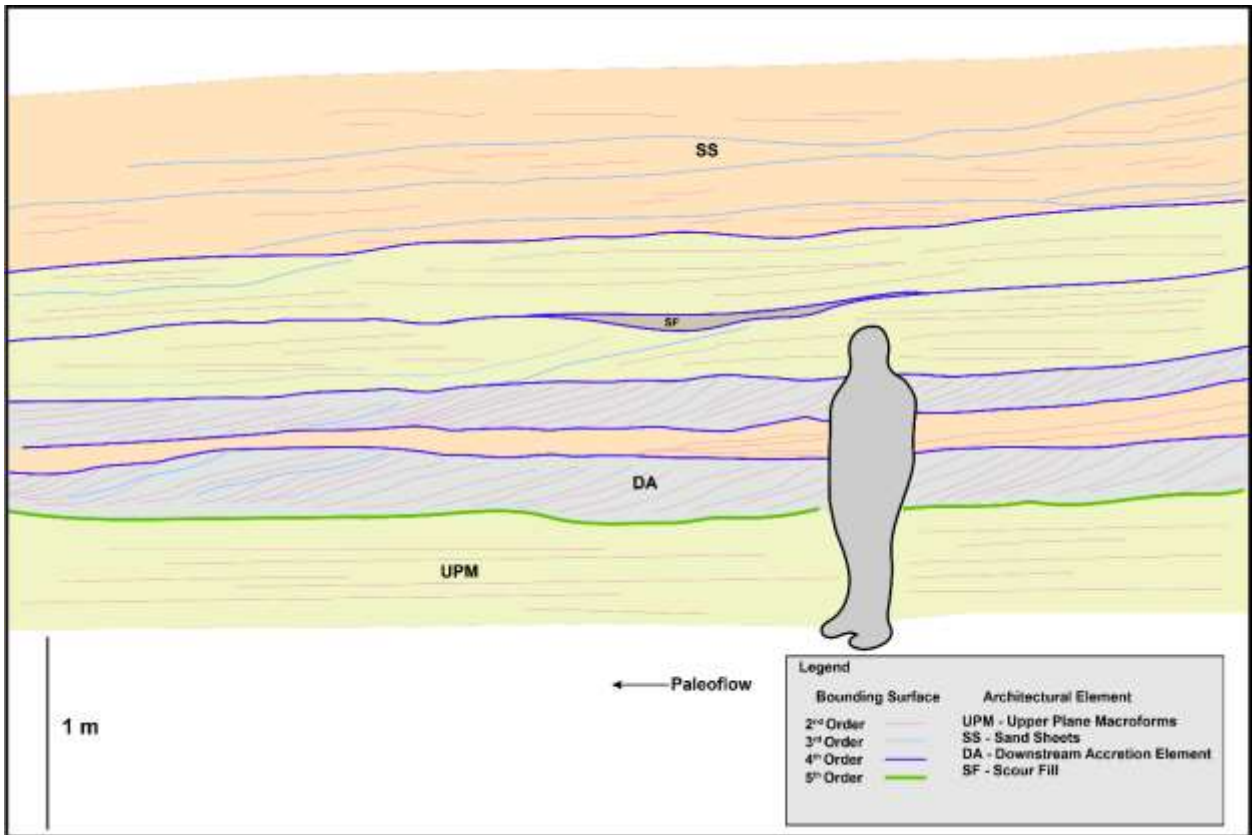


Figure 21. Architectural analysis of the Upper Sandstone Unit showing more ephemeral conditions. Elements are distinguished by color. UPM, Upper Plane Macroforms = yellow. SS, Sand Sheets = orange. DA, Downstream Accretion = blue. SF, Scour Fill = grey.

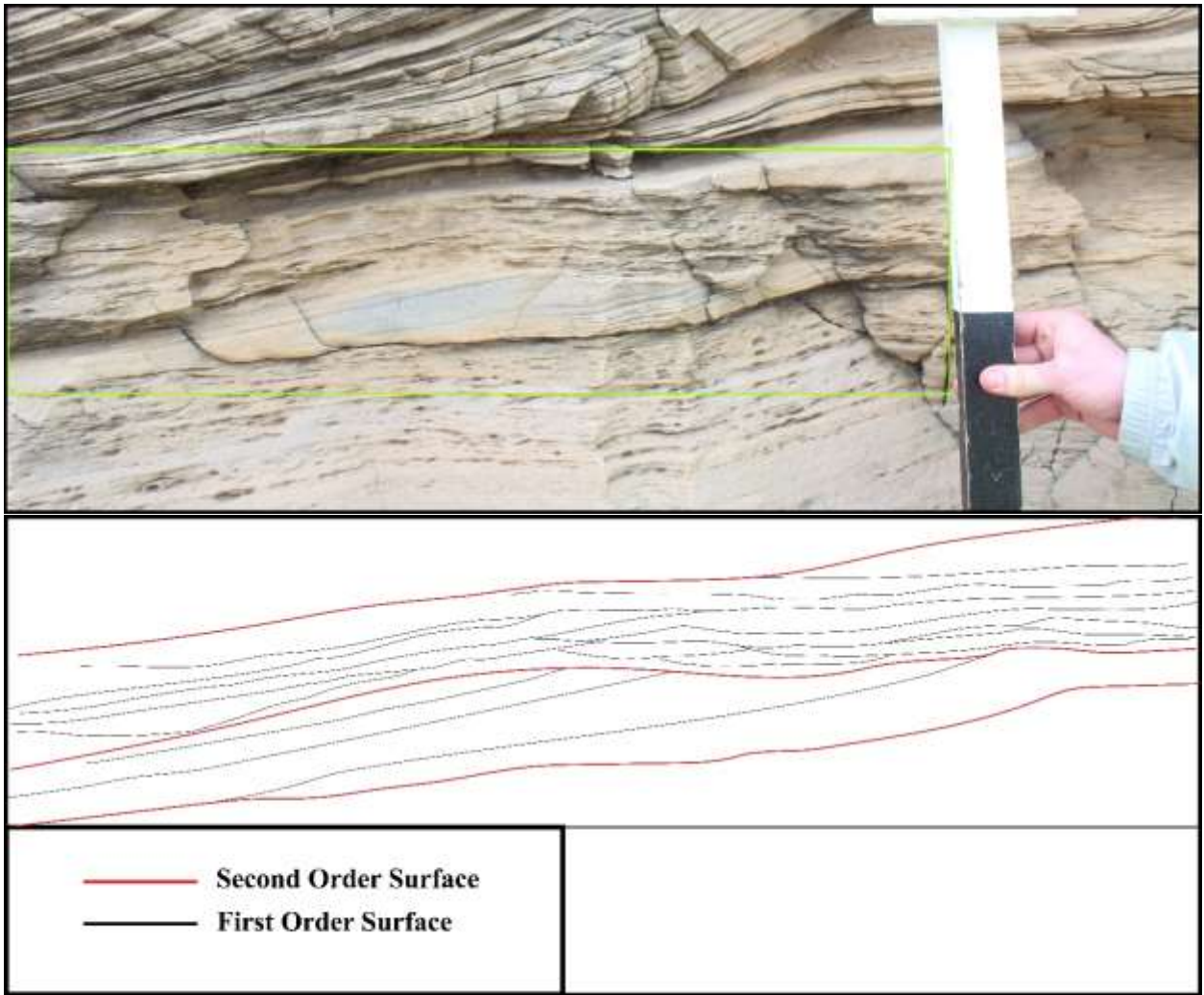


Figure 22. Architecture of the Upper Sandstone showing upper-plane deposition. Paleoflow to the left.

Paleochannel Conditions of the Middle Sandstone Member

Distinctive fluvial architectural and paleochannel characteristics of the middle sandstone member, and to a lesser extent the lower sandstone member, contrast with recent studies of Dockum Group deposits in west Texas (Lamb, 2019; Walker, 2020). One striking difference in the architecture of the Santa Rosa Formation is the height of 2nd order bar accretion surfaces bounded by 4th order macroform surfaces that represent interchannel transverse bar forms. Average thicknesses of these bars ranged from 1.7 m (n=6) in the lower strata of the middle sandstone unit to 0.76 m (n=8) in the upper strata of the middle

sandstone unit, with an overall average dune height of 1.358 m. True average bar thicknesses may be higher due to the erosive and amalgamated nature of the fluvial system, so these are minimum bar thicknesses. Based on these averages, paleochannel bankfull depth was at least 1.4 m on average (e.g., Bridge and Tye, 2000; Holbrook and Wanas, 2014)

Another useful approximation of flow depth is thickness of unit bars. More recently, a study by Alexander et al. (2020) reveals slipfaces of transverse bars only portray approximately 30% of true bankfull deposits in flood sediments of the Missouri River. Using an estimation from Figure 23 of approximately 2.5 m for the foresets of unit bars, bankfull conditions could have easily been in excess of 7.5 meters for some of the larger channels.



Figure 23. Large-scale downstream accreting elements of the Middle Sandstone Unit, indicative of large transverse unit bars. Bars are over two meters, arguing the formative river was at least 2 m in depth, and more likely up to three times bankfull depth. (Alexander et al., 2020)

Depositional Model for the Santa Rosa Formation

The depositional trend of the Santa Rosa Formation evolves from a perennial mixed braided/meandering system to a highly variable system categorized by seasonal ephemeral streams in the youngest strata of the Santa Rosa Formation. This pattern of change over Santa Rosa deposition is expressed on the changes in architecture between ascending members.

Initiation of the Santa Rosa Formation started with deposition of the lower sandstone unit on top of Permian sediments, in northward flowing streams that show a perennial mixed braided/meandering pattern. These were large rivers on the order of seven meters deep. The major 250 Ma peak seen in provenance data of the lower sandstone unit is similar to the well-developed 250 Ma peak in the geosol seen in younger Dockum Group deposits (Figure 3, Figure 4). This geosol potentially records the upland landscape that was feeding lower sandstone drainages. These rivers with thick LA accretion sets that produced large-scale point bar deposits signify high paleowater discharge that was perennial in nature.

The middle sandstone unit was also deposited in mixed meandering/braided streams that had bankfull paleodepth estimates of well over two meters, based on large-scale 2nd order accretion surfaces. The fining-upward and amalgamated channel fills of the middle sandstone member point to a perennial braided-to-meandering system that had a low accommodation rate compared to sediment supply that promoted lateral and vertical amalgamation of sand bodies as well as the lack of preservation of overbank elements like floodplain muds and paleosols. Analysis of the barforms and bedforms, with dominant downstream and lateral accretion elements that dominant 2nd order large-scale bar surfaces show that the middle sandstone unit was deposited in perennial, high bedload, high discharge streams (Miall, 1996) . Water discharge, accommodation, and sediment supply was relatively

constant due to the lack of abundant reactivation surfaces recording bar exposure and reworking, as well as the thickness of 2nd order bar accretion surfaces arguing for high river depth and width (Miall, 1996; Holbrook and Wanas, 2014).

The mudstone unit was deposited in a low-energy fluvial floodplain that shows single-story, ribbon-like channel bodies encased in floodplain mud that was commonly pedogenically overprinted. These deposits represent an environment that was not adjacent to the main trunk channel, as the common ripple lithofacies and thin splay-like sand bodies represent deposition in a low-energy setting distal to the main channel. Channel sedimentation could not keep up with accommodation so the major lithology preserved is vertically aggraded floodplain mudstone, similar to mud-prone deposits of the Chinle Formation (Blakey and Gubitosa, 1984; Tanner, 2000; Hartley and Evenstar, 2018).

The upper sandstone unit was deposited in a highly seasonal, ephemeral fluvial setting prone to high discharge variability. In contrast to the previous fluvial units, the upper sandstone shows signs of episodic discharge with abundant 3rd order reactivation surfaces representing multiple flow events within channels. 5th order surfaces are not distinctly convex-up, as bars within channels were not well developed over continued perennial flow. Channel depths were shallow and wide hosting sheet flows, with bankfull channel estimates only measuring 2 to 4 meters in depth. Supercritical flow was abundant, with upper plane bedforms commonly seen in outcrop and antidunes locally.

Provenance for the Santa Rosa Group and Greater Dockum Group

Detrital Zircons and the Source of Dockum and Chinle Formation Sediments

Dockum rivers sourced from the Ouachita Mountains to the southeast and crossed Grenville basement on the way to deposition in the Palo Duro Basin. Grenville-aged grains

comprise the dominant source in a majority of samples, typically averaging between 25-35% of samples. The next most abundant grains source from Appalachian/Ouachita and Gondwanan terranes. The abundance of Grenville-aged grains, as well as significant abundances of Appalachian and Gondwanan-aged grains in most samples supports a general southeastern source terrane for the Dockum Group from the previously lifted Ouachita front. As significant is the low abundance of Midcontinent and Yavapai-Mazatzal grains, arguing sediment input from western, northern, or northeastern sources that must tap these basement provinces was minimal.

This supports Dickinson and Gehrels (2008) work which grouped Ouachita, Grenville, and Gondwanan sources into a single large and generally southeastern source area for both the Chinle Formation and the Dockum Group. Abundant Grenville-aged zircons in the down-dip Chinle Formation of the Colorado Plateau lead prior investigators to propose a continental-scale northwestern drainage flowing from a reactivated Ouachita front into back-arc basins of the Chinle Formation west of the Rocky Mountains (Riggs et al., 1996; Dickinson and Gehrels, 2008; Dickinson et al., 2010a; Dickinson, 2018). Equivalent Dockum sediments source from the Ouachita front as well. This also argues that the Chinle and Dockum Group source was the same, and supports earlier assertions arguing the Chinle and Dockum record a common continental drainage system. The sections below detail the trends in the source area at the formation level.

Late Triassic Volcanic Zircon Input Trends

The Tecovas and Trujillo Formations do not show the abundance of Late Triassic grains that the basal geosol or Cooper Canyon Formation preserve. During the Permian and Triassic Periods, two extant volcanic arc margins were present, and these overlap in volcanic

activity also existed at this time. The East Mexico Arc was active from around 300 Ma to 240 Ma (Wengler et al., 2019), and was located to the south to southeast of the Palo Duro Basin during the Permian and Triassic Periods. The other arc was the incipient Cordilleran Arc, which was considered to be volcanically active from 260 Ma to 200 Ma (Riggs et al., 2020). Prominent pulses of volcanic and plutonic origin are associated with the Cordilleran margin in western Pangea, such as at 220 Ma, as well as 250 Ma (Davis, 2019; Riggs et al., 2020). Volcanic activity was present, but not consistent with regard to the Cordilleran arc, as there were periods of waning or little volcanic activity within the rock record (Davis, 2019). Late Triassic zircon abundance in the Dockum Group could reflect volcanic input modulated by intermittency of arc-related volcanic ash sources. Alternatively, the variation in Triassic volcanic abundance could be lithological. Particularly, excess zircons in the geosol could be because well-developed paleosols record long-term subaerial landscapes, and may have better accumulated air-fall zircon grains sampled over a longer duration. Fine-grained overbank environments were sampled in all formations, however. Biases toward finer-grained environments do not appear to be the cause.

It is also feasible that wind transport could have been aided due to intense and highly seasonal monsoons that reversed wind patterns inland toward basins such as the Palo Duro Basin (Dubiel et al., 1991; Winguth and Winguth, 2013; Lamb, 2019). In this case, significant pulses of airfall deposits would have been prevalent in the basal and upper deposits, with the sand-dominant Tecovas and Trujillo Formations recording a waning phase of Cordilleran volcanism, and/or weakening monsoonal conditions. Since the Dockum Group was deposited in tropical latitudes (Dubiel et al., 1991), prevailing easterly winds should have blown ash westward and away from the Palo Duro area. Strong monsoons could reverse

these winds toward interior Dockum locations. The Tecovas, Trujillo, and Cooper Canyon Formations each are dominated by upper-flow-regime likely tied to megamonsoonal conditions (Walker and Holbrook, in press). Absence of monsoonal climate conditions during Tecovas and Trujillo time is not supported by this evidence. The hypothesis of a gap in volcanism at this time for the lack of zircons is thus preferred.

Another intriguing aspect of Kernel Density Estimate (KDE) signatures in the Cooper Canyon Formation is the spike in Permian-Triassic grains. Permian-Triassic grains generally are 6-7% more abundant than the abundance of the previous two formations. Triassic age peaks that are wholly Late Triassic (215 Ma, 220 Ma, 230 Ma) appear in the Cooper Canyon time that were not apparent in older samples collected from the Tecovas and Trujillo formations at the same locations. The only active arc within this Late Triassic time frame in the region of modern-day west Texas and eastern New Mexico is the Cordilleran Arc, as the East Mexico Arc became dormant just before the beginning of the Late Triassic (Dickinson and Gehrels, 2008; Barboza-Gudiño et al., 2010; Wengler et al., 2019). Therefore, it is interpreted that these signals are a result of volcanic aerosol input from the Cordilleran Arc. Multiple studies of Triassic deposits on the western Cordilleran margin show that there was a cessation of arc influence between 225-245 Ma from western sources of Chinle deposits, and that there is evidence that zircon input was not only detrital in origin but that plinian eruption events deposited ashes containing euhedral zircons into Chinle Formation basins (Riggs et al., 2003; Riggs et al., 2013; Riggs et al., 2020). This gap of volcanism in the rock record is also seen farther to the east in the Palo Duro Basin, and suggests that these eruptive events are temporally related and a result of aforementioned megamonsoonal circulation that persisted throughout Late Triassic time.

Zircon data from this study shows a regional trend of mudstone deposits with a high yield of Late Triassic grains in the younger strata as well as basal mudstone strata of the Dockum Group. This could point further to a regional imprint of megamonsoonal conditions in Late Triassic strata of the southwest, including the Dockum Group at the extreme end. Lithologic bias of elevated paleosols or undisturbed floodplain deposits remains to be studied fully in Late Triassic deposits, but data from this study points to an initial trend of preference towards mudstones that could signify a climatic or volcanic influence during the Late Triassic deposition of the Dockum Group and distal Chinle Formation.

The absence of Late Triassic grains in the Dockum Group argue Dockum deposition extends into the end of the Triassic Period. Abundant zircons of ~212 Ma in the Cooper Canyon argue deposition lasted at least until this time at the end of the Norian. Samples clustered about 220 Ma in the geosol argue the entire Dockum Group is younger and confined into the Late Norian. Further inspection of Dockum samples with laser ablation techniques and/or additional samples could further test this assertion.

The Anomalous 250 Ma peak

The prominent peak seen in the geosol samples of PDG1, PDG2, and 256paleosol at 250 Ma is also seen in the sample S2, which is a sample of the lower sandstone unit within the Santa Rosa Formation in Santa Rosa, New Mexico. This records the initiation of the Triassic Period. It is noteworthy that this peak is not seen in the uppermost Santa Rosa sample, with sample S5 containing a slight peak at 260 Ma. This peak could represent evidence that the regional geosol captured a Mesozoic volcanic source of this age. Paleosol deposits were prone to retaining a larger signature of these 250 Ma aged grains, and potentially record a regional elevated terrain starting at the beginning of the Triassic that

allowed ash falls to incorporate into long-lived soils of the landscape. An alternative is that this peak could signify a detrital source, but is highly unlikely due to these samples being in prominently well-defined paleosols. Lower Santa Rosa paleocurrents come from the south (Figure 13), and not directly from the same source area as Dockum Group sediments. Zircons stripped from these soils could have been incorporated into the Santa Rosa at this time. Sample S6, a distal sample farther west collected from the Redonda Lake Formation of the Dockum Group, equivalent to the Cooper Canyon Formation, contains a pronounced 250 Ma peak as well, arguing a periodic influx of sediment from these younger Mesozoic sources locally and later.

Similar provenance signatures are seen in the basal Shinarump Conglomerate west of the Rockies in the Chinle Formation (Dickinson and Gehrels, 2008). Pre-Shinarump paleosol formation is similar to Dockum Group paleosol formation, with well-developed paleosols developed on elevated interfluvial surfaces, often considered to be age equivalent to the age of the Shinarump Conglomerate deposited in the paleovalleys (Demko et al., 1998; Tanner, 2003). The presence of prominent age peaks around 250 Ma within Dockum and Chinle Formation deposits could be evidence that there was a much older landscape that encompassed a majority of southwest Laurentia physiographic surfaces during the Triassic Period, which was incorporated into overlying fluvial deposits during Late Triassic time.

Provenance Changes within the Santa Rosa Formation

Samples collected of the Santa Rosa Formation reveal a vertical shift in provenance during the duration of deposition. There is a stark contrast in signature in younger aged grains (<750 Ma) between the two initial samples. S2, at the base of the section, records a higher amount of these younger grains (51%) when compared to S5 (31%) at the top of the

section. An up-section shift is also apparent in the KDE (Figure 10), with age peak decreases in both Permian-Triassic aged grains and Gondwanan aged grains, as well as an increase in Appalachian aged grains. There is also an increase of 10% from S2 to S5 in Grenvillian grains. This increase in Grenvillian grains can be attributed to a change in source area reflected in paleocurrent data from south to more eastern sources, where Grenvillian aged terranes were most abundant flanking the Ouachita highlands. The Grenvillian and other southerly sourced grains are likely reworked from sediments above these basement terranes. They could theoretically come from reworked grains from northerly sources along the Ouachita front. The absence of Yavapai-Mazatzal and Mid-Continent grains argues against any northerly sourced rivers that could have crossed these terranes. Increases upward in Yavapai-Mazatzal ages can potentially be attributed to proximity of the basin to Yavapai-Mazatzal paleodrainages being temporally incorporated into Santa Rosa Formation. This increased incorporation of Yavapai-Mazatzal basement in the basal Santa Rosa was also noticed by (Dickinson et al., 2010b).

The decrease in Permian-Triassic grains upward from 19% in S2 to 3% in S5 could be a result of erosion of the prior exposed landscape that defined the region earlier in the Triassic, and incorporation of ashes collected in intervening soils developed over these Permo-Triassic formations. An alternative explanation is that these two samples correlate to similar signatures within the Dockum Group, with S2 resembling geosol signatures, and S5 recording an absence of Permian-Triassic grains similar to the Tecovas and Trujillo Formations. The latter is not likely, owing to the fact that no Late Triassic grains are found in any Santa Rosa sample, as well as prior investigations that place the Santa Rosa beneath Dockum units stratigraphically, and thus too young to capture reworked Dockum grains

(Darton, 1922; Gorman and Robeck, 1946; Lupe, 1977).

Sample S8 provides further indication that exposed landscape was eroded through time to incorporate a greater percentage of eastern-sourced grains, with a gradual shift from Permo-Triassic terranes to older Cambrian and Grenville aged terranes through time. This is in agreement with previous samples collected from the up dip sections in the Dockum Group.

Palo Duro Geosol

The geosol has a distinct and predominant age peak in all three of the samples at 250 Ma, distinguishing this unit from the overlying Dockum strata. The abundance of Permian-Triassic grains is also relatively prominent, ranging from 14-22% for the three samples. The remaining samples of the two sections produce an average of 5.3% of Permian-Triassic grains, with none showing the prominent Kernel Density Estimate (KDE) peaks of the geosol.

The age peaks of ~250 Ma show an abundance of grains of Early Triassic (Olenekian) age, which is situated just above the Permian-Triassic boundary (PTB) (251.9 Ma) within the rock record. This is at a time where Pangea was at its full equatorial extent across the paleoequator (Dubiel, 1994), and where monsoonal conditions were prevalent in western subtropical Pangea (Dubiel et al., 1991; Dubiel and Hasiotis, 2011; Winguth and Winguth, 2013). Models show that at this time, there was potential for extreme seasonal low pressure systems owing to the latent heat differentiation of the Pangean landmass. These penetrated inner Pangea during Chinle Formation deposition, and timed with extreme volcanism events that also could have promoted global-scale anoxia of oceans at the PTB (Winguth and Winguth, 2013). The East Mexico Arc was active at 250 Ma, but prevailing

monsoonal winds likely did not flow this far north. Also, the fact that the Ouachita thrust belt likely blocked any possibility for northerly flowing streams to incorporate sediment into the Palo Duro Basin making input from the East Mexico Arc not likely (Barboza-Gudiño et al., 2010). These volcanos could be a source of zircons in this part of the peak.

There is also a signature of Midcontinent and Yavapai-Mazatzal sources in the geosol samples. The Palo Duro Basin is situated within the Midcontinent Granite-Rhyolite Province during the Late Triassic and could have incorporated grains from these provinces, as these are rare in other deposits. The paleosol is not channel deposition and, given their strong horizonation, likely was well-drained and did not experience heavy accumulation from flooding. Derivation of Yavapai-Mazatzal terranes could be a result of eolian transport of grains from adjacent Yavapai-Mazatzal provinces to the north and northwest, or alternatively from transport reworking deposits from Midcontinent source areas. These would have accumulated over long durations and integrated by reworking into a stable paleosol, but not necessarily preserve in actively accumulating fluvial strata, particularly if these rivers did not source from these terrains at that time. The volcanic activity in the Corilleran Arc at this time could have been a prime source of zircons for these elevated terrains.

The peak at ~250 Ma represents a dynamic landscape that lasted at least from just before 250 Ma into Late Triassic time. This surface records at least 20 million years of nondeposition, incorporating ash-fall deposits from the west due to the monsoonal wind pattern as well as an eolian input from a regional range of basement terranes. These deposits were incorporated into the subaerial soils that became the well-defined paleosols preserved in Palo Duro Canyon and Highway 256, as well as being incorporated into the overlying fluvial deposits during Late Triassic time.

A sample (S8) from the middle sandstone unit of the Santa Rosa Formation collected in Santa Rosa as a check of prior samples, confirms an up section change in sourcing of detrital grains toward more easterly sources such as Appalachian or Cambrian dominant terranes. The dominant shift in paleo flow from south to east, as well as a shift to greater Grenville-aged grain populations points further to dominant eastern sources. An increase from S2 to S5 in Cambrian-aged grains suggests this eastern source. This is in accordance with CDF data from S2 and S5 that indicates a shift to a more active tectonic setting, with rift settings promoting an increased influence on the depositional system at the time, with major sedimentation occurring in the middle sandstone unit.

Tecovas Formation

The Tecovas Formation samples show a dominance of Grenvillian aged grains with age peaks of 1030-1050 Ma throughout both sections, arguing for a predominant southeasterly source that crossed Grenvillian basement in the foreland of the reactivated Ouachita highlands (Dickinson et al., 2010b). Grenville abundances average 30% in Tecovas Formation samples, compared to the average of 23% Grenvillian grains in geosol samples. Sample 256TC3 from the basal Tecovas sandstone also includes the dominant 250 Ma peak characteristic of the underlying geosol, but Tecovas samples from Palo Duro show only muted 250 Ma signatures. K-S values show a high (p values less than 0.05) probability that the geosol and overlying channel sandstones and associated mudstones of the Tecovas Formation are from statistically different populations. The one basal sand with the 250 Ma peak likely records reworking of zircons from the underlying geosol, rather than a continued 250 Ma source. There is also a distinct increase in abundance of Appalachian grains in Tecovas Formation grains, as evidenced in age peaks of 410 and 415 Ma in these samples

that is not present in geosol samples. This argues for hinterland extension of the drainages that larger tapped more distant Ouachita sources beyond the Grenville mountain front.

The Tecovas Formation samples are channelized sandstones and associated overbank floodplain deposits that record early Dockum Group channel deposition (Lamb, 2019; Walker and Holbrook, in press). CDFs produced show a pronounced change of distribution with regard to geosol and Tecovas samples (Figures 8,9). The geosol (samples PDG2 and PDG1) shows higher amounts of younger, potentially air fall grains within the samples when compared the Tecovas Formation (samples PDTE1 and PETE3). These distributions can be attributed to the tectonic shift from a stable interior to a rifting basin, allowing older source terranes to be tapped and shed via fluvial processes into the basin during Dockum Group deposition. Initial channel formation eroded elevated topography occupied by the geosol, incorporating subordinate 250 Ma and Midcontinent age peaks more typical of the geosol, reflected in the most basal Tecovas sample. Increased regional sourcing from remnant Ouachita highlands during later Tecovas time is recorded by increases in Appalachian and Grenville-aged grains that reached the basin due to northwest flowing streams originating from the Ouachita front, and a loss of reworked geosol zircons. This marked a significant change in provenance drainage reorganization toward more southerly mountain sources, likely driven by shifts in paleoclimate and/or paleotectonics at this time and burial of the Geosol. Geosol samples in this study mostly resemble the passive margin regimes of Cawood et al. (2012), while Tecovas samples more resemble rift basin regimes of Cawood et al. (2012) that incorporate signatures of older provinces. This is likely because Tecovas samples coincide with Late Triassic nascent rifting of Pangea and initial formation of the Gulf of Mexico, which promoted a regional north-sloping paleogradient due to thermal upwelling

that reactivated Ouachita highlands and associated basins. The minimal zircons from northern Midcontinent and the lack of Yavapai-Mazatzal zircons in Tecovas samples argues that drainages became increasingly extended into southwest sources in Tecovas time, and northern sourcing for rivers remained negligible.

Trujillo Formation

The Trujillo Formation records a dominant sourcing of grains from Grenville aged terranes (31.5%), similar to the Tecovas Formation, as well as other dominant southeastern sources of Appalachian and Gondwanan origin (16.5% each). Thus, it can be stated that the Trujillo Formation paleodrainages were still sourcing from Ouachita highlands, and that a marked provenance change from the Tecovas is not apparent. Statistical results show that the distributions of Trujillo and Tecovas samples show a 70.18% degree of likeness (Figure 7), with values approaching 100% signifying that the two distributions are likely similar. One interesting trend seen is a distinct shift in paleoflow within the Dockum Group at this time. Lamb (2019) recorded a slight shift of paleoflow to the north and west with regard to the Tecovas and Trujillo Formation respectively. The similarity in data suggests an autogenic shift of sourcing within the Ouachita and Marathon suture, with the Trujillo Formation recording local shifts in catchment within the reactivated uplift.

One recognizable feature of the dataset is that the Tecovas and Trujillo Formation do not show the abundance of Triassic grains that the basal geosol or Cooper Canyon Formation preserve. The 250 Ma salient decreases upward in the Dockum section into the Trujillo Formation compared to both the geosol and Tecovas deposits. Abundances of Permian-Triassic grains within these deposits decreases up section from 11% in the lower Tecovas (256TR4) to 1% in the Trujillo (256TR2). Sample 256TR4 could represent the last signal of

the pre-Late Triassic regional landscape prior to Dockum Group sedimentation. Topographic highs rich in 250 Ma zircons recorded by the basal-Dockum geosol were likely eroded down and adjacent basins filled prior and during Trujillo deposition, with only intraformational reworking of grains from the Trujillo Formation to the end of Dockum sedimentation. This could reflect limited arc influence during this span of the Late Triassic in contrast to the activity that occurred in Late Triassic times near the western coast of equatorial Pangea.

The dearth of Triassic grains in the Tecovas and Trujillo Formations could be explained by a gap in volcanism. Two extant volcanic arc margins were present in the Triassic, and overlap in volcanic activity. The East Mexico Arc was active from around 300 Ma to 240 Ma (Wengler et al., 2019), and was located to the south to southeast of the Palo Duro Basin during the Permian and Triassic Periods. The other arc was the incipient Cordilleran Arc, which is considered to be volcanically active from 260 Ma to 200 Ma (Riggs et al., 2020). Prominent pulses of volcanic and plutonic origin are associated with this margin in western Pangea, such as at 220 Ma, as well as 250 Ma (Davis, 2019; Riggs et al., 2020). Volcanic activity was present, but not consistent with regard to the Cordilleran arc, as there were periods of waning or little volcanic activity (Davis, 2019). The Dockum Group could have been deposited with well-developed paleosols recording long-term subaerial landscapes, accumulating air-fall zircon grains of Cordilleran origin transported to inner Pangea. It is feasible that transport could have been aided due to intense and highly seasonal monsoons that reversed easterly equatorial wind patterns inland toward basins such as the Palo Duro Basin (Dubiel et al., 1991; Winguth and Winguth, 2013; Lamb, 2019).

The contribution of the Yavapai-Mazatzal and Midcontinent terranes is constantly minor throughout the span of Tecovas and Trujillo deposition, but there is some variance in

peak ages for their relatively small contributions (Figures 3 and 4). One explanation for these minor contrasts in age peaks is that hinterland feeder streams integrated basement rock from different drainages areas up-dip into the headwaters of the paleodrainage related to catchment evolution. A similar case of tributary influence is recorded in the down-dip Chinle Formation, where southern tributaries contributed secondary sedimentary components from the Mogollon highlands as well as Triassic plutons of the Cordilleran Arc (Dickinson, 2018). Yavapai-Mazatzal terranes abundances are slightly higher in the Trujillo Formation, and the fluctuation in distribution seen in Trujillo Formation, as well as throughout the west Texas sections, is most likely a result of interplay of older Yavapai-Mazatzal terranes being intruded by Midcontinent anorogenic granite (Dubiel, 1994; Dickinson et al., 2010b). Dockum Group tributaries during the Late Triassic tapped these basement rocks in different proportions and quantities, as igneous intrusion was not widespread throughout the area of deposition (Figure 1). Furthermore, remnant topography of the Ancestral Rocky Mountains could have been uplifted at the same time due to the same thermal reactivation event causing subsidence in the Palo Duro Basin, causing Yavapai-Mazatzal terranes and Midcontinent granites to be subaerially exposed in different areas and/or at different times during deposition of the Dockum Group (Gehrels et al., 2011).

Cooper Canyon Formation

The Cooper Canyon Formation records a similar provenance trend as the Tecovas and Trujillo Formations, with nearly identical proportions of Grenvillian (31%), Appalachian (19%), Gondwanan (19%), and Midcontinent (14%) aged zircons. One distinct change in the distribution is the presence of Cambrian aged grains in the range of 530-540 Ma. These Cambrian grains have been associated with sediment shedding off of the Amarillo-Wichita

Uplift and transported in a paleodrainage known as the Eagle paleoriver that also deposited sediment to basins in modern-day Colorado and Utah (Dickinson and Gehrels, 2008). Age peaks in the Highway 256 section seem to trend up section toward the Ancestral Rocky Mountain (ARM) age range, and the Cooper Canyon sample in Palo Duro samples record a similar 540 Ma peak that is not present in underlying deposits. Since the evolution of this signal occurs in the youngest Dockum deposits in west Texas, it could correspond to reorganization of the Eagle paleoriver. The Eagle paleoriver may have swung into the West Texas corridor, more likely, part of the Eagle Drainage was transferred southward into Texas to generate this new contribution from the ARM to the north after sedimentation of the Tecovas and Trujillo Formation.

Another intriguing aspect of Kernel Density Estimate (KDE) signatures in Cooper Canyon is the reintroduction of Permian-Triassic grains. Permian-Triassic grains generally are 6-7% more abundant than the abundance of the younger Trujillo and Tecovas formations. As well as Triassic age peaks that are wholly Late Triassic (215 Ma, 220 Ma, 230 Ma) appear in the Cooper Canyon time that were not apparent in older samples collected from the Tecovas and Trujillo formations at the same locations. The only active arc within this Late Triassic time frame is the Cordilleran Arc, as the East Mexico Arc became dormant just before the beginning of the Late Triassic (Dickinson and Gehrels, 2008; Barboza-Gudiño et al., 2010; Wengler et al., 2019). Therefore, it is interpreted that these Late Triassic signals are a result of volcanic aerosol input from the Cordilleran Arc. Multiple studies of Triassic deposits on the western Cordilleran margin show that there was a cessation of input for volcanic zircons between 225-245 Ma in the Chinle deposits to the west (Riggs et al., 2003; Riggs et al., 2013; Riggs et al., 2020). Paleosols below the Tecovas and Trujillo Formations

have zircons with a 250 Ma peak before this gap, but the Tecovas and Trujillo generally lack Triassic zircons, beyond a few in the lower section that are easily attributed to reworking of the underlying paleosol. The appearance of Triassic zircons in the Cooper Canyon Formation that post-date the 225-245 Ma gap in Cordilleran volcanism argues that the Cooper Canyon deposited after this gap as well. The lack of Triassic zircons in the Tecovas and Trujillo Formations argues these formations deposited coeval with this gap.

Overall, the samples within these two sections show high probability that sample distributions are from the same source (Figure 7). According to Satkoski et al. (2013), likeness values of > 60% represent high probability of likeness of distributions. Out of 210 total comparisons, only 37 represented distributions that had less than 60% likeness values. The dominant source for the Cooper Canyon is thus the Ouachita Mountains to the south, the same as for the Tecovas and Trujillo Formations.

Regional Provenance Comparison

Regional Samples – Westward Correlations Dockum Group Samples

Dockum Group samples of west Texas bear similarities with Dockum Group samples in New Mexico. The Travesser Park Formation is postulated to be one of the youngest deposits of the Late Triassic Dockum Group (Lucas et al., 1987). These deposits are equivalent or younger than the Cooper Canyon Formation.

Although a distinct Late Triassic peak is not apparent in the lower Travesser Formation sample (S3), there is a distinct peak Late Triassic peak (215 Ma) in the upper Travesser Formation sample S7. Permian-Triassic grains are relatively low when compared to deposits in west Texas with S3 only having an abundance of 1% and S7 having an abundance of 3%. The only samples in west Texas that show Late Triassic KDE signatures

are entirely within the Cooper Canyon Formation, the uppermost formation of the Dockum Group in west Texas. Samples 256CCS4 and 256CCS3 show the exact same age peak at 215 Ma, as well as sample PDCC4 containing a 220 Ma age peak. Moreover, Cooper Canyon samples at Palo Duro (PDCC4) and Travesser Park (S7) samples show a 1.00 K-S test value, and one of the higher likeness values seen in this data set at 83.7%. Likeness values of S7 when compared to Cooper Canyon Formation sediments at the 256 outcrop average a likeness value of 71.2%.

A main argument to a younger Chinle-Dockum paleodrainage within Late Triassic time is the U-Pb evidence of a dominant age peak at 530-540 Ma shedding off the Amarillo-Wichita Uplift and passing through the Palo Duro Basin (Dickinson and Gehrels, 2008). This signature is seen in Cooper Canyon deposits within the Palo Duro Basin, specifically samples PDCC4, 256CCS3, 256CCS4, 256CCS1. Secondary peaks are seen within both distal samples S3 and S7 in New Mexico, but not as dominant as seen within proximal west Texas samples of the Dockum Group. One reason for this regional decrease could be a result of tributary influence farther away from the source, as the Dockum Group would be as close as 50 km to this Cambrian province, in contrast to the regional samples S3 and S7 down dip (Dickinson et al., 2010b). Overall, this further supports a younger paleodrainage which had a dynamic evolution from northernly paleoflow to a more westernly paleoflow and eastern source region as the Late Triassic progressed.

The high similarity in age and source between the Cooper Canyon sample at Palo Duro, and to a lesser extent the Cooper Canyon Formation samples at Highway 256, argue for a high probability that the Cooper Canyon Formation of the uppermost Dockum Group in west Texas was time coincident and positionally connected to deposits of the Travesser

Formation in northeastern New Mexico. The paleodrainage that connected these two regions was most likely the youngest part of the Late Triassic northwesterly flowing Eagle paleodrainage of Late Triassic time (Dickinson and Gehrels, 2008). The Traversser Formation was not confined by the Matador Arch and Amarillo Uplift like the Cooper Canyon Formation of west Texas (McGowen et al., 1983). The northwestern tilting that drove flow direction was most likely a result of dynamic back-arc subsidence from the Cordilleran margin to the west (Dickinson, 2018) with possible gradient effects from the reactivation and uplift of the Ouachita highlands during this time as well.

Lithological Effects on Data Abundance and Potential Implications

Zircon type and abundance could potentially vary between samples according to lithofacies. Prior statistical (Vermeesch, 2012), hydrological (Lawrence et al., 2011), temporal and regional (Sharman and Malkowski, 2020), and lithological (Gehrels et al., 2020) studies test this assertion. This section compares zircon type (volcanic vs detrital) and abundance by lithology and depositional environment for the Dockum Group.

Lithology alone shows minimal contrast between samples (Table 5). Fine-grained samples (clay-sized) vs coarse grained samples (non-clay sized) yield similar results with clay-sized samples averaging ~242 grains, and coarse-grained samples averaging ~224 grains for similar sized samples. Average abundances for young Late Triassic grains show a similar trend, with fine-grained samples producing a slightly higher average at 1.78% vs. 1.59% for the coarse-grained average. More contrast is apparent when comparing depositional environment of individual samples.

Clay-sized samples from paleosols and lacustrine deposits yield a relatively high normalized abundance of Late Triassic grains. The geosol that is regional to west Texas

shows relatively high abundances (~4%) of Late Triassic grains in the Palo Duro section (samples PDG2 and PDG1). The geosol in 256 yields no grains of Late Triassic age. Notably, the Tecovas Formation channels have incised the paleosol considerably at the Highway 256 section, and the paleosol does not show the same amount of thickness or maturity when compared to the geosol in Palo Duro Canyon. The geosol grades into Tecovas Formation floodbasin sediments. Lacustrine sediments also show relatively high abundances of Late Triassic grains. More specifically, lacustrine samples PDCC4, 256CCS3, 256CCS2, and 256CCS1 show relatively high amounts of Late Triassic grains, with ranges from ~3.2% to 4.01%. The lacustrine and paleosol sample generally preserve young/ash-fall zircons better than the channel and bar deposits.

Subaerially mature landscapes, like those reflected in the Palo Duro geosol, can incorporate air-fall ashes containing primary zircons through pedological processes such as bioturbation, rooting, and desiccation. Samples PDG2 and PDG1 both show these long-term pedological traits, as well as variated coloring due to the fluctuating seasonal climate that persisted in the Late Triassic. Other critical evidence that points to an elevated and well-drained terrain accumulating zircons is the fact that all basal paleosol samples show primary kernel density age peaks around 250 Ma, with smaller secondary age peaks of equal or younger age going up in section (Figures 3,4, and 5). This is possible evidence that the geosol present during Dockum Group deposition lasted across the 220 Ma peak for more than 20 million years, incorporating zircons over this duration. Later local erosion of this geosol shed into channelized deposits of the Dockum Group, with decreasing input through time. Dockum samples PDTE1, 256TC3, and 256TR4 are channelized deposits that show this geochronologic trend of reworking from the paleosol. The Palo Duro geosol likely records

most if not all of the late Early, Middle, to early Late Triassic Period.

Lacustrine deposits of the Dockum Group are prevalent, and show a similar tendency toward preservation of relatively abundant Late Triassic grains. The Cooper Canyon Formation in both Palo Duro Canyon and Highway 256 outcrops is predominately lacustrine in origin, with deltaic components and terminal splays prograding into shallow lakes (Lamb, 2019). Samples from highly laminated, clay-sized lacustrine deposits of the Cooper Canyon Formation as well as abandoned channel fills of the Tecovas and Trujillo Formations show distinct abundances of young zircons compared to more sandy deposits and most floodplain muds of the same formation. Predominantly laminated lacustrine deposits of the Cooper Canyon Formation that lacked evidence of significant coarse-clastic deposition (Samples PDCC4, 256CCS3, 256CCS2, 256CCS1) had particularly high abundances of Late Triassic grains. Sample 256CCS3 is interpreted here as a preserved ash bed that was deposited on a lake bottom, and shows the second highest abundance of actual Late Triassic grains in the dataset. Several potential conditions contribute to high abundance of young ash-fall zircons in lake settings, such as lack of bioturbation, negligible sedimentation rates, and absence of reworking fluvial currents (Königer and Stollhofen, 2001). Samples that are associated with sandy progradational lacustrine deltas in the Cooper Canyon Formation (i.e. Samples 256CCS1, 256CCS2) preserve less primary pyroclastic zircons relatively, most likely because clastic input incorporated comparatively higher proportions of detrital zircons from associated floodplains and channel drainages (Ducassou et al., 2019).

The Tecovas and Trujillo Formation do not show the abundance of Late Triassic grains that the basal geosol or Cooper Canyon Formation preserve. Since lacustrine samples were collected from both, this likely records a gap in volcanic ash accumulation in this part

of west Texas, rather than a lithological bias.

Paleotectonic and Paleoclimate Implications of the Dockum Group and Santa Rosa Formation

Regional Tectonics

The current study argues that Chinle, Dockum, and Santa Rosa strata are preserved parts of a collective Late Triassic fluvial depositional system that originated from the contemporary Ouachita/Grenvillian front in the area of modern Texas and dispersed northwestward across modern west Texas and eastern New Mexico into areas of the modern Colorado Plateau. The abundance of Grenvillian aged grains, as well as Appalachian and Gondwanan aged grains points to a dominant southeast source from the Ouachita highlands for all these strata. Zircons from these sources are ubiquitous in the Chinle Formation and paleoflow trends are similarly from the southwest where basement provinces dominate. Similar zircon trends are clear from the Dockum Group and Santa Rosa Formation in the areas projected up dip from these Chinle exposures.

The assertion here for a common Ouachita source area for Triassic strata across the U.S. southwest also implies a significant regional shift in the continental gradient during the Triassic that generated a regional shift in gradient from the Ouachita highlands toward the northeast into both the Palo Duro and Chinle depositional basins. This agrees with the hypothesis of Dickinson et al. (2010b) that thermal reactivation during the Triassic associated with the incipient rifting of Pangea allowed for a regional gradient that sourced reactivated Grenvillian and Ouachita topography via fluvial drainages into basins that were also associated with this reactivation experiencing dynamic subsidence in western Texas. Furthermore, the middle sandstone unit of the Santa Rosa Formation captured the initiation of this regional gradient, as the increase in Grenvillian grains and dominant westerly flow

initiating in this section point to a significant tectonic shift in source area from the lower Santa Rosa. Data from this study argue this gradient persists through Dockum Group deposition, as zircon age, distribution, and paleoflow remained relatively the same (W/NW trending). This agrees with earlier assertions of Dickinson (2018) who argued for a similar SW Chinle and Dockum source. A temporal migration of paleoflow to the northwest could be evidence that back-arc subsidence that governed Chinle Formation deposition (Dickinson, 2018) also affected Dockum Group deposition. The high provenance similarity and correlative Cambrian signature (~540 Ma) between the Travesser Formation located in the northeast corner of New Mexico (sample S7) and the Cooper Canyon Formation (sample PDCC4) points to a gradual shift toward the end of Dockum fluvial sedimentation to the north, which sourced a higher abundance of Amarillo-Wichita uplift terranes..

Santa Rosa Formation

Various tectonic and climatic implications can be hypothesized based on the sedimentology, architectural analysis, as well as detrital zircon data of the Santa Rosa Formation. Since Santa Rosa deposition occurred in inner Pangea (~1500 km from Pangean paleocoast), there should be no base level effect on stratigraphy. The two main controls are tectonics and climate.

At the base of the Santa Rosa Formation lies the lower sandstone unit, which records northern flowing perennial braided streams of subarkose lithology, as well as the dominant 250 Ma age peak seen in the younger Dockum Formation deposits. The dominant flow direction is to the north. The overlying middle sandstone unit records a paleocurrent shift, with larger scale perennial mixed braided/meandering streams of quartzarenite lithology flowing to the west. There is also evidence of high-bedload medium to coarse-grained

bedforms as well as evidence of convoluted cross-bedding. This change in bedload and source direction points to a potential tectonic uplift that lowered accommodation and allowed these braided channels to incise and amalgamate at the belt, and potentially the valley scale. This increase in slope also led to more conglomerate facies within the middle sandstone unit when compared to the lower sandstone. The lower sandstone could have been derived from the southern end of the Marathon-Ouachita belt, as the subarkose lithological content is evidence of a closer source area, but records similar high abundances of Grenvillian, Appalachian, and Gondwanan aged grains.

There are some potential sources for tectonic uplift proximal and distal to the Tucumcari Basin where the middle sandstone unit was deposited. Sediment could have been sourced from regions that experienced reactivation and uplift due to the thermal effects of Gulf of Mexico rifting. Proximal sources could have been the Frio Uplift as well as the Matador Arch, containing Wolfcampian-aged marine limestones (Broadhead, 1988). The Frio Uplift is situated to the east, and separates the Tucumcari and Palo Duro Basin. The medium to coarse-grained, high bedload deposition, extrabasinal conglomerates containing carbonate nodules, and lack of Santa Rosa deposition in the Palo Duro Basin could be direct evidence of a proximal uplift that increased paleogradient and allowed for braided stream deposition in the middle sandstone unit. An alternate hypothesis is that the middle sandstone unit could also mark the reactivation of the relatively distal Ouachitas, as the high quartz content points to a distal source region.

A climatic factor also has to have controlled deposition of the middle sandstone unit, as paleochannel bankfull depth estimates ranging over 10 meters cannot be governed by tectonics and is an anomaly in Triassic red bed strata. There are multiple studies that model

or provide evidence that the Triassic climate was monsoonal or highly seasonal (Parrish, 1993; Dubiel, 1994; Demko et al., 1998; Winguth and Winguth, 2013; Lamb, 2019; Walker, 2020). More specifically, Parrish (1993) hypothesized that monsoonal climate would reach a maximum sometime during the Triassic, as well as a “full” monsoon model where these conditions would reverse equatorial winds and promote rainfall 600-1200 km into inner Pangea. If this was monsoonal-driven deposition, it does not look like the ephemeral settings of the Dockum Group and upper sandstone of the Santa Rosa Formation. There is evidence in the Late Triassic Chinle Formation in New Mexico of perennial fluvial settings occurring in arid environments where seasonality would produce ephemeral flow (Deluca and Eriksson, 1989). Moreover, there is also evidence in the Chinle Formation that elevated highlands were humid and allowed constant groundwater recharge into the system that allowed for perennial flow, seen in perennial Chinle deposits (Blakey and Gubitosa, 1984). Monsoon systems are also hypothesized to bring higher annual amounts of total rainfall that would keep fluvial systems flowing in a perennial fashion (Dubiel et al., 1991).

Based on this evidence, as well as the architecture of the middle sandstone with 2nd order large-scale bedforms with lack of reactivation surfaces, along with paleochannel estimates indicative of a perennial system, the middle sandstone is interpreted to have formed in monsoonal conditions that provided high annual amounts of rainfall which allowed for constant recharge of the fluvial system, even in seasonal arid conditions.

The mudstone unit represents an environmental change to predominately overbank and floodplain elements. One potential factor that could have caused this change was that aggradation of the middle sandstone led to autocyclic avulsion as the fluvial system aggraded to keep up with deposition. Tectonic uplift could have waned, allowing a decrease in gradient

as aggradation started to control deposition instead of degradation. The change from medium-grained sediment to finer-grained deposits points to an increase in accommodation as well (Holbrook and Schumm, 1999).

An allogenic factor that could have caused this environmental change could have been a decrease in sediment supply due to a decrease in gradient because of waning uplift and/or erosion of source area. Monsoonal effects on long-term decadal to millennial time scales can cause aggradation or degradation on a fluvial system as well, dictated by sediment load and stream power. Ancient and modern examples of this allogenic factor have been documented in the Chinle Formation, and the modern Indian monsoonal climate with both studies indicating that paleolatitude migration into different climate zones as the main factor (Gibling et al., 2005; Singh et al., 2009)

Another explanation for aggradation of the thick mudstone unit could be that localized Permian salt became mobilized sometime during the Triassic. A localized sink around Santa Rosa has been documented and interpreted to be a function of salt mobility (Kelley, 1972). This could have led to localized increased subsidence into salt sinks that promoted avulsion. Similar circumstances have been documented in the Chinle Formation in the Four Corners area (Prochnow et al., 2006; Hartley and Evenstar, 2018).

The upper sandstone unit records a change in fluvial style with regard to the middle sandstone unit, from perennial conditions to a flash-flood ephemeral system that records multiple 3rd order flood event surfaces on an alluvial plain with channel depths estimates of 2 – 4 meters, and architectural elements filled with upper plane bed deposition. Walker and Holbrook (2020) proved that estimated slope in west Texas was likely not large enough to promote the supercritical flow structures observed in outcrop, and thus climate was what

dictated the high-energy discharge rates. This study interprets climate as the main factor in the deposition of the upper sandstone unit as well. The 3rd order surfaces that represent deposition within single flood events, often occurring with different orientations, along with the lack of perennial channel depth points to short, intense seasonal flood events separated by otherwise arid conditions without significant discharge. In contrast to perennial flow, these ephemeral streams were not able to denudate and create thick bankfull depths.

There is much literature that points to monsoonal conditions of the Chinle Formation reaching maximum strength in the Triassic, and the waning into the end of the Triassic and terminating with Jurassic erg deposition, due to the nascent rifting of the Gulf of Mexico and paleolatitude migration from tropical 5-15 degrees north of the paleoequator to arid latitudes 30 degrees north of the paleoequator (Dubiel et al., 1991; Parrish, 1993; Dubiel, 1994). The Chinle Formation, as well as the Dockum Group, would have been situated at higher latitudes which would have not experienced maximum megamonsoonal conditions in the later stages of the Triassic (Dubiel, 1994). This migration also caused seasonal monsoon activity to wane. Based on the data presented in this study as well as Walker (2020), estimated flow depths of channel sandstones decrease with younger age in Santa Rosa Formation up into Dockum Group strata. The contrast in fluvial style from perennial to ephemeral flow, along with shallowing of flow depths could be a result of this waning. Total annual total rainfall rates would have decreased to conditions that could not sustain perennial flow during upper sandstone unit deposition and continued during deposition of the Dockum Group.

Paleosol variation in the Chinle Formation shows that the Late Triassic underwent a significant climatic change from wet climate and high water tables at the base of the Chinle Formation to fluctuating, low water tables towards the end of Chinle deposition (Dubiel and

Hasiotis, 2011). Dubiel and Hasiotis (2011) also determined that this paleosol variation recorded a temporal change in seasonality, with monsoonal seasons with longer months at the beginning of Chinle deposition waning to monsoonal conditions occurring in a shorter span of months towards the end of the Chinle Formation. They also state that the arid conditions at the end of Chinle deposition resulted in decreases in fluvial discharge and sediment load, with older deposits showing increased discharge and sediment load due to the wetter conditions. This study shows similarities to the findings of Dubiel and Hasiotis (2011), with high sediment load, high discharge perennial fluvial drainages at the base of the Santa Rosa Formation transitioning to more extreme seasonal, flash-flood ephemeral fluvial systems in the upper strata of the Santa Rosa Formation and Dockum Group.

Overall, this study provides radiometric and sedimentological evidence that a megamonsoonal regime dictated fluvial style and climate in deposits of Triassic age east of the Rockies. Monsoonal conditions are seen to have potentially reached a maximum at the base of the Santa Rosa Formation, with consistent waning through the Santa Rosa Formation and into the Late Triassic Dockum Group. Further studies of regional architecture of the Santa Rosa, as well as stratigraphic age dates of these strata could lead to a more complete record of the timing of climate and tectonics in southwest Laurentia in the Triassic Period, and how these strata are connected temporally to the Chinle Formation.

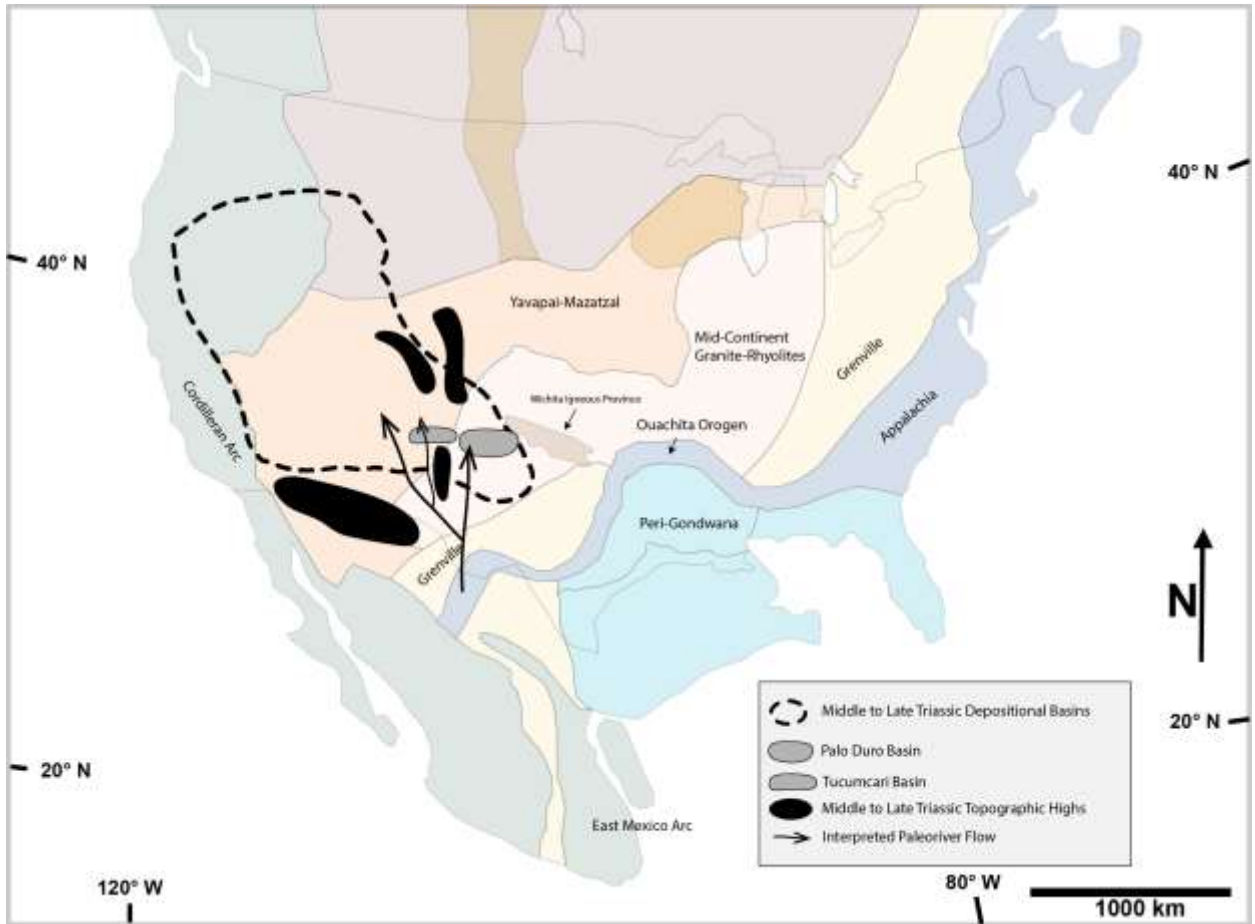


Figure 24. Interpretation of paleodrainage source and direction during deposition of the lower sandstone unit of the Santa Rosa Formation.

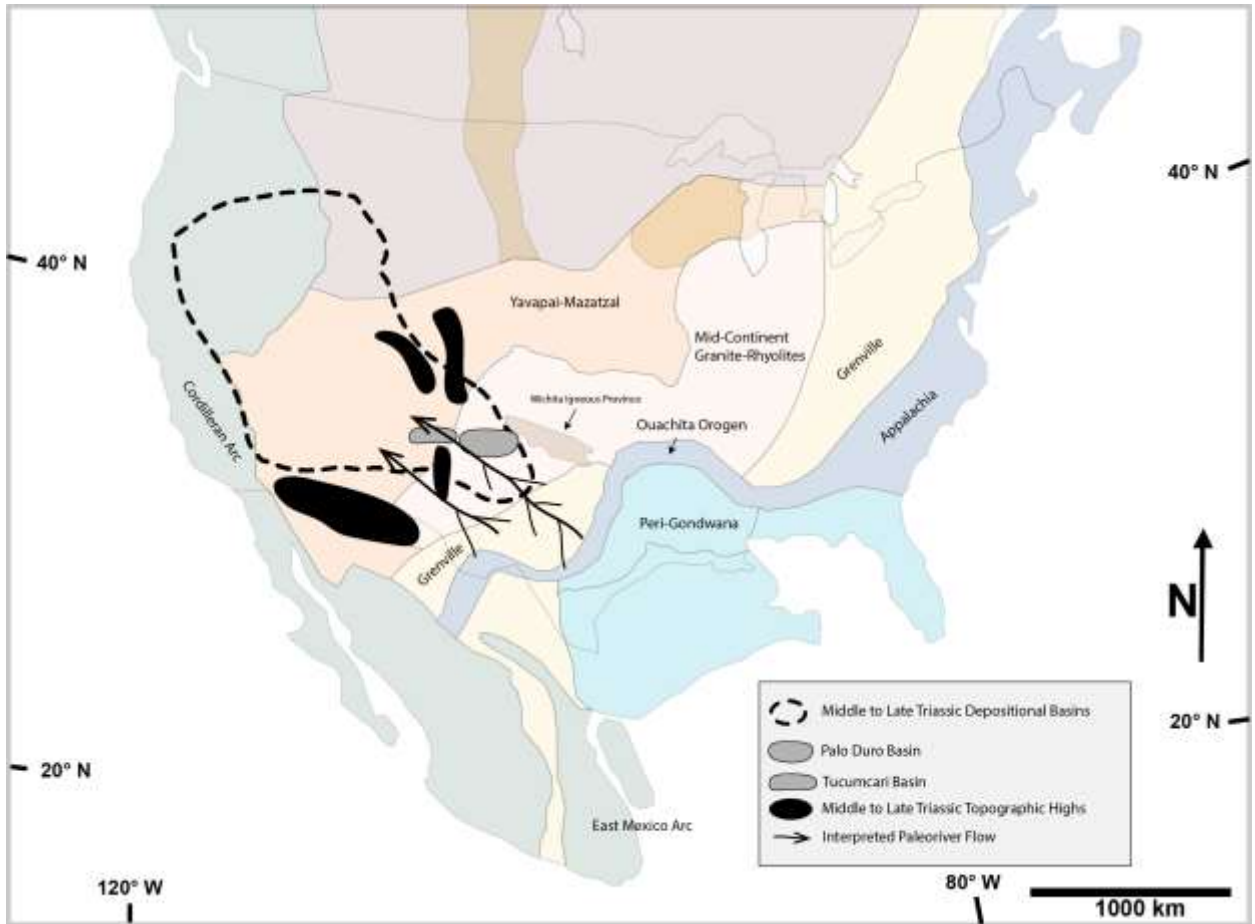


Figure 25. Interpretation of paleodrainage source and direction during deposition of the middle/upper sandstone unit of the Santa Rosa Formation.

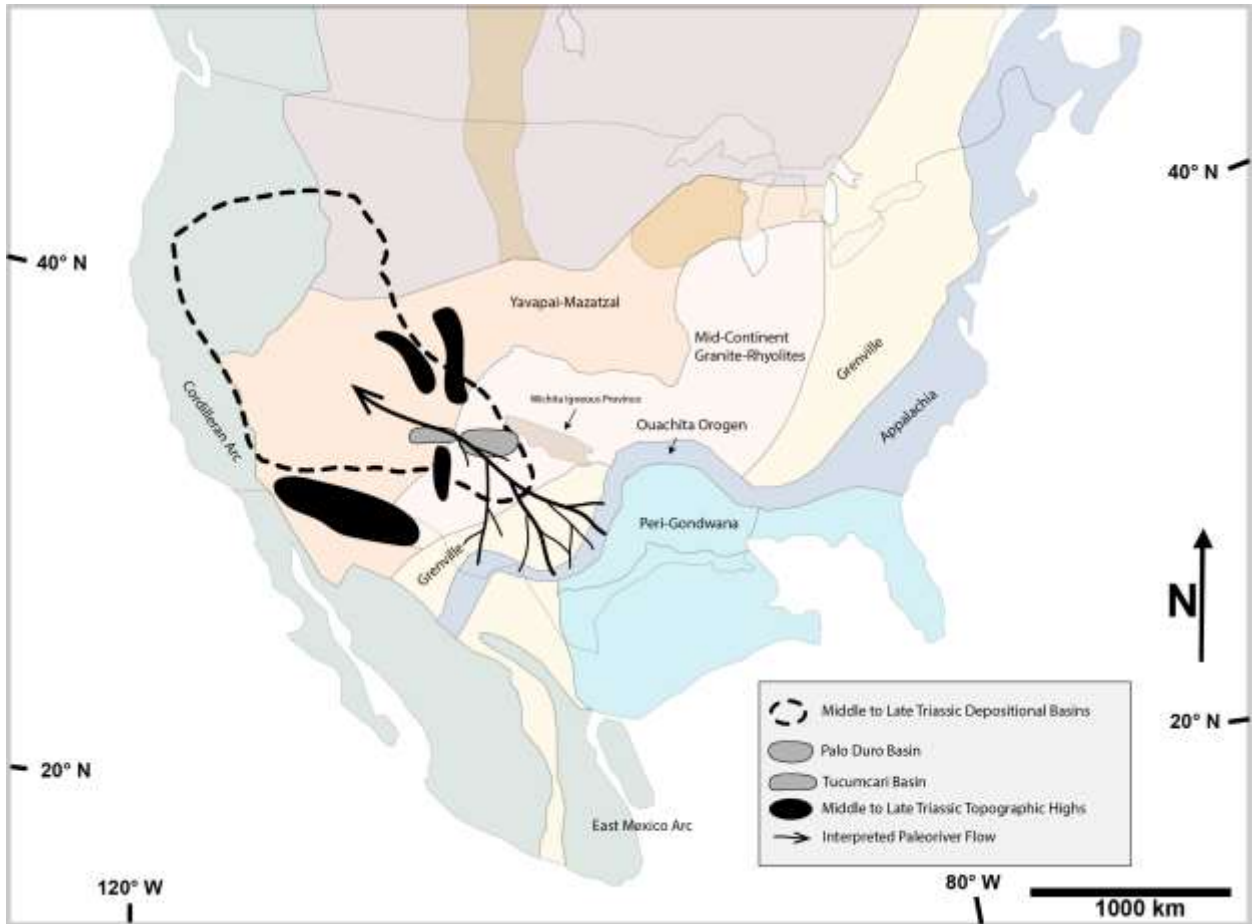


Figure 26. Interpretation of paleodrainage source and direction during deposition of the Tecovas Formation of the Dockum Group.

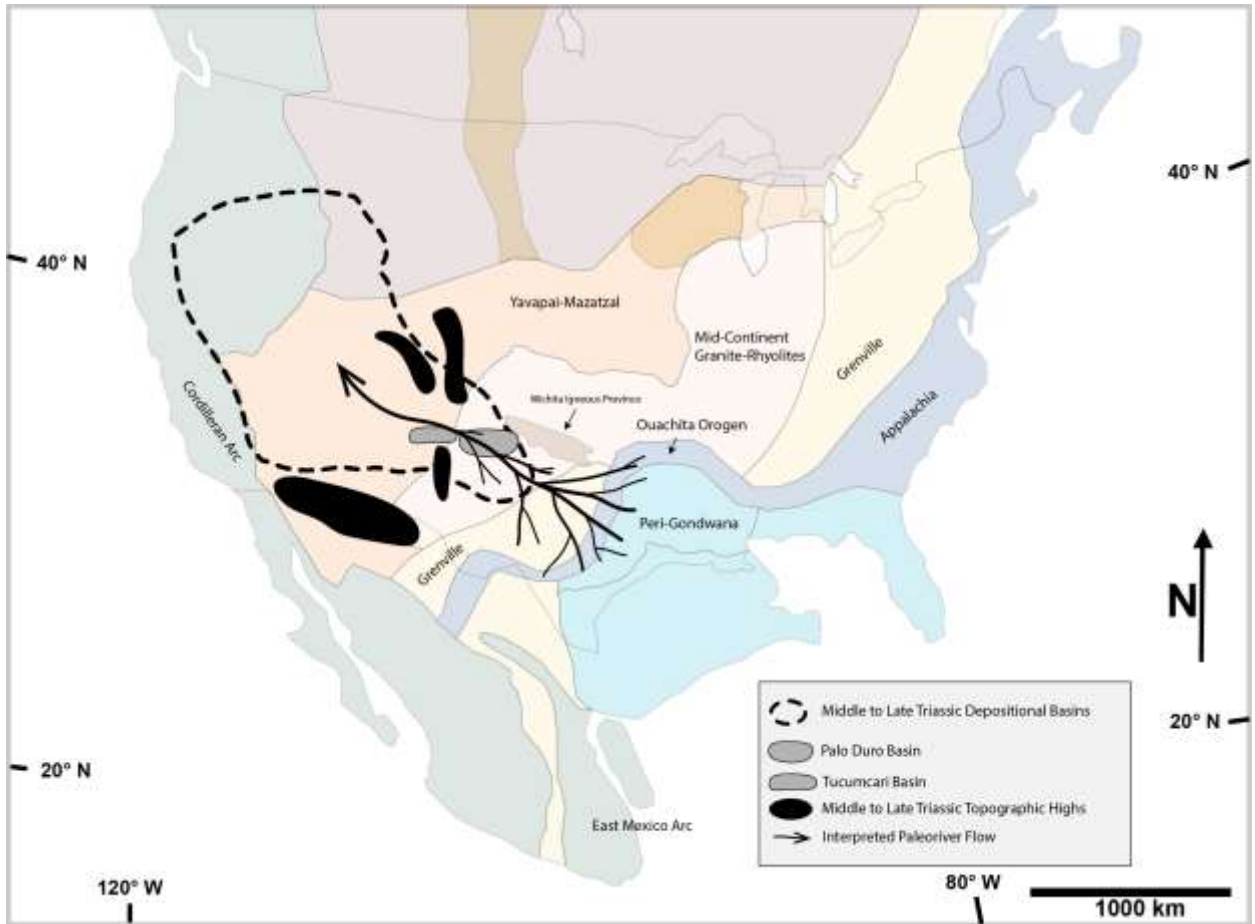


Figure 27. Interpretation of paleodrainage source and direction during deposition of the Trujillo Formation of the Dockum Group.

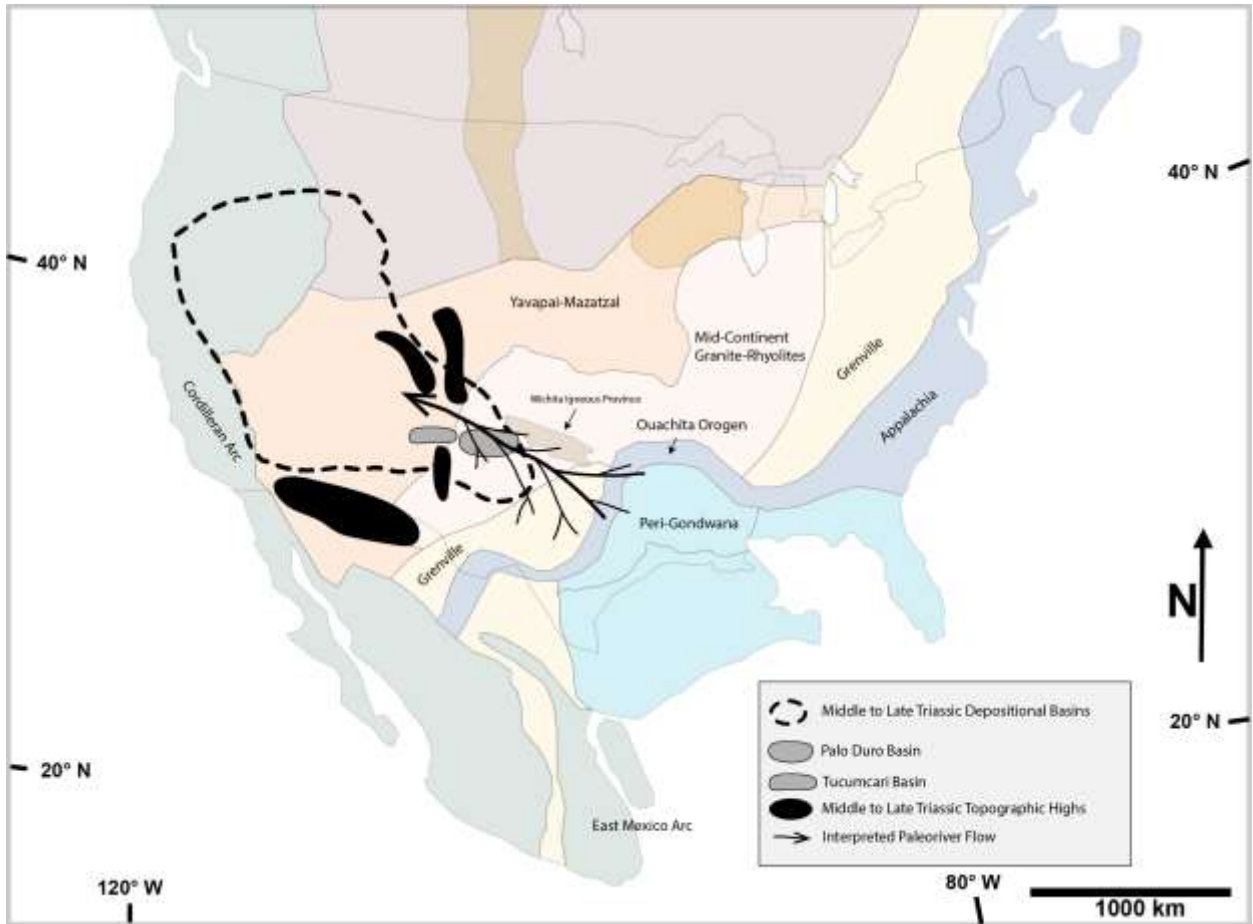


Figure 28. Interpretation of paleodrainage source and direction during deposition of the Cooper Canyon Formation of the Dockum Group.

Conclusions

1. Provenance analysis of Dockum Group strata in west Texas provides further evidence that the Chinle Formation and Dockum Group record a common paleodrainage sourcing from the Ouachita Belt in southeast Texas. From deposition of the Santa Rosa Formation in eastern New Mexico to deposition of the Dockum Group in Texas, the fluvial system shows shifts of sourcing within the orogenic belt to the south and southeast, potentially due to the breakup of Pangea and/or effects of back-arc subsidence from arc formation in western Pangea. The fluvial system records the gradual migration of the paleodrainage northward.

2. Strata of the Cooper Canyon Formation and Travesser Formation show high likeness of sourcing and are temporally at the same stratigraphic age. This region of equatorial Pangea during the Triassic shows evidence that topographic highs affected depositional trends, similar to barriers seen in the down-dip Chinle Formation.
3. A distinct age peak of 250 Ma contained in the provenance data of the geosol strata of west Texas points to a regional landscape that was incorporating eolian input, including primary ash-falls, for at least 20 million years before deposition of the overlying Dockum Group strata in west Texas. This could signify monsoonal conditions were present at approximately this time that reversed easterly equatorial wind patterns to promote temporary eastward migration of aerosol ash into the Palo Duro and Tucumcari Basins.
4. The Santa Rosa Formation records earlier evidence of monsoonal conditions within the Triassic Period. The Middle Sandstone Unit records a potential maximum strength of monsoonal conditions, with large bankfull channels recording persistent water supply. The strength of monsoonal conditions wanes into the younger Upper Sandstone Unit, with deposition in ephemeral streams. It is interpreted that this trend continued with deposition of the stratigraphically younger Dockum Group deposits, with extreme flash-flood events separated by extended times of dryness. This trend is seen in stratigraphically equivalent Chinle Formation, and is interpreted to be a byproduct of progressive paleolatitude migration due to incipient rifting of the Pangea and the Formation of the Gulf of Mexico.
5. The lack of abundance in Late Triassic grains in the Tecovas and Trujillo Formations points to a gap in volcanism, and not lithological sample bias.
6. This work provides evidence of a younger Late Triassic age for the Dockum Group (lasting between 220 Ma and 212 Ma), with further testing to confirm these younger ages

with more precise geochronology methods.

References

- Alexander, J. S., McElroy, B. J., Huzurbazar, S., and Murr, M. L., 2020, Elevation gaps in fluvial sandbar deposition and their implications for paleodepth estimation: *Geology*, v. 48, no. 7, p. 718-722.
- Ash, S. R., and Creber, G. T., 1992, Palaeoclimatic interpretation of the wood structures of the trees in the Chinle Formation (Upper Triassic), Petrified Forest National Park, Arizona, USA: *Palaeogeography, Palaeoclimatology, Palaeoecology*, v. 96, no. 3, p. 299-317.
- Barboza-Gudiño, J. R., Zavala-Monsiváis, A., Venegas-Rodríguez, G., and Barajas-Nigoche, L. D., 2010, Late Triassic stratigraphy and facies from northeastern Mexico: Tectonic setting and provenance: *Geosphere*, v. 6, no. 5, p. 621-640.
- Bazard, D., and Butler, R., 1991, Paleomagnetism of the Chinle and Kayenta Formations, New Mexico and Arizona: *Journal of Geophysical Research*, v. 96, p. 9847-9871.
- Blakey, R. C., and Gubitosa, R., 1984, Controls of sandstone body geometry and architecture in the Chinle Formation (Upper Triassic), Colorado Plateau: *Sedimentary Geology*, v. 38, no. 1, p. 51-86.
- Boone, J. L., 1979, Lake margin depositional systems of the Dockum Group (Upper Triassic) in Tule Canyon, Texas Panhandle.
- Bordy, E. M., John Hancox, P., and Rubidge, B. S., 2004, Fluvial style variations in the Late Triassic–Early Jurassic Elliot formation, main Karoo Basin, South Africa: *Journal of African Earth Sciences*, v. 38, no. 4, p. 383-400.
- Bridge, J. S., 2003, *Rivers and floodplains: forms, processes, and sedimentary record*, John Wiley & Sons.
- Broadhead, R. F., 1988, Petroleum geology of Pennsylvanian and Lower Permian strata, Tucumcari Basin, east-central New Mexico: *New Mexico Bureau of Mines and Mineral Resources*, v. 119, p. 76.
- Cazeau, C. J., 1962, Upper Triassic deposits of west Texas and northeastern New Mexico: University of North Carolina at Chapel Hill.
- Darton, N. H., 1922, Geologic structure of parts of New Mexico: Chapter E in *Contributions to economic geology, 1921, Part II.--Mineral fuels, 726-E*.
- Davis, H. M., 2019, *Permo-Triassic Cordilleran Arc Magmatism and Detrital Zircon Record in Triassic Sedimentary Strata in The Inyo Mountains, Eastern California* [M.S.]: Northern Arizona University, 239 p.
- Deluca, J. L., and Eriksson, K. A., 1989, Controls on synchronous ephemeral- and perennial-river sedimentation in the middle sandstone member of the Triassic Chinle Formation, northeastern New Mexico, U.S.A:

- Sedimentary Geology, v. 61, no. 3, p. 155-175.
- Demko, T. M., Dubiel, R. F., and Parrish, J. T., 1998, Plant taphonomy in incised valleys: Implications for interpreting paleoclimate from fossil plants: *GEOLOGY*, v. 26, no. 12, p. 1119-1122.
- Dickinson, W., 2018, Tectonosedimentary Relations of Pennsylvanian to Jurassic Strata on the Colorado Plateau: Special Paper of the Geological Society of America, v. 533, p. 1-184.
- Dickinson, W. R., 1981, Plate tectonic evolution of the southern Cordillera: *Arizona Geological Society Digest*, v. 14, p. 113-135.
- Dickinson, W. R., Dickinson, W. R., Gehrels, G. E., and Gehrels, G. E., 2010a, Insights into North American Paleogeography and Paleotectonics from U–Pb ages of detrital zircons in Mesozoic strata of the Colorado Plateau, USA: *International Journal of Earth Sciences*, v. 99, no. 6, p. 1247-1265.
- Dickinson, W. R., and Gehrels, G. E., 2008, U-PB AGES OF DETRITAL ZIRCONS IN RELATION TO PALEOGEOGRAPHY: TRIASSIC PALEODRAINAGE NETWORKS AND SEDIMENT DISPERSAL ACROSS SOUTHWEST LAURENTIA: *JOURNAL OF SEDIMENTARY RESEARCH*, v. 78, no. 11-12, p. 745-764.
- Dickinson, W. R., Gehrels, G. E., and Stern, R. J., 2010b, Late Triassic Texas uplift preceding Jurassic opening of the Gulf of Mexico: Evidence from U-Pb ages of detrital zircons, Volume 6: BOULDER, GEOLOGICAL SOC AMER, INC, p. 641-662.
- Dubiel, R., and Hasiotis, S., 2011, Deposystems, Paleosols, and Climatic Variability in a Continental System: The Upper Triassic Chinle Formation, Colorado Plateau, U.S.A, Volume 97, p. 393–421.
- Dubiel, R., Hasiotis, S., and Demko, T., 1999, INCISED VALLEY FILLS IN THE LOWER PART OF THE CHINLE FORMATION, PETRIFIED FOREST NATIONAL PARK, ARIZONA: COMPLETE MEASURED SECTIONS AND REGIONAL STRATIGRAPHIC IMPLICATIONS OF UPPER TRIASSIC ROCKS: *National Park Service Paleontological Research*, v. 4, p. 127-139.
- Dubiel, R. F., 1994, Triassic Deposystems, Paleogeography, and Paleoclimate of the Western Interior: *AAPG Bulletin*, v. Mesozoic Systems of the Rocky Mountain Region, USA, p. 35.
- Dubiel, R. F., Parrish, J. T., Parrish, J. M., and Good, S. C., 1991, The Pangaeon Megamonsoon: Evidence from the Upper Triassic Chinle Formation, Colorado Plateau: *PALAIOS*, v. 6, no. 4, p. 347-370.
- Ducassou, C., Mercuzot, M., Bourquin, S., Rossignol, C., Pellenard, P., Beccalotto, L., Poujol, M., Hallot, E., Pierson-Wickmann, A. C., Hue, C., and Ravier, E., 2019, Sedimentology and U-Pb dating of Carboniferous

- to Permian continental series of the northern Massif Central (France): Local palaeogeographic evolution and larger scale correlations: *Palaeogeography, Palaeoclimatology, Palaeoecology*, v. 533, p. 109228.
- Fildani, A., McKay, M. P., Stockli, D., Clark, J., Dykstra, M. L., Stockli, L., and Hessler, A. M., 2016, The ancestral Mississippi drainage archived in the late Wisconsin Mississippi deep-sea fan: *Geology*, v. 44, no. 6, p. 479-482.
- Finch, W. I., and Geological, S., 1988, Principal reference section for the Santa Rosa Formation of middle and late Triassic age, Guadalupe County, New Mexico: Department of the Interior, U.S. Geological Survey.
- Finch, W. I., Lupe, R., and Ash, S. R., 1988, Principal reference section for the Santa Rosa formation of Middle and Late Triassic age, Guadalupe County, New Mexico, 1804.
- Fritz, T. L., 1991, Depositional history of the mid-late Triassic Santa Rosa Formation, Eastern New Mexico.
- Gehrels, G., 2011, Detrital Zircon U-Pb Geochronology: Current Methods and New Opportunities, *Tectonics of Sedimentary Basins*, p. 45-62.
- Gehrels, G., Giesler, D., Olsen, P., Kent, D., Marsh, A., Parker, W., Rasmussen, C., Mundil, R., Irmis, R., Geissman, J., and Lepre, C., 2020, LA-ICPMS U-Pb geochronology of detrital zircon grains from the Coconino, Moenkopi, and Chinle formations in the Petrified Forest National Park (Arizona): *Geochronology U6* v. 2, no. 2, p. 257-282.
- Gehrels, G., Valencia, V., and Pullen, A., 2006, Detrital Zircon Geochronology by Laser-Ablation Multicollector ICPMS at the Arizona LaserChron Center: *The Paleontological Society Papers*, v. 12, p. 67-76.
- Gehrels, G. E., Blakey, R., Karlstrom, K. E., Timmons, J. M., Dickinson, B., and Pecha, M., 2011, Detrital zircon U-Pb geochronology of Paleozoic strata in the Grand Canyon, Arizona: *Lithosphere*, v. 3, no. 3, p. 183-200.
- Gibling, M. R., Tandon, S. K., Sinha, R., and Jain, M., 2005, Discontinuity-Bounded Alluvial Sequences of the Southern Gangetic Plains, India: Aggradation and Degradation in Response to Monsoonal Strength: *Journal of Sedimentary Research*, v. 75, no. 3, p. 369-385.
- Gorman, J. M., and Robeck, R. C., 1946, *Geology and asphalt deposits of north-central Guadalupe County, New Mexico*, 44.
- Guynn, J., and Gehrels, G., 2010, Comparison of detrital zircon age distributions in the KS test: University of Arizona, Arizona LaserChron Center, Tucson.
- Hartley, A., and Evenstar, L., 2018, Fluvial architecture in actively deforming salt basins: Chinle Formation, Paradox Basin, Utah: *Basin Research*, v. 30, no. 1, p. 148-166.

- Holbrook, J., and Schumm, S. A., 1999, Geomorphic and sedimentary response of rivers to tectonic deformation: a brief review and critique of a tool for recognizing subtle epeirogenic deformation in modern and ancient settings: *Tectonophysics*, v. 305, no. 1-3, p. 287-306.
- Holbrook, J., and Wanas, H., 2014, A fulcrum approach to assessing source-to-sink mass balance using channel paleohydrologic parameters derivable from common fluvial data sets with an example from the Cretaceous of Egypt: *Journal of Sedimentary Research*, v. 84, no. 5, p. 349-372.
- Holbrook, J. M., and Allen, S. D., 2021, The case of the braided river that meandered: Bar assemblages as a mechanism for meandering along the pervasively braided Missouri River, USA: *Bulletin*, v. 133, no. 7-8, p. 1505-1530.
- Horn, B., Goldberg, K., and Schultz, C., 2017, Interpretation of massive sandstones in ephemeral fluvial settings: A case study from the Upper Candelária Sequence (Upper Triassic, Paraná Basin, Brazil): *Journal of South American Earth Sciences*, v. 81.
- Kelley, V. C., 1972, Geology of the Fort Sumner sheet, New Mexico: New Mexico Bureau of Mines and Mineral Resources, v. Bulletin 98, p. 55.
- Königer, S., and Stollhofen, H., 2001, Environmental and Tectonic Controls on Preservation Potential of Distal Fallout Ashes in Fluvio-Lacustrine Settings: The Carboniferous–Permian Saar–Nahe Basin, South–West Germany: *IAS Special Publication*, v. 30, p. 263-284.
- Lamb, G. H., 2019, An architectural analysis and depositional interpretation of the Dockum Group in the West Texas High Plains: Texas Christian University.
- Lawrence, R., Cox, R., Mapes, R., and Coleman, D., 2011, Hydrodynamic fractionation of zircon age populations: *Geological Society of America Bulletin*, v. 123, p. 295-305.
- Lehman, T., and Chatterjee, S., 2005, Depositional setting and vertebrate biostratigraphy of the Triassic Dockum Group of Texas: *Journal of Earth System Science*, v. 114, no. 3, p. 325-351.
- Lucas, S., Heckert, A., and Hunt, A., 2001, Triassic stratigraphy, biostratigraphy and correlation in east-central New Mexico: *New Mexico Geological Society*, v. 51, p. 85-102.
- Lucas, S., Hunt, A., and Hayden, S., 1987, The Triassic System in the Dry Cimarron Valley, New Mexico: *New Mexico Geological Society*, v. 38, p. 97-117.
- Lucas, S. G., 1985, Middle Triassic Amphibian from the basal Santa Rosa Formation, east-central New Mexico: *New Mexico Geological Society*, v. 36th Field Conference Guidebook, p. 171-184.

- Lucas, S. G., and Hunt, A. P., 1987, Stratigraphy of the Anton Chico and Santa Rosa Formations, Triassic of East-Central New Mexico: *Journal of the Arizona-Nevada Academy of Science*, v. 22, no. 1, p. 21-33.
- Ludwig, K. R., 2008, User's Manual for Isoplot 3.6: Berkeley Geochronology Center.
- Lupe, R. D., 1977, Depositional History of the Triassic Santa Rosa Sandstone, Santa Rosa, New Mexico: *Geological Society of America*, v. Abstracts with Programs, no. 9:61.
- Martz, J., 2008, Lithostratigraphy, chemostratigraphy, and vertebrate biostratigraphy of the Dockum Group (Upper Triassic), of southern Garza County, West Texas: *Lithostratigraphy, Chemostratigraphy, And Vertebrate Biostratigraphy Of The Dockum Group (Upper Triassic), Of Southern Garza County, West Texas*.
- McGowen, J., Granata, G., and Seni, S., Depositional setting of the Triassic Dockum Group, Texas Panhandle and eastern New Mexico 1983, *Rocky Mountain Section (SEPM)*.
- McGowen, J. H., Granata, G. E., and Seni, S. J., 1979, Depositional framework of the lower dockum group (triassic): Texas Panhandle, Bureau of Economic Geology, University of Texas at Austin, v. Book, Whole.
- Meadows, N. S., and Beach, A., 1993, Structural and climatic controls on facies distribution in a mixed fluvial and aeolian reservoir: the Triassic Sherwood Sandstone in the Irish Sea: *Geological Society, London, Special Publications*, v. 73, no. 1, p. 247.
- Miall, A., *The Geology of Fluvial Deposits: Sedimentary Facies, Basin Analysis, and Petroleum Geology* 1996.
- Parrish, J. T., 1993, Climate of the Supercontinent Pangea: *The Journal of Geology*, v. 101, no. 2, p. 215-233.
- Parrish, J. T., Rasbury, E. T., Chan, M. A., and Hasiotis, S. T., 2019, Earliest Jurassic U-Pb ages from carbonate deposits in the Navajo Sandstone, southeastern Utah, USA: *GEOLOGY*, v. 47, no. 11, p. 1015-1019.
- Pavlak, S. J., 1979, Stratigraphy and Sedimentary Petrology of the Moss Back Member of the Late Triassic Chinle Formation, North Temple Wash-San Rafael Desert Area, Emery County, Utah: University of Southern California.
- Plink-Björklund, P., 2015, Morphodynamics of rivers strongly affected by monsoon precipitation: Review of depositional style and forcing factors: *Sedimentary Geology*, v. 323, no. C, p. 110-147.
- Prochnow, S. J., Atchley, S. C., Boucher, T. E., Nordt, L. C., and Hudec, M. R., 2006, The influence of salt withdrawal subsidence on palaeosol maturity and cyclic fluvial deposition in the Upper Triassic Chinle Formation:

- Castle Valley, Utah: *Sedimentology*, v. 53, no. 6, p. 1319-1345.
- Riggs, N. R., Ash, S. R., Barth, A. P., Gehrels, G. E., and Wooden, J. L., 2003, Isotopic age of the Black Forest Bed, Petrified Forest Member, Chinle Formation, Arizona: An example of dating a continental sandstone: *GEOLOGICAL SOCIETY OF AMERICA BULLETIN*, v. 115, no. 11, p. 1315-1323.
- Riggs, N. R., Lehman, T. M., Gehrels, G. E., and Dickinson, W. R., 1996, Detrital zircon link between headwaters and terminus of the upper triassic chinle-dockum paleoriver system: *Science*, v. 273, no. 5271, p. 97.
- Riggs, N. R., Reynolds, S. J., Lindner, P. J., Howell, E. R., Barth, A. P., Parker, W. G., and Walker, J. D., 2013, The Early Mesozoic Cordilleran arc and Late Triassic paleotopography: The detrital record in Upper Triassic sedimentary successions on and off the Colorado Plateau: *Geosphere*, v. 9, no. 3, p. 602-613.
- Riggs, N. R., Sanchez, T. B., and Reynolds, S. J., 2020, Evolution of the early Mesozoic cordilleran arc; the detrital zircon record of back-arc basin deposits, Triassic Buckskin Formation, western Arizona and southeastern California, USA, Volume 16: BOULDER, Geological Society of America, p. 1042-1057.
- Rubio Cisneros, I. I., and Holbrook, J., 2021, Fluvial interpretations of stratigraphic surfaces across Upper Triassic to Lower-Middle Jurassic continental red beds northeastern Mexico: *Journal of South American earth sciences*, v. 110, p. 103366.
- Seni, S. J., 1978, Genetic stratigraphy of the Dockum Group (Triassic), Palo Duro Canyon, Panhandle, Texas.
- Sharman, G. R., and Malkowski, M. A., 2020, Needles in a haystack: Detrital zircon UPb ages and the maximum depositional age of modern global sediment: *Earth-Science Reviews*, v. 203, p. 103109.
- Singh, B. P., Tandon, S. K., Singh, G. P., and Pawar, J. S., 2009, Palaeosols in early Himalayan foreland basin sequences demonstrate latitudinal shift-related long-term climatic change: *Sedimentology*, v. 56, no. 5, p. 1464-1487.
- Tanner, L., 2000, Palustrine-Lacustrine and Alluvial Facies of the (Norian) Owl Rock Formation (Chinle Group), Four Corners Region, Southwestern U.S.A: Implications for Late Triassic Paleoclimate: *Journal of Sedimentary Research*, v. 70.
- , 2003, Pedogenic features of the Chinle Group, Four Corners region: Evidence of Late Triassic aridification: *New Mexico Geological Society Guidebook*, v. 54, p. 269-280.
- Tanner, L. H., and Lucas, S. G., 2006, Calcareous paleosols of the Upper

- Triassic Chinle Group, Four Corners region, southwestern United States: Climatic implications: Geological Society of America Special Papers, v. 416, p. 53.
- Van der Voo, R., Mauk, F. J., and French, R. B., 1976, Permian-Triassic continental configurations and the origin of the Gulf of Mexico: *Geology*, v. 4, no. 3, p. 177.
- Vermeesch, P., 2012, On the visualisation of detrital age distributions: *Chemical Geology*, v. 312-313, p. 190-194.
- Wakefield, O. J. W., Hough, E., and Peatfield, A. W., 2015, Architectural analysis of a Triassic fluvial system: The Sherwood Sandstone of the East Midlands Shelf, UK: *Sedimentary Geology*, v. 327, p. 1-13.
- Walker, S. P., 2020, Profiles and paleohydrology of supercritical rivers, the Triassic Dockum group of West Texas: Texas Christian University.
- Walper, J. L., 1977, Paleozoic tectonics of the southern margin of North America.
- Wengler, M., Barboza-Gudiño, J. R., Thomsen, T. B., and Meinhold, G., 2019, Sediment provenance of Triassic and Jurassic sandstones in central Mexico during activity of the Nazas volcanic arc: *Journal of South American Earth Sciences*, v. 92, p. 329-349.
- Winguth, A., and Winguth, C., 2013, Precession-driven monsoon variability at the Permian–Triassic boundary — Implications for anoxia and the mass extinction: *Global and Planetary Change*, v. 105, p. 160-170.

Vita

Personal Background

Blake Bezucha

Dallas, Texas

Education

Diploma, Bishop Lynch High School

Bachelor of Science, UT-Austin

Experience

Research Assistant, Bureau of Economic
Geology

Teaching Assistant, TCU

Professional Memberships

Fort Worth Geological Society

Dallas Geological Society

Abstract

GEOCHRONOLOGIC CONNECTIONS BETWEEN THE CHINLE FORMATION AND DOCKUM GROUP

By Blake Bezucha

Department of Geosciences

Texas Christian University

Thesis Advisor: Dr. John Holbrook, Professor of Geology

The Late Triassic Chinle Formation and the correlative Dockum Group span most of the southwestern United States, exposed in outcrop from Texas to Nevada. Although the Chinle Formation west of the Rocky Mountains is extensively studied and dated and shown to be lithostratigraphically and broadly time equivalent to the more eastern Dockum Group, a more refined geochronologic correlation is needed to confirm western Chinle strata is equivalent to Dockum strata east of the Rockies in basins such as the Palo Duro and Tucumcari Basins. This study provides clarity to initial assessments for provenance of the Dockum Group and paleogeographical ties to the Chinle Formation through various sedimentological and geochronological methods, painting a clearer picture of the Late Triassic during a megamonsoonal climate and initial rifting of the Gulf of Mexico.